“The best of both worlds” – Connecting remote sensing and Arctic communities for safe sea ice travel

by

Rebecca Segal
B.Sc., University of Victoria, 2013

A Thesis Submitted in Partial Fulfillment
of the Requirements for the Degree of

MASTER OF SCIENCE

in the Department of Geography

© Rebecca Segal, 2019
University of Victoria

All rights reserved. This thesis may not be reproduced in whole or in part, by photocopy
or other means, without the permission of the author.

Supervisory Committee

"The best of both worlds" – Connecting remote sensing and Arctic communities for safe sea ice travel

by

Rebecca Segal
B.Sc., University of Victoria, 2013

Supervisory Committee

Dr. Randall Scharien, Department of Geography
Supervisor

Frank Duerden, Department of Geography
Departmental Member

Abstract

This thesis examines the role of remote sensing technology in providing information to northern residents of Kugluktuk and Cambridge Bay, Kitikmeot region of Nunavut, Western Canadian Arctic, for the purpose of improving sea ice trafficability and safety. The main objectives of this thesis include 1) the identification of northern community sea ice information needs that can be addressed using remote sensing, and 2) the creation of remote sensing-based products showing sea ice surface roughness information useful to community sea ice trafficability and safety. Thesis outcomes include the refinement and dissemination of information and products with these communities. Research methods involved interviews with northern community members that were analysed using thematic analysis, as well as quantitative assessments of sea ice roughness using satellite datasets. Maps of sea ice surface roughness were created using Sentinel-1 synthetic aperture radar and the Multi-angle Imaging Spectroradiometer, and were evaluated against fine-scale airborne LiDAR data.

Keywords: Arctic sea ice, Inuit knowledge, remote sensing, sea ice roughness, safety and navigation, Synthetic Aperture Radar (SAR), Multi-angle Imaging SpectroRadiometer (MISR), cryosphere climate change

Table of Contents

Supervisory Committee **ii**

Abstract **iii**

Table of Contents **iv**

List of Tables **vi**

List of Figures **viii**

Acknowledgments **xii**

Chapter 1 – Introduction **1**

1.1 Context 1
1.1.1 Northern communities and sea ice trafficability 1
1.1.2 Local on-ice trafficability and sea ice surface roughness 3

1.2 Inuit Qaujimajatuqangit and remote sensing 5

1.3 Thesis structure 6

1.4 Co-author contributions 7

1.5 References 8

Chapter 2 - "The best of both worlds" - Connecting remote sensing and Arctic communities for safe sea ice travel Part 1 - Uncertain trafficability **15**

2.1 Acknowledgements 15

2.2 Abstract 16

2.3 Introduction 17

2.4 Background 19

2.5 Study area 22

2.6 Methods 25
2.6.1 Research approach and community data 25
2.6.2 Greyscale and classified SAR maps 26

2.7 Results and Discussion 29
2.7.1 Changes impacting sea ice use 29
2.7.2 Evaluation of SAR-based maps 35
2.7.3 Comparison to other trafficability studies 44
2.7.4 Online integration 49

2.8 Conclusions 51

2.9 References 53

Chapter 3 - The best of both worlds" - Connecting remote sensing and Arctic communities for safe sea ice travel Part 2 –Surface roughness **66**

3.1 Acknowledgements 66

3.2 Abstract 67

3.3 Introduction 68

3.4 Methods 72
3.4.1 Study area and research design 72
3.4.2 Data processing 77
3.4.3 Multi-scale comparisons 79
3.4.4 Decomposition and classification using Sentinel-1 and RADARSAT-2 79

3.5 Results 80
3.5.1 Broad-scale comparison 80
3.5.2 Fine-scale comparison 83
3.5.3 Roughness indices 88
3.5.4 Ice type classification 89

3.6 Discussion 91
3.6.1 MISR NDAI 91
3.6.2 Sentinel-1 HH backscatter 93
3.6.3 Impact of snow 95
3.6.4 Other data and recommendations 96

3.7 Conclusions 97

3.8 References 99

Chapter 4 - Conclusions **108**

4.1 Summary 108

4.2 Community engagement with remote sensing products 110

4.3 Future research and recommendations 111

Appendix A **114**

A.1 SAR processing 115

A.2 References 117

Appendix B **118**

B.1 Study region sea ice regime 118

B.2 HH backscatter processing 118

B.3 NDAI and HH backscatter relationships by ice type 122

B.4 HH backscatter by region 123

B.5 Other data and recommendations (continued) 124

B.6 References 129

List of Tables

Table 2.1. Major sea ice features and their occurrence in the context of hazardous ice conditions, as described by residents of Kugluktuk and Cambridge Bay, Nunavut. 33

Table 2.2. Major sea ice feature use and change, as described by residents of Kugluktuk and Cambridge Bay, Nunavut. Features a – j are described in the text and Table 2.1..... 34

Table 2.3. The traditional or current practices used to navigate sea ice conditions a - j, and the information ideally desired by travelers. Features a – j are described in Table 2.1 and the text. 37

Table 2.4. Evaluation of SAR-based maps in the context of their ability to provide safety and trafficability information about sea ice conditions a - j, and the potential benefits of the information provided. Features a – j are described in Table 2.1 and the text. Information originates from interview data unless italicized..... 38

Table 3.1. Information about the sensors and products used to assess sea ice backscatter and surface roughness. Abbreviations are as follows: S = Sentinel; Des = descending; Asc = ascending; EW = extended wide-swath; GRD = ground range detected; FQn = fine quad pol; Bxx=band number; Fxx = Format version number; ALS = airborne laser scanner; SLC = single-look complex; NA = not applicable. SLC images are used in section 3.4.4 exclusively. 76

Table 3.2. Confusion matrices for MYI detection using a H-alpha Wishart classification on Sentinel-1 imagery (dual-pol) and H-A-alpha Wishart classification on RADARSAT-2 imagery (quad-pol). Producer's accuracy measures the probability

of omission error whereas user's accuracy measures commission error. Kappa is a measure of actual vs. chance agreement in the classification, as calculated in Congalton (1991). 91

Table A.1. Semi-structured interview question guideline for May-June 2017 field season. 114

Table A.2. Information about the Sentinel-1 products processed and used in maps brought to the communities. Where indicated (*), classified maps were also created. Abbreviations are as follows: S = Sentinel; Des = descending; Asc = ascending; and EW = extended wide-swath. All images are in ground range detected (GRD) format. 116

Table B.1. Information about the sensors and products used to investigate the effect of incidence angle on Sentinel-1 backscatter over FYI and MYI in M'Clintock Channel, winter 2017. Abbreviations are as follows: S = Sentinel; Des = descending; Asc = ascending; EW = extended wide-swath; GRD = ground range detected. 121

Table B.2. FYI C-band HH backscatter observed across Arctic roughness regimes. 123

Table B.3. Current and near-future satellite-based payloads that may be useful (high quality and/or affordable) for providing sea ice surface trafficability information to northern communities. 128

List of Figures

Figure 2.1. Map showing the locations of Cambridge Bay and Kugluktuk, distinguished by red dots, in Nunavut's Kitikmeot Region Subdivision (red dashed lines; from the 2017 Canadian census). Other populated places are shown as black dots..... 24

Figure 2.2. Sample SAR-based maps. a) is greyscale, and b) is classified by roughness level. 28

Figure 2.3. Maps showing: a-c) the locations of thin sea ice or open water areas identified by local experts as dangerous seasonally or year-round. Maps show important places mentioned in interviews (black dots) and dangerous areas across a) the Kitikmeot region, b) the Kugluktuk region, and c) the Cambridge Bay region. This is not a comprehensive list of dangerous areas: some thin sea ice areas are missing near Lewes Island, dangerous areas closer to other Kitikmeot communities would be better known by the residents of those communities, and other areas may appear with a changing climate. a) Main travel routes (grey lines) and important places (grey dots) identified by the Inuit Heritage Trust (http://ihti.ca/eng/iht-proj-plac.html). 40

Figure 2.4. Top: greyscale Sentinel-1 HH-band SAR-based map of 1-30 April 2019 images on the Google Earth Engine platform. Bottom: classified roughness map viewed on the SIKU website (https://beta.siku.org) using the selected date of 1 April 2019. 50

Figure 3.1 a) The study area, showing Sentinel-1 (orange), MISR (blue) and LiDAR (yellow) data coverage. The dashed grey line indicates the coverage of inset b),

which shows LiDAR-derived root mean square roughness, overlaid on the 9-14 April 2017 Sentinel-1 mosaic. 73

Figure 3.2. Sea ice surface roughness features near Kugluktuk on 28 May 2018 (a-b) and Cambridge Bay on 21 May 2018 (c-d). a) Area of snow-covered moderately rough sea ice with upturned blocks (N 67˚56.936’, W 114˚41.526’); b) close-up of a typical ice block seen in the foreground of a), with dimensions: length = 127 cm, width = 24 cm, height = 135 cm, and thickness = 14 cm; c) image showing the thickness of sea ice when it broke (~10 cm, each marked interval is 1 cm); and d) a sea ice fracture (pressure ridge) ~2-3 m in height and ~ 4.5 m wide (N 69˚03.724, W 105˚40.165’)..... 75

Figure 3.3. Box and whisker plot showing HH backscatter and NDAI by sea ice type... 81

Figure 3.4. For DFYI in Victoria Strait: a) relationship between mean HH backscatter and NDAI; b) standard regression residuals from a) plotted spatially; c) NDAI; and d) HH backscatter. 82

Figure 3.5. Measured sea ice surface roughness (black) compared to Sentinel-1 HH backscatter (orange) and MISR NDAI (blue) along a LiDAR flightline from Victoria Strait to M’Clintock Channel. 84

Figure 3.6. Relationship of surface roughness to satellite-derived roughness by ice type: a) NDAI for FYI, b) HH backscatter for FYI, c) NDAI for MYI, d) HH backscatter for MYI, e) NDAI for a balanced set of ROIs by ice type (N = 29 for FYI and N = 28 for MYI), and f) HH backscatter for a balanced set of ROIs by ice type (*N* = 26 for FYI and *N* = 23 for MYI). Plots show linear regressions with 95% confidence intervals and threshold values (dotted horizontal lines) used for

the creation of maps showing *smooth ice, moderately rough ice*, and *rough sea ice*. 86

Figure 3.7. Thresholded roughness maps from a) NDAI and b) HH backscatter. Overlaid ROIs show measured roughness along a LiDAR flight path. Insets of c) NDAI and d) HH backscatter, are indicated by a dotted black line. 87

Figure 3.8. Modeled roughness based on regression fits from measured roughness and a) NDAI and b) HH backscatter from Figure 3.6. 89

Figure 3.9. Evaluation of a) the Sentinel-1-based H-alpha dual pol Wishart classification and its ability to detect areas of MYI (yellow) and FYI (green). Images are from April 2017 in Victoria Strait. Comparisons are made to: b) the RADARSAT-2-based H-A-alpha quad pol Wishart classification, c) the corresponding weekly regional sea ice chart produced by the Canadian Ice Service; and d) Sentinel-1 HH backscatter (in dB). In e) the difference between the a) and b) is shown, with grey representing areas where the two classifications agree, and blue (red) representing areas where Sentinel-1 found MYI (FYI) but RADARSAT-2 found FYI (MYI). Images f) and g) are insets of a) and b) respectively, denoted by the white boxes in the outset images. 90

Figure B.1. Sentinel-1 HH-band backscatter from a) FYI and b) MYI targets, given as cubic functions of incidence angle for gamma-nought and sigma-nought calibrations. The effect of incidence angle is less for gamma-nought calibration and is similar between FYI and MYI types. In c) the effect of ten-degree incidence angle intervals is shown as HH gamma nought backscatter ranges, for FYI and MYI types. 120

Figure B.2. Relationship between mean Sentinel-1 HH backscatter and mean MISR NDAI for FYI (top) and MYI (bottom) types. 122

Acknowledgments

I would like to thank all the people who welcomed me into the north and who shared their stories and love of the sea ice. Your kindness, appreciation for learning, and desire for remote sensing images is an inspiration that helps me stay motivated.

To my supervisor Dr. Randy Scharien – Thank you very much for your support. Each time I came to you with new ideas for funding applications, data, conferences, training, etc., you consistently enabled me to grow and explore. I feel very privileged to have been given so much over the past three years – great independence, amazing opportunities, and wonderful experiences.

Dr. Frank Duerden –a great thank you for the many lively discussions and coffees. You provided very necessary research focus (tables!) and support.

I also want to recognise Dr. Trevor Lantz, who gave me research training, an introduction to northern research, and inspiration for some of the approaches and writing techniques used in this thesis. I would not be on this path without your guidance and assistance.

Many thanks to current and past ICE lab members (Sasha Nasonova, Silvie Cafarella, Katia Tavri, Parnian Rezania, Vishnu Nandan, Trilby Buck, James Balchin, Jessica McLean, and Andy Wynden) and to the other geography graduate students who are always happy to offer advice or moral support.

Last but not least – a huge thanks to my friends and family who have been (hopefully willingly) coerced into learning about sea ice, remote sensing, and northern communities. I am lucky to have such a great group of supporters!

Chapter 1 – Introduction

1.1 Context

1.1.1 Northern communities and sea ice trafficability

Most Arctic communities are situated on the marine coastline, where sea ice is highly intertwined with the lives of Arctic residents. Life events occur on sea ice trails and they are considered places in and of themselves (Aporta, 2009). Furthermore, sea ice provides a platform for travel that connects communities to one another; allows access to recreation and hunting grounds; and is embedded in the cultural fabric of northern life (Aporta, 2004; Laidler, 2007). However, while sea ice has been a long-term component of the northern seascape, changes to communities and the environment have profound impacts to travel on and around sea ice.

Inuit traditional, current, and future knowledge systems, or Inuit Qaujimajatuqangit (IQ), contain extensive information about safe navigation practices from personal observations and interpersonal communications. However, sea ice trafficability and safety is impacted by the adoption of modern lifestyles. Modern lifestyles are associated with new sources of technology and technologically-derived knowledge like snowmobiles, GPS, and weather reports; as well as changed societal practices like decreased time spend on the sea ice, and the disruption of traditional knowledge communication about on-ice safety to younger generations (Brinton, 2018; Ford, 2005; Ford et al., 2006a, 2006b; Heyes, 2011; Laidler et al., 2011; Panikkar et al., 2018). Access to the sea ice, which is dependent on the ability to safely navigate risks and requires adequate safety and navigation knowledge, experience with travel and inclement

conditions and possession of functional equipment, has decreased with the lifestyle changes associated with settled communities. Experienced, high-risk tolerant Inuit in the Nunangat region now have 101 days more access to land and sea ice trails per year when compared to less experienced, low-risk tolerant Inuit travelers (Ford et al., 2019). These findings suggest that there is an opportunity for informational materials to help improve land and sea ice accessibility.

Climate change is impacting the Arctic more than most other areas of the world (ACIA, 2005; Bush & Lemmen, 2019; Meier et al., 2014). Sea ice extent and thickness are decreasing, multi-year ice (MYI) is being replaced by first year ice (FYI), and the open water season is lengthening (Comiso & Hall, 2014; Lindsay & Schweiger, 2015; Markus et al., 2009; Meier et al., 2014; Stroeve et al., 2014). Northerners have observed increasingly unpredictable travel conditions (Deemer et al., 2018; Krupnik & Jolly, 2002; Meier et al., 2014; Nickels et al., 2005). Impacts are also expected to include infrastructure degradation and cultural site losses, changes in resource availability, and shifts in northern daily activities and culture; however, at the local scale factors like local environmental conditions, historical ability to deal with stressors, and local capacity will modulate responses to change (Arctic Monitoring and Assessment Programme, 2011; Duerden, 2004; Meier et al., 2014; Prowse et al., 2009; Stuckenberger, 2010).

Remote sensing products are able to provide fine resolution, broad-scale information about sea ice. Consultations have revealed that access to remote sensing information is desired by many northern residents, particularly as social and environmental conditions change (Bell et al., 2014; Druckenmiller et al., 2009; Gauthier et al., 2010; Laidler et al., 2011). In particular, synthetic aperture radar (SAR) has been

used to inform industry-related sea ice hazard detection and produce operational sea ice maps for decades. However, determining what information is useful to northern communities, and how satellite data or satellite-derived products can be used to address these information needs, has not yet been explored with most Arctic communities. This thesis provides a first assessment of sea ice information needs for the communities of Kugluktuk and Cambridge Bay in the Kitikmeot region of Nunavut, Western Canadian Arctic.

1.1.2 Local on-ice trafficability and sea ice surface roughness

Numerous studies have noted community desires for sea ice topographical information (Aporta, 2004; Bell et al., 2014; Dammann et al., 2018; Druckenmiller et al., 2013; Ford et al., 2008; Laidler et al., 2011), also known as macroscale sea ice surface roughness and referred to in this thesis as *roughness*. Roughness is identified as a major sea ice trafficability and safety information need that can be addressed using remote sensing techniques. Consequently, research efforts focus on this information need, and quantitatively analyse remote sensing products to characterise roughness.

Roughness is characterised by a range of features including: level, undeformed sea ice; structures formed by convergent or divergent stressors like pressure ridges, cracks, leads, ice rubble, rafted ice, and hummocks; snow features like sastrugi, dunes, and variable depth; and melt features like saturated snow (slush) and melt water ponds. Sea ice roughness is caused by seasonal and multi-year ice types undergoing thermodynamic and dynamic-deformation processes. It is important at spatio-temporal scales applicable to travel by snowmobile; that is, in sub-metre to metre-scales (>0.1 m), over large areas and at frequent intervals throughout the season. While several studies

have used satellite and/or LiDAR datasets to characterise roughness, few have focused on roughness in relation to trafficability by local northern sea ice users (Dammann et al., 2018; Gauthier et al., 2010).

In this thesis, two satellite datasets, C-band frequency Sentinel-1 SAR and optical Multi-angle Imaging SpectroRadiometer (MISR), are investigated for their abilities to provide data on winter-period macroscale surface roughness at scales applicable to serving on-ice trafficability information needs. The Sentinel-1 constellation is operated by the European Space Agency (ESA), while MISR, hosted on the Terra platform, is operated by the National Aeronautics and Space Administration (NASA). Both satellite datasets are assessed by comparing derived image data to high-resolution roughness data measured by an airborne LiDAR system. SAR is desirable for roughness mapping because of its ability to regularly obtain imagery regardless of cloud cover or darkness, and the sensitivity of measured backscatter to surface roughness where dielectric property contrasts occur (air/snow and snow/ice interfaces) (Dammann et al., 2018). MISR provides optical data from 9 cameras with different viewing geometries and has a descending orbit that allows directional reflectances to be used to infer surface roughness (Nolin, 2004; Nolin & Payne, 2007).

Defining, observing, and creating products that display sea ice roughness in ways that are useful to northern communities is a developing area of research. To characterise roughness at fine scales, often simple vertical-roughness functions like deviation from a mean surface, or more complicated vertical and horizontal autocorrelations or variogram-style functions are applied at set length-scales or within objects (contiguous groups of image pixels aggregated by spectral or other properties) (Beckers et al., 2015; Landy et

al., 2015; Li, 2018; Nasonova et al., 2018; Newman et al., 2014; Nolin & Mar, 2019; Petty et al., 2017). For broader-scale roughness datasets like those often used in satellite remote sensing, complex roughness metrics (e.g., normalised differential angular index, neighbourhood-style analyses like terrain ruggedness, calculated parameters like radar texture, depolarization or intensity), or semi-automated techniques are becoming more prevalent (Fors et al., 2016; Gegiuc et al., 2018; Li, 2018; Nolin & Mar, 2019). However, current sea ice research methods still reflect ongoing efforts to connect image-based roughness data to physical and in situ properties at appropriate scales.

By comparing Sentinel-1 and MISR datasets to LiDAR data over winter sea ice, this thesis identifies where the relationships between the satellite sensor-computed roughness and LiDAR-measured roughness are strong, and conditions that cause these relationships to break down. Also highlighted are areas where the two satellite sensors have unequal utility in the quantification of roughness and the subsequent creation of roughness maps.

1.2 Inuit Qaujimajatuqangit and remote sensing

This thesis synthesises knowledge derived from IQ and remote sensing to evaluate the role that the latter can play in providing information about sea ice conditions in the context of a changing climate. The use of both knowledge systems is essential because it allows for the discussion of achievable priorities and outcomes from the perspectives of both northerners and researchers. Various experts with knowledge about sea ice use, northern community needs, or remote sensing all offer valuable insight for improving the role of remote sensing products in northern communities. This study makes connections between remote sensing technology and IQ through northern partners

who identify remote sensing-related needs and whose feedback guides product development and assessment. The perspectives of northerners inform the current and potential applications of remote sensing products and assist in the evaluation of current information product utility, accuracy, and accessibility. A two-way (or multi-directional) exchange of information enables the current remote sensing-based map content and context to be better understood by all parties. From conception to completion, this thesis has benefited from the assistance of many people and organizations both inside and outside the Arctic.

1.3 Thesis structure

Two main research questions are investigated: 1) What are the impediments to modern and future marine trafficability and safety, as determined by and for communities of the Western Canadian Arctic; and 2) How can openly available satellite tools be used effectively to improve on-ice trafficability and safety related to sea ice surface roughness?

The second chapter addresses research question 1 using qualitative data collected through interviews with community members in the Western Canadian Arctic. Information exchanges regarding local sea ice conditions, ice information priorities, and the role of remote sensing primarily occurred during three field seasons in Kugluktuk and Cambridge Bay. The identification of sea ice surface roughness as a main impediment to marine trafficability and safety is then used to create research question 2, which is addressed in Chapter 3 by assessing two freely available satellite sensors, Sentinel-1 and MISR, for their abilities to contribute to sea ice surface roughness maps using a comparison to high-resolution airborne LiDAR data.

The fourth chapter discusses the main contributions and applications of this thesis research and its relationships to existing research. This chapter also provides recommendations for future research directions.

Appendices A and B contain the supplementary materials prepared to accompany Chapters 2 and 3, respectively.

1.4 Co-author contributions

This thesis exists due to co-author collaborations. Dr. Randy Scharien provided oversight and editing for Chapters 1-4. Frank Duerden provided research focus and editing for Chapter 1, 2 and 4. Dr. Chui-Ling Tam assisted with fieldwork methods. For Chapter 3, Silvie Cafarella provided analysis suggestions and Dr. Andrew Tedstone provided pre-processed MISR data.

1.5 References

ACIA. (2005). *Arctic climate impact assessment* (p. 1042). New York, New York: Cambridge University Press. Retrieved from www.cambridge.org/9780521865098

Aporta, C. (2004). Routes, trails and tracks: Trail breaking among the Inuit of Igloolik. *Études/Inuit/Studies*, *28*(2), 9–38. https://doi.org/10.7202/013194ar

Aporta, C. (2009). The trail as home: Inuit and their pan-Arctic network of routes. *Human Ecology*, *37*(2), 131–146. https://doi.org/10.1007/s10745-009-9213-x

Arctic Monitoring and Assessment Programme. (2011). *Snow, water, ice and permafrost in the Arctic (SWIPA): Climate change and the cryosphere*. Oslo, Norway. Retrieved from www.amap.no

Beckers, J. F., Renner, A. H. H., Spreen, G., Gerland, S., & Haas, C. (2015). Sea-ice surface roughness estimates from airborne laser scanner and laser altimeter observations in Fram Strait and north of Svalbard. *Annals of Glaciology*, *56*(69), 235–244. https://doi.org/10.3189/2015AoG69A717

Bell, T., Briggs, R., Bachmayer, R., & Li, S. (2014). Augmenting Inuit knowledge for safe sea-ice travel: The SmartICE information system. In *Oceans - St. John's, 2014* (pp. 1–9). https://doi.org/10.1109/OCEANS.2014.7003290

Brinton, M. (2018). Risk and uncertainty regarding Inuit transportation in the face of climate change. *Boise State University Theses and Dissertations*. https://doi.org/10.18122/td/1372/boisestate

Bush, E., & Lemmen, D. S. (Eds.). (2019). *Canada's changing climate report.* Ottawa, Ontario: Government of Canada. Retrieved from http://publications.gc.ca/collections/collection_2019/eccc/En4-368-2019-eng.pdf

Comiso, J. C., & Hall, D. K. (2014). Climate trends in the Arctic as observed from space. *Wiley Interdisciplinary Reviews: Climate Change*, *5*(3), 389–409. https://doi.org/10.1002/wcc.277

Dammann, D. O., Eicken, H., Mahoney, A. R., Saiet, E., Meyer, F. J., & George, J. C. "Craig." (2018). Traversing sea ice: Linking surface roughness and ice trafficability through SAR polarimetry and interferometry. *IEEE Journal of Selected Topics in Applied Earth Observations and Remote Sensing*, *PP*(99), 1–18. https://doi.org/10.1109/JSTARS.2017.2764961

Deemer, G. J., Bhatt, U. S., Eicken, H., Posey, P. G., Hutchings, J. K., Nelson, J., … Creek, K. (2018). Broadening the sea-ice forecaster toolbox with community observations: A case study from the northern Bering Sea. *Arctic Science*, *4*, 47–70. https://doi.org/10.1139/AS-2016-0054

Druckenmiller, M. L., Eicken, H., George, J. C. "Craig," & Brower, L. (2013). Trails to the whale: Reflections of change and choice on an Iñupiat icescape at Barrow, Alaska. *Polar Geography*, *36*(1–2), 5–29. https://doi.org/10.1080/1088937X.2012.724459

Druckenmiller, M. L., Eicken, H., Johnson, M. A., Pringle, D. J., & Williams, C. C. (2009). Toward an integrated coastal sea-ice observatory: System components and a case study at Barrow, Alaska. *Cold Regions Science and Technology*, *56*(2–3), 61–72. https://doi.org/10.1016/j.coldregions.2008.12.003

Duerden, F. (2004). Translating Climate Change Impacts at the Community Level. *Arctic*, *57*(2), 204–212.

Ford, J. D. (2005). Living with climate change in the Arctic | Worldwatch Institute. *Worldwatch Institute*, *18*(5), 18–21.

Ford, J. D., Clark, D., Pearce, T., Berrang-Ford, L., Copland, L., Dawson, J., … Harper, S. L. (2019). Changing access to ice, land and water in Arctic communities. *Nature Climate Change*, 1. https://doi.org/10.1038/s41558-019-0435-7

Ford, J. D., Pearce, T., Gilligan, J., Smit, B., & Oakes, J. (2008). Climate change and hazards associated with ice use in Northern Canada. *Arctic, Antarctic, and Alpine Research*, *40*(4), 647–659. https://doi.org/10.1657/1523-0430(07-040)[FORD]2.0.CO;2

Ford, J. D., Smit, B., & Wandel, J. (2006a). Vulnerability to climate change in the Arctic: A case study from Arctic Bay, Canada. *Global Environmental Change*, *16*(2), 145–160. https://doi.org/10.1016/j.gloenvcha.2005.11.007

Ford, J. D., Smit, B., Wandel, J., & MacDonald, J. (2006b). Vulnerability to climate change in Igloolik, Nunavut: What we can learn from the past and present. *Polar Record*, *42*(2), 127. https://doi.org/10.1017/S0032247406005122

Fors, A. S., Brekke, C., Gerland, S., Doulgeris, A. P., & Beckers, J. F. (2016). Late summer Arctic sea ice surface roughness signatures in C-Band SAR data. *IEEE Journal of Selected Topics in Applied Earth Observations and Remote Sensing*, *9*(3), 1199–1215. https://doi.org/10.1109/JSTARS.2015.2504384

Gauthier, Y., Tremblay, M., Bernier, M., & Furgal, C. (2010). Adaptation of a radar-based river ice mapping technology to the Nunavik context. *Canadian Journal of Remote Sensing*, *36*(S1), S168–S185. https://doi.org/10.5589/m10-018

Gegiuc, A., Similä, M., Karvonen, J., Lensu, M., Mäkynen, M., & Vainio, J. (2018). Estimation of degree of sea ice ridging based on dual-polarized C-band SAR data. *The Cryosphere*, *12*(1), 343–364. https://doi.org/10.5194/tc-12-343-2018

Heyes, S. A. (2011). Cracks in the knowledge: Sea ice terms in Kangiqsualujjuaq, Nunavik. *The Canadian Geographer / Le Géographe Canadien*, *55*(1), 69–90. https://doi.org/10.1111/j.1541-0064.2010.00346.x

Krupnik, I., & Jolly, D. (2002). *The Earth is faster now: Indigenous observations of Arctic environment change*. Arctic Research Consortium of the United States.

Laidler, G. J. (2007). *Ice, through Inuit eyes: Characterizing the importance of sea ice processes, use, and change around three Nunavut communities.* (Ph.D.). University of Toronto, Toronto, Ontario.

Laidler, G. J., Hirose, T., Kapfer, M., Ikummaq, T., Joamie, E., & Elee, P. (2011). Evaluating the Floe Edge Service: How well can SAR imagery address Inuit community concerns around sea ice change and travel safety? *Canadian Geographer / Le Géographe Canadien*, *55*(1), 91–107. https://doi.org/10.1111/j.1541-0064.2010.00347.x

Landy, J. C., Isleifson, D., Komarov, A. S., & Barber, D. G. (2015). Parameterization of centimeter-scale sea ice surface roughness using terrestrial LiDAR. *IEEE Transactions on Geoscience and Remote Sensing*, *53*(3), 1271–1286. https://doi.org/10.1109/TGRS.2014.2336833

Li, Y. (2018). *Sea ice and ice sheet surface roughness characterization and its effects on bi-directional reflectance* (Thesis). Texas A & M University, College Station, Texas. Retrieved from https://oaktrust.library.tamu.edu/handle/1969.1/173578

Lindsay, R., & Schweiger, A. (2015). Arctic sea ice thickness loss determined using subsurface, aircraft, and satellite observations. *The Cryosphere*, *9*(1), 269–283. https://doi.org/10.5194/tc-9-269-2015

Markus, T., Stroeve, J. C., & Miller, J. (2009). Recent changes in Arctic sea ice melt onset, freezeup, and melt season length. *Journal of Geophysical Research: Oceans*, *114*(C12), C12024. https://doi.org/10.1029/2009JC005436

Meier, W. N., Hovelsrud, G. K., van Oort, B. E. H., Key, J. R., Kovacs, K. M., Michel, C., … Reist, J. D. (2014). Arctic sea ice in transformation: A review of recent observed changes and impacts on biology and human activity. *Reviews of Geophysics*, *52*(3), 185–217. https://doi.org/10.1002/2013RG000431

Nasonova, S., Scharien, R. K., Haas, C., & Howell, S. E. L. (2018). Linking regional winter sea ice thickness and surface roughness to spring melt pond fraction on landfast Arctic sea ice. *Remote Sensing*, *10*(1), 37. https://doi.org/10.3390/rs10010037

Newman, T., Farrell, S. L., Richter-Menge, J. A., Conner, L. N., Kurtz, N. T., Elder, B. C., & McAdoo, D. (2014). Assessment of radar-derived snow depth over Arctic sea ice. *Journal of Geophysical Research: Oceans*, *119*(12), 8578–8602. https://doi.org/10.1002/2014JC010284

Nickels, S., Furgal, C., Buell, M., & Moquin, H. (2005). *Unikkaaqatigiit - Putting the human face on climate change: Perspectives from Inuit in Canada*. Ottawa,

Ontario: Inuit Tapiriit Kanatami, Nasivvik Centre for Inuit Health and Changing Environments at Université Laval and the Ajunnginiq Centre at the National Aboriginal Health Organization. Retrieved from http://www.inuitknowledge.ca/sites/ikc/files/attachments/20060726-Unikkaaqatigiit-book-complete-web.pdf

Nolin, A. W. (2004). Towards retrieval of forest cover density over snow from the Multi-angle Imaging SpectroRadiometer (MISR). *Hydrological Processes*, *18*(18), 3623–3636. https://doi.org/10.1002/hyp.5803

Nolin, A. W., & Mar, E. (2019). Arctic sea ice surface roughness estimated from multi-angular reflectance satellite imagery. *Remote Sensing*, *11*(1), 50. https://doi.org/10.3390/rs11010050

Nolin, A. W., & Payne, M. C. (2007). Classification of glacier zones in western Greenland using albedo and surface roughness from the Multi-angle Imaging SpectroRadiometer (MISR). *Remote Sensing of Environment*, *107*(1–2), 264–275. https://doi.org/10.1016/j.rse.2006.11.004

Panikkar, B., Lemmond, B., Else, B., & Murray, M. (2018). Ice over troubled waters: Navigating the Northwest Passage using Inuit knowledge and scientific information. *Climate Research*, *75*(1). Retrieved from https://www.openchannels.org/literature/22121

Petty, A. A., Tsamados, M. C., & Kurtz, N. T. (2017). Atmospheric form drag coefficients over Arctic sea ice using remotely sensed ice topography data, spring 2009-2015. *Journal of Geophysical Research: Earth Surface*, *122*, 1472–1490.

Prowse, T. D., Furgal, C., Wrona, F. J., & Reist, J. D. (2009). Implications of climate change for Northern Canada: Freshwater, marine, and terrestrial ecosystems. *AMBIO: A Journal of the Human Environment*, *38*(5), 282–289. https://doi.org/10.1579/0044-7447-38.5.282

Stroeve, J. C., Markus, T., Boisvert, L., Miller, J., & Barrett, A. (2014). Changes in Arctic melt season and implications for sea ice loss. *Geophysical Research Letters*, *41*(4), 2013GL058951. https://doi.org/10.1002/2013GL058951

Stuckenberger, A. N. (2010). Les Inuit et le changement climatique / The Inuit and climate change. *Études/Inuit/Studies*, *34*(1), 5–19.

Chapter 2 - "The best of both worlds[1]" - Connecting remote sensing and Arctic communities for safe sea ice travel

Part 1 - Uncertain trafficability

Rebecca A. Segal[a], Randall K. Scharien[a], Frank Duerden[a], Chui-Ling Tam[b]
[a]Department of Geography, University of Victoria
[b]Department of Geography, University of Calgary

2.1 Acknowledgements

We gratefully acknowledge the hospitality, assistance, and expertise of the residents and partnered organizations in both Kugluktuk and Cambridge Bay. We thank the hunters and elders who shared wisdom during interviews and sea ice excursions, Jessica MacLean for assistance with interview transcription, Trilby Buck for support in the field, as well as Andy Wynden and Sasha Nasonova for programming support. We acknowledge a beneficial partnership with Ocean Networks Canada and the University of Victoria's Climate Lab. This research was supported by the Marine Environmental Observation Prediction and Response (MEOPAR) network and Irving Shipbuilding Inc. project number 1.22, Polar Knowledge Canada (POLAR; NST-1718-0024), the W. Garfield Weston Foundation through the Association of Canadian Universities for Northern Studies (ACUNS), the Natural Sciences and Engineering Research Council of

[1] Resident of Kugluktuk

Canada (NSERC), the Royal Canadian Geographical Society (RCGS), the Arctic Institute of North America (AINA), and the University of Victoria. Sentinel-1 data are freely provided by the European Space Agency. Interviews comply with the Human Research Ethics Board at the University of Victoria (protocol 17-130) as well as Nunavut Research Institute licenses 04 008 17R-M, 04 010 18R-M, and 04 008 18R-M.

2.2 Abstract

Northern communities are increasingly interested in technology that provides information about the sea ice environment and reduces trafficability uncertainty. Microwave synthetic aperture radar (SAR) remote sensing is widely used to observe sea ice independently of sunlight and cloud cover; however, access to SAR in northern communities has been limited. This study 1) defines the sea ice features that influence trafficability for two communities in the Western Canadian Arctic; 2) identifies the utility of SAR for reducing uncertainty associated with these features; and 3) describes methods for sharing SAR maps. Three field seasons (2017/8) were used to engage residents in locally-guided research, where applied outputs were evaluated by participants. We found that SAR data inform and improve sea ice safety, trafficability, and education. Information from technology is desired to complement Inuit Qaujimajatuqangit-based understanding of sea ice features including surface roughness, thin sea ice, early/late season conditions, slush/water on sea ice, sea ice encountered by boats, and ice fractures. Floe edges were not a priority. Sea ice surface roughness is identified as the main condition where benefits to trafficability from SAR-based mapping are regarded as substantial. Classified roughness maps are designed using thresholds representing

domains of sea ice surface roughness (smooth ice/*manniqtuk hiku*; moderately rough ice/*manitutun hiku*; rough ice/*manitpiatuk hiku*; dialect is *Inuinnaqtun*). These maps show excellent agreement with local observations. Overall, SAR maps tailored for on-ice use are beneficial for, and desired by, northern community residents and we recommend that high-resolution products be routinely made available in communities in both soft- and hard-copy formats.

2.3 Introduction

In this study, we explore how information from satellite remote sensing technologies can be used to supplement and improve the sea ice safety and trafficability of local travelers in Arctic communities. Arctic residents have expressed interest in accessing information from synthetic aperture radar (SAR) imagery to complement their understanding of changing sea ice conditions and to plan livelihood activities (Bell et al., 2014; Druckenmiller et al., 2009; Gauthier et al., 2010; Laidler et al., 2011). Many of the traditional indicators used to assess sea ice quality (e.g., winds, moving ice, multi-year ice (MYI), openings such as cracks, leads and ice edges, etc.), can theoretically be studied using SAR images (Laidler et al., 2011). The utility of SAR and techniques such as polarimetry and interferometry have been demonstrated for assessments of trafficability: the ability to safely and efficiently navigate across sea ice environments (Dammann, 2017; Dammann et al., 2018a). SAR has the potential to be used in combination with modern and traditional information sources to create baseline datasets, support safe travel to hunting sites and between communities, and preserve the cultural well-being of residents of Arctic coastal communities who use the sea ice as an extension of the land

(Aporta, 2009; Dammann et al., 2018b; Laidler, 2006, 2007; Laidler et al., 2011; Lindsay et al., 2012; Meier et al., 2014; Nickels et al., 2005).

SAR has been used to assess sea ice conditions and safety relevant to Alaskan and eastern Arctic communities (Eicken et al., 2011; Laidler et al., 2011; Bell et al., 2014; Dammann et al., 2018a, 2018b). The Western Canadian Arctic, and particularly the Canadian Arctic Archipelago, has a unique ice regime where community ice information needs remain undefined (Howell et al., 2009). Sea ice information needs can vary widely, even between communities in close proximity to one another (Fisheries and Oceans Canada, 2012; Ford et al., 2008; Laidler et al., 2008a; Laidler & Elee, 2008; Laidler & Ikummaq, 2008). These dissimilarities make it necessary to determine impediments to sea ice trafficability that Arctic communities face, the ability of SAR to address these impediments, and the spatiotemporal scales at which sea ice information is helpful. This study focuses on 1) defining the sea ice features that influence trafficability, as encountered by the residents of Kugluktuk and Cambridge Bay; 2) identifying the utility of SAR for reducing uncertainty associated with these sea ice features; and 3) describing methods for sharing SAR-based products in ways that are useful to these communities. Section 2.4 describes the implications of community and sea ice changes on sea ice use and introduces cryospheric microwave remote sensing information. The study area is detailed in section 2.5, and research methods are described in section 2.6. Results and discussion are given in section 2.7, followed by concluding statements in Section 2.8. A quantitative assessment of open-access satellite tools for improving community on-ice trafficability and safety related to sea ice surface roughness is found in Part 2 (Chapter 3).

2.4 Background

Climate change has impacted the Arctic more than most other areas of the world (ACIA, 2005; Bush & Lemmen, 2019; Meier et al., 2014; Serreze et al., 2000). Sea ice extent and thickness is decreasing, with the decline accompanied by a substantial loss of older MYI (Comiso & Hall, 2014; Lindsay & Schweiger, 2015; Markus et al., 2009; Meier et al., 2014). First year ice (FYI) now comprises 70% of sea ice in the Arctic basin, compared to 38% in the 1980s (Stroeve et al., 2014). Many of these changes are a result of increased air temperatures (Bekryaev et al., 2010; Overland, 2009), ocean temperatures (Steele et al., 2008), and sea ice export out of the central Arctic during positive Arctic Dipole anomaly phases (Wu et al., 2006). Decreases in albedo, driven by MYI loss, are changing solar heat-related feedback patterns and leading to further warming (Letterly et al., 2018; Perovich et al., 2008). The open water season length is increasing (Markus et al., 2009; Stroeve et al., 2014), leading to changes in processes like ice deformation, fetch, and coastal erosion (Meier et al., 2014). Coastal areas are particularly impacted by climate change. Sea ice found within 50 km of the land has decreased by 25% in the early summer over the Arctic, with the greatest declines in the East Siberian and Chukchi Sea areas (>40%) (Bhatt et al., 2010).

While changes in sea ice have impacts globally through large-scale weather and climate impacts and feedbacks, Arctic residents, industries, and ecosystems are impacted locally. Local climate change impacts include increasingly unpredictable conditions, directly or indirectly related to sea ice (Deemer et al., 2018; Krupnik & Jolly, 2002; Meier et al., 2014; Nickels et al., 2005). Impacts directly or indirectly related to sea ice include increasingly unpredictable conditions, infrastructure and cultural heritage sites

loss, resource accessibility change, and northern community daily activity/cultural shifts (Arctic Monitoring and Assessment Programme, 2011; Laidler, 2007; Laidler et al., 2008b; Meier et al., 2014; Prowse et al., 2009; Stuckenberger, 2010). The consequences of dynamic ice conditions are likely to be unequally distributed between shipping, industry, and community stakeholders (Bell et al., 2014; Dawson et al., 2017; Dowsley et al., 2010; Pizzolato et al., 2014).

Trafficability is a key activity impacted by sea ice features and processes that evolve both seasonally, and inter-annually (Dammann et al., 2018b). Hazards are conditions or events that have the potential to harm people, causing damage that is physical, psychological, possibly including loss of life (Ford et al., 2008). The degree of hazard exposure (risk) associated with trafficability is impacted by environmental conditions (e.g., time of year and ice type), social conditions (e.g., degree of familiarity with the area, reliance on technology, and understanding of climate-related changes), as well as the potential consequences of disaster (Eicken & Mahoney, 2015; Ford et al., 2008; Lépy, 2008). Furthermore, trafficability, hazards, and risks depend on the type of sea ice use. For example, trafficability and safety concerns associated with shipping activities where travelers navigate through ice are different than those encountered by Inuit traveling on ice (Dammann, 2017; Eicken & Mahoney, 2015; Laidler et al., 2008b; Rolph et al., 2018; Stephenson et al., 2011). Trafficability, hazards, and risks are associated with particular sea ice conditions, and as a result they are unevenly distributed in space and time.

As major social changes and natural variability in sea ice conditions are further compounded by climate change, northern communities are increasingly interested in

scientific information designed to improve safety by increasing information and reducing uncertainty (Laidler et al., 2011; Panikkar et al., 2018). Inuit traditional, current, and future knowledge systems (Inuit Qaujimajatuqangit, or IQ) contain extensive information about the sea ice environment, obtained from personal experiences as well as knowledge passed through generations. However, there is a gap in knowledge transfer that has resulted in younger generations possessing less IQ than elders (Ford, 2005; Ford et al., 2006b; Laidler, 2007; Laidler et al., 2011). With changes including the development of settled communities, wage economies, a variety of lifestyle options, and the adoption of technology, the use of sea ice is different and more limited than in the past (Brinton, 2018; Ford et al., 2006b, 2006a; Heyes, 2011; Laidler et al., 2011; Panikkar et al., 2018). Consequently, younger people are often more assisted by, and reliant on, technology that complements their IQ (Laidler, 2007), although IQ remains imperative for staying safe should technology fail (Clark et al., 2016a; Ford et al., 2006b; Laidler et al., 2011; Panikkar et al., 2018).

Furthermore, the increase in unpredictable and variable weather that makes the conditions in sea ice environments more difficult to predict using IQ (Druckenmiller et al., 2009; Ford et al., 2006a, 2008; Ford & Smit, 2004; Krupnik & Jolly, 2002; Laidler, 2007; Nickels et al., 2005; NTI, 2001; Rolph et al., 2018; Stammler-Gossmann, 2010). Search and rescue events in Nunavut more than doubled between 2006 and 2015 due to conditions like environmental exposure, loss of IQ and changes in culture, economic stress, more powerful and complicated equipment, despite limited supplies for search and rescue missions (Clark et al., 2016a, 2016b; Nunavut Emergency Management, 2017). The ability to identify key sea ice features and seasonal development is critical for

reducing travel time, fuel cost, equipment deterioration, and risk, while improving safety (Ford et al., 2008; Laidler et al., 2008b, 2011).

Microwave remote sensing is used to observe sea ice independently of sunlight and cloud cover, conditions which severely limit optical sensors (Bertoia et al., 1998; Teleti & Luis, 2013). SARs are active microwave systems capable of providing image data at spatial resolutions of ~1-1000 m and swath widths of ~30-500 km. Various SAR frequencies, transmit/receive polarizations, modes of operation (resolutions and swath widths), and incidence angles are used to reveal parameters like sea ice extent, type, deformation, drift, melt state, and surface flooding (Chan & Koo, 2008; Dierking, 2013; Ersahin et al., 2014; Scharien et al., 2014; Teleti & Luis, 2013). Accessibility to SAR data is increasing, with the European Space Agency's Sentinel-1 constellation of two polar-orbiting satellites offering frequent and open-access data, and the recent and expected launches of more SAR satellites in the near future (e.g., RADARSAT Constellation Mission in June 2019).

2.5 Study area

The marine areas used by Kugluktuk (Qurluktuk) and Cambridge Bay (Iqaluktuuttiaq) residents are situated in the Kitikmeot administrative region of Nunavut in the Canadian Western Arctic (Figure 2.1). The marine portion of the Kitikmeot includes Larsen Sound, Queen Maud Gulf, Coronation Gulf, and Bathurst Inlet. Kugluktuk, the westernmost community in Nunavut, is located on the north coast of mainland Canada next to Coronation Gulf and is on the western edge of the Coppermine River mouth. The Hamlet of Kugluktuk has 1491 residents on the 2016 census (Statistics Canada, 2017b). Cambridge Bay is located on the southeast coast of Victoria Island,

adjacent to Dease Strait. The Hamlet of Cambridge Bay, with a 2016 population of 1766 residents (Statistics Canada, 2017a), is a growing transportation and administrative centre and a regular stop-over for vessels traveling the Northwest Passage (Calihoo & Romaine, 2010). The majority of people in Kugluktuk and Cambridge Bay are Inuk, at 1340 and 1430 people respectively, and the dominant Inuktitut dialect of both communities is Inuinnaqtun (Statistics Canada, 2017a, 2017b).

Like most Arctic communities, residents in both Kugluktuk and Cambridge Bay are highly dependent on sea ice for travel and subsistence (Aporta, 2009; Calihoo & Romaine, 2010; Johnson & Arnold, 2010; Panikkar et al., 2018). Hunters and trappers supply their families and networks with traditional food, and professional guides accompany tourists and researchers on sea ice. Both communities have cell phone service, and many residents use snowmobiles and other technological devices or products like weather reports, InReach, and GPS (Panikkar et al., 2018). Additionally, due to the presence of the Canadian High Arctic Research Station (CHARS), relationships between scientists and local residents in the Kitikmeot are increasingly encouraged, and fine-scale data for the development and ground-truthing of new remote sensing techniques are available.

Annual sea ice is a dominant feature of the Kitikmeot marine environment for more than nine months of the year. The average date of freeze-up between 1982-2010 was 22 October for both communities, while break-up was 2 July in Kugluktuk and 16 July in Cambridge Bay, with an open water season in-between (Canadian Ice Service, 2011). Landfast FYI dominates Coronation Gulf, Dease Strait, and Dolphin & Union Strait, and MYI is usually present in M’Clintock Channel and, to a lesser extent, Queen

Maud Gulf (Canadian Ice Service, 2011). While floe edges are adjacent and economically important to many Arctic communities, near Kugluktuk and Cambridge Bay the sea ice approaches 100% concentration.

Figure 2.1. Map showing the locations of Cambridge Bay and Kugluktuk, distinguished by red dots, in Nunavut's Kitikmeot Region Subdivision (red dashed lines; from the 2017 Canadian census). Other populated places are shown as black dots.

2.6 Methods

2.6.1 Research approach and community data

Traditional ways of knowing were connected with science to a) identify information needs regarding improved sea ice trafficability, and b) evaluate the effectiveness of SAR for reducing uncertainty associated with these needs. This study was built upon established collaborative relationships with northern residents and organisations, connections with southern organizations, and existing literature.

Residents of Kugluktuk and Cambridge Bay were engaged formally and informally to create a locally-guided research project with an applied output product, as recommended by Ford et al. (2018), Grimwood et al. (2012) and Tondu et al. (2014). Engagement occurred during three community visits: spring/fall 2017, and spring 2018; it was sustained remotely via phone, email, and social media. Three public meetings were held: two in Kugluktuk and one in Cambridge Bay. Informational evening sessions, two in each community at local grocery stores, extended discussions to those interested and informed the community of project goals. Hamlets, Hunters and Trappers Organizations, and the Kitikmeot Inuit Association were also made aware of the research and given the opportunity to provide guidance on research design and local protocols. Informal engagement (e.g., attending local events, sharing conversations over tea, etc.) was also a very successful tool for developing relationships and gaining local insights.

Semi-structured interviews on the topics of sea ice trafficability and SAR image evaluation were conducted during all field visits (Table A.1). Participant recruitment focused on residents aged 14+ who use sea ice for travel and subsistence. Fewer interviews were held with people who no longer travel or have less experience but were

interested in participating and knowledgeable about the environment. All interviews involved viewing prototype SAR image-based maps created specifically for the interview process (see section 2.6.2) and included an optional participatory mapping component. SAR data are from the Sentinel-1 mission, which provides imagery in the C-band frequency commonly used for ice charting purposes (ESA, 2018b). Potential interview participants were suggested by engaged organizations, other participants (snowball sampling), or directly encountered. Interview and workshop compositions were flexible, with 1-7 interviewees. Some participants were present at more than one session. In total, 47 interviewees participated formally over 37 sessions that included 7 workshops (>2 interviewees), with 20 people participating formally on more than one occasion. Sea ice excursions in both spring and fall were conducted to allow residents to identify and discuss specific areas or features related to sea ice, travel and trafficability. Three formal on-ice interviews were conducted.

Interview transcripts were analysed using thematic coding in NVivo Pro 11. Codes were drawn from thematic information patterns encountered in interviews and attached to relevant interview text (e.g., coded “MYI” and “rough ice”), then aggregated or separated as required during analysis and assembled into themes (e.g., sea ice surface roughness). Naturally, there is considerable overlap among the themes identified, as sea ice information was discussed organically and without categorization by participants.

2.6.2 Greyscale and classified SAR maps

Prototype greyscale SAR-based maps of winter and shoulder-season sea ice conditions were printed on A2-sized paper to use as engagement tools and visual demonstrations of the capabilities of SAR (Figure 2.2). Hard copies were left in the

communities in the spring, and soft copies were distributed in winters 2017-2019 by email and social media. These maps contained processed Sentinel-1 images (see Appendix A section A.1). Winter period images were the main focus because the ice is landfast and thick. Shoulder season images served as discussion points for seasonal trafficability hazards.

Initial interviews revealed that delineating areas based on sea ice roughness degree using SAR would benefit both communities. Classified roughness maps (e.g., Figure 2.2b) were created by thresholding winter backscatter values to delineate three classes representing “smooth”, “moderately rough”, and “rough” sea ice roughness domains. Thresholds were initially determined by manual selection, as it was anticipated that refinement and validation based on community input and quantitative analyses would be necessary (see Chapter 3). Domains were colour-coded into classes representing sea ice snowmobile travel that is 1) easy (green; < -20 dB), 2) slow but passable with caution (orange; >= -20 and <= -18 dB), and 3) impassable or takes considerable effort (red; > -18 dB). In the local Inuinnaqtun language these categories are *manniqtuk hiku* (smooth ice), *manitutun hiku* (moderately rough ice), and *manitpiatuk hiku* (rough ice). The prevalence of the English words “smooth,” “sort of rough,” and “rough,” in interviews along with the matching Inuinnaqtun words further indicate that the SAR categories are of local importance. Classified maps were used to generate specific discussion points and improvement suggestions for subsequent field seasons. Map colours were changed based on discussion with northern residents and the CIS, to green, yellow, and purple respectively, to convey less alarming navigation suggestions through more pleasing colours (see section 2.7.4; Figure 2.4).

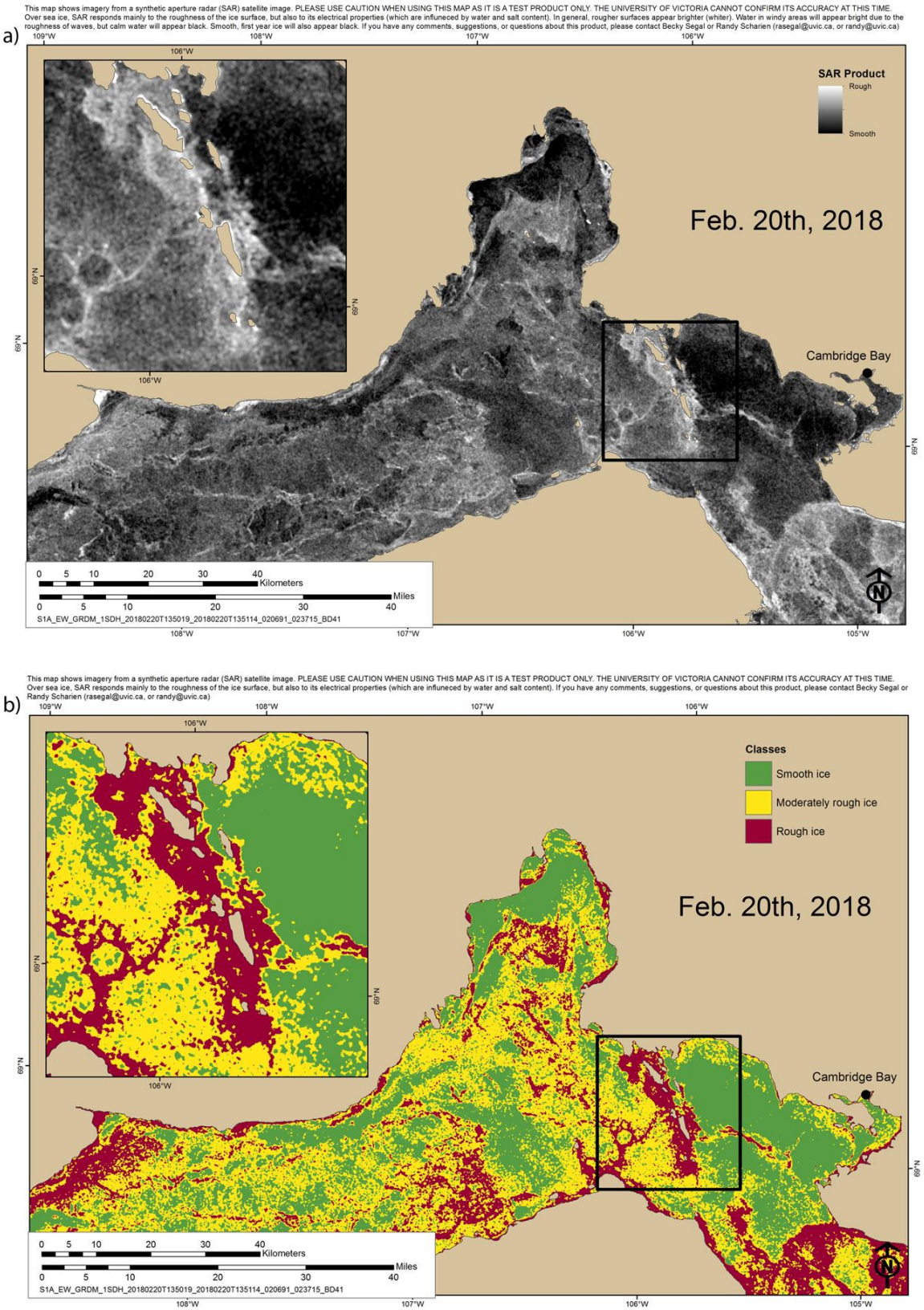

Figure 2.2. Sample SAR-based maps. a) is greyscale, and b) is classified by roughness level.

2.7 Results and Discussion

2.7.1 Changes impacting sea ice use

2.7.1.1 Community changes

Social changes and the adoption of modern technologies were highlighted during interviews as two ways that travel and safety are changing significantly. People have varied degrees of competence with the skills necessary for sea ice travel, and most spend less time on the ice than previous generations. Participants of all ages from both communities cited an IQ gap between young people and elders, noting that many search and rescue events are caused by people getting lost or being inadequately prepared to travel safely. Many people work jobs or split their time between multiple interests, reducing the time available for sea ice use. Purchasing and maintaining equipment like snowmobiles necessitates participation in the modern economy. Furthermore, increases in population means that it is more difficult to track who is in town, and results in increased nearby hunting pressure. High hunting pressure creates a need to travel longer distances to find animals, over an increasingly uncertain sea ice environment. However, when animals do come near town, less experienced (opportunistic) hunters may encounter hazards for which they are not equipped. Another cultural change is also occurring: some women are hunting, which is traditionally a male task, and becoming sea ice guides.

The prevalence of technology and its rapid change was emphasised. Participants primarily discuss the use of snowmobiles, boats, all-terrain vehicles, GPS, InReach, cell phones, weather information, SAR-based maps, radio, and social media technologies: these are used before, during, and after travel. Technologies change the way travel is

conducted and have mixed impacts on travel safety. For example, snowmobiles, unlike dog teams, can break down and leave travelers stranded; however, they allow for faster travel while carrying more supplies and do not require looking after a dog team. Some people blend old traditions with new by bringing dogs on snowmobiles to help with hunting and guarding. A woman in Kugluktuk described technology and IQ: many people use GPS, weather reports, and traditional knowledge and "combine it all together and … have the best of both worlds. I think that's what people should be learning." Many participants pointed out the ability of community members to adapt to widespread technological change and wanted access to, and the choice of, using modern technology.

2.7.1.2 Environmental changes

"I think it's changing. I think it used to be, like that people would say, 'oh, it's thick, it's usually frozen by this time, let's go.' But, now that things are changing, people are realizing that, like, 'oh, we're not going to go out.'" – resident of Kugluktuk

Interview data provide information about sea ice conditions, related community concerns, as well as the role of technologies in adaptation. The ice conditions relevant to trafficability include the features and seasonal regimes, labelled a – j, arising from thematic analysis and participant terminology or structure:

a) smooth FYI: seasonal sea ice that grows in calm conditions.

b) moderately rough and rough FYI: the sea ice surface contains slabs of broken ice embedded, typically ~15-60 cm thick and <1 to 6+ m high; may also contain pressure ridges. Ice slab density and size varies. May be thicker (piled up) or thinner (insulated by snow) than smooth sea ice.

c) MYI: smooth and bumpy (hummocky) surface, often very thick, with low salt content. If next to FYI floes, there can be a “skateboard style” drop between floes that is often hidden by snow cover.

d) snow on sea ice: precipitation deposition; wind causes builds up behind ice pieces and makes long snowdrifts.

e) thin ice: ice that will not hold the weight of a person or snowmobile, related to season or fast-moving water (ocean current or river outflow) that thins ice from the bottom.

f) early ice: seasonal regime associated with freeze-up that begins when ice becomes safe for travel and ends when winter conditions persist. Sea ice is thin and unstable. Its formation influences sea ice conditions throughout the ice season.

g) late ice: seasonal regime associated with break-up that begins when ice deteriorates by rotting in strong current/near-shore areas and accumulates sea ice fractures and surface slush/water. Ice is broken by winds and tides, until ice chunks float freely; it ends when marine boat travel becomes possible.

h) slush/water on ice: ice-coloured/light blue ponds contain surface water, but dark blue, muddy looking, or grey-black ponds indicate melt holes. Slush, water, or refrozen melt ponds may disguise ice thickness.

i) ice encountered by boats: boating begins when small local boats are launched in the ocean in spring and ends when sea ice blocks boat travel. Boaters travel through, over, and on sea ice, pulling boats with snowmobiles.

j) ice fractures: includes cracks, leads, and pressure ridges. Cracks are narrow, typically long fissures through the sea ice. Pressure ridges are either fractures with open or

snow-covered water bordered by piled up sea ice, ~1.2 m to 4.5 m in height (type 1), or ridges that form when sea ice releases pressure and buckles upward, which can be very tall (type 2). Leads are wide splits through the sea ice, generally not crossable. Fractures appear deceptively narrow when ice edges are thin or snow-covered. They can shift and open/close with the tide, especially in spring.

The occurrence of ice conditions a – j, as well as their associated usage and changes, are described in Tables 2.1 and 2.2 respectively. A myriad of changes in these sea ice features were noted during interviews, including observations of rougher and thinner sea ice, warmer ocean temperatures, different areas or timings of thin sea ice and open water, changed snowfall patterns, longer open water seasons (later freeze-up and earlier break-up), more slush, and possible movement of ice fractures. Both Kugluktuk and Cambridge Bay interviewees reported that environmental changes are creating increased uncertainty about sea ice conditions and trafficability.

Table 2.1. Major sea ice features and their occurrence in the context of hazardous ice conditions, as described by residents of Kugluktuk and Cambridge Bay, Nunavut.

	Feature	Occurrence
a.	FYI (smooth)	Develops in low wind and weak current areas during freeze-up, and in areas that freeze after the surrounding ice (e.g., fall leads).
b.	FYI (moderately rough/rough)	Develops in high wind (~80-100 kmph)/strong current areas during freeze-up. Slabs catch wind and result in more force on the ice. Often found near the shore. Slabs may melt and decrease roughness (typically in late spring but may also occur in fall).
c.	MYI	Uncommon in Coronation Gulf but encountered further north.
d.	Snow on ice	First snowstorm after freeze-up fills depressions. Snow accumulates and may cover rough sea ice. Winter/spring storms create hard-packed snow mounds (snow roughness). Becomes soft during spring melt.
e.	Thin ice	Areas either persist through winter or are seasonal. Often in fast-moving water and similar locations across years (e.g., between islands). Ice roads become thin early.
f.	Early season ice	Early ice forms adjacent to the communities due to fresh water and land influences. Areas north of Coronation Gulf and areas with strong current freeze later.
g.	Late season ice	Timing more variable than freeze-up. Coppermine River break-up speeds sea ice melt by flowing on the ice (Kugluktuk). Snow delays ice melt through insulation.
h.	Slush/water on ice	Widespread during fall/spring; only in areas of moving water in winter. Accumulates near the coastline in spring, especially if heavy snow. Melt ponds flood the sea ice in late spring, and subsequently drain leaving dry craters.
i.	Ice encountered by boats	Boating begins when cracks near town turn into leads wide enough (9-12 m from shore). Usually in June when the Coppermine River breaks (Kugluktuk), or early August (Cambridge Bay). Ends with freeze-up.
j.	Ice fractures	Strong current and near-shore areas, often in similar locations across years. Type 2 pressure ridges are usually far from land. Pressure ridges form in late fall/early winter and open in spring (becoming cracks/leads). Most cracks appear and widen in spring. Leads usually form from cracks/pressure ridges in late spring.

Table 2.2. Major sea ice feature use and change, as described by residents of Kugluktuk and Cambridge Bay, Nunavut. Features a – j are described in the text and Table 2.1.

ID	Usage	Changes and Consequences
a	Facilitates rapid snowmobile travel (~50-110 kmph), good fuel efficiency, light wear on equipment.	Becoming rougher in recent years.
b	Slow and difficult travel (~5-30 kmph; zig-zag and shorten tow lines); hard on equipment; lower fuel efficiency; hard to navigate in dark/bad weather. Polar bear range area. Good for emergency shelters. Less predictable travel; increased risk of accidents and breakdowns.	May be rougher in recent years. Exacerbates risk of accidents or breakdowns, consumes time, and increases costs. Delayed freeze-up may cause formation to occur during windier time of year.
c	Smoother than rough FYI but rougher than smooth FYI. Polar bear range area. Good for drinking water.	Not discussed; presence near town too infrequent.
d	Modifies ice surface to smoother/rougher. Insulates sea ice and controls ice thickness. Fall snow makes travel easier. Snow accumulation may allow rough ice to be trafficable. Rough snow and soft snow both decrease trafficability.	Possible changes due to winter storm frequencies.
e	Risk of falling through the sea ice; cause travelers to hug shorelines.	Thinning connected to warmer ocean and changing snowfall patterns. New/larger open water areas now found; e.g., Cape Krusenstern area.
f	Use begins when sea ice is 5-15 cm thick (risk-tolerant and experienced travelers near communities) or ~0.6-0.9 m thick (further from land). On-ice travel is preferable to terrestrial travel due to relative lack of snow cover.	Delayed/prolonged: historical use in September/ October now November/ December. Observations of under-ice slush not developing due to warmer water (early season ice now needs to be thicker to have the same strength, delaying travel).
g	Use ends when cracks or leads become too dangerous (June or July). Most stop use when ice is difficult to access from shore but still safe.	Timing is naturally variable but may be ~1 month earlier and more rapid.
h	Melt holes and deep melt ponds indicate quickly thinning sea ice, need to be avoided and deter many people from travel. Snowmobiles can get stuck in slush/water, break through re-frozen melt pond ice lids and skid, or stop running if the belt gets wet. Sleds may spin due to loss of friction over melt ponds. Travel in cool evenings may be easier when soft slush/snow is firmer.	Coastline slush more of an issue in recent years.
i	Must plan boat travel to avoid being trapped inside/outside the community by ice. Longer boating season beneficial for those with boats, but not for on-ice activities. Must be aware of shifting ice (particularly MYI) causing waves dangerous to small vessels.	Ice-free season is ~1 month longer than in the past (both communities). People doing more boating trips, boating earlier in spring and later in fall (mid-October in Cambridge Bay, mid-November in Kugluktuk).
j	Used as landmarks to identify locations. Regularly crossed when narrow, otherwise crossed using a natural sea ice bridge (transcurrent-style shift that leaves a bridge-like structure across the crack/fault), making a sea ice bridge (a last resort), or by jumping a snowmobile (water skipping). Location for ocean hunting animals. Possible to fall through fractures into open water (fairly common); precautionary flotation suits in spring may be used. Can be difficult to see in darkness or poor weather.	Most did not notice changes. New cracks and zig-zagging cracks (used to be straight) observed. Cracks near Locker Point have moved north over the past ~30 years by a few hundred metres, measured by a Kugluktuk hunter using GPS. Number of pressure ridges may have increased over the past 10-15 years (Kugluktuk). Pressure ridges used to be straight from Long Point to the mainland; recently went sideways.

2.7.2 Evaluation of SAR-based maps

"This [SAR map] is fantastic; this is incredible. And this very much is the reality. Yes, it's very much indicative of what you see" – resident of Cambridge Bay

2.7.2.1 Users and experience

SAR-based maps are considered useful by residents who currently use the sea ice for hunting, trapping, camping, fishing, guiding, or other projects because maps reveal sea ice surface conditions in unknown areas. As SAR images show sea ice information relevant to IQ, many participants think they would be a beneficial educational tool for schools and people who cannot observe the sea ice conditions directly. Participants in both communities noted that the Canadian Rangers (sub-component of the Canadian Armed Forces), Coast Guard, and Search and Rescue organisations would benefit from accessible SAR-based products, some of whom had already received RADARSAT-2 SAR images and training for navigation. Most people had no prior experience with SAR imagery, but there were more participants with training in Cambridge Bay than Kugluktuk. Prior to this study, RADARSAT-2 images, which are restricted rather than open access and expensive, were only made available by the Canadian Ice Service once or twice a year in each community, specifically for planned excursions. Only one participant in each community regularly uses Canadian Ice Service sea ice charts, although they both orally disseminate this information with a limited number of others.

Most participants felt that the demonstrated SAR-based maps were easy to understand once they knew the base image capture date, but many people desired access to SAR image training. Others feel that knowledge sharing by word-of-mouth within the community would be sufficient. Sample SAR images paired with annotations and

photographs are recommended as a way of providing context to make the imagery understandable and should be considered in the future.

2.7.2.2 Features

Participants want SAR- or technology-based information about all the sea ice conditions from Table 2.2 that impact safety and trafficability. A comparison between traditional practices of information gathering and the information desired for safe travel is detailed in Table 2.3. The evaluation of SAR-based maps and realised or perceived benefits (where applicable) are given in Table 2.4. Information needs are not equally important in their impact on safety or trafficability because some features' impacts are more easily avoided or mitigated than others. Sea ice surface roughness was identified as the main ice condition where benefits to trafficability from SAR-based mapping are regarded as substantial. Rough sea ice makes travel slow, difficult, hazardous, and expensive.

Thin sea ice areas were more difficult to recognise using SAR imagery but were still a high priority. Consequently, we developed a supplemental dataset showing areas identified by local participants as typically having thin ice (or open water). These data will be added to maps in the future (Figure 2.3).

Table 2.3. The traditional or current practices used to navigate sea ice conditions a - j, and the information ideally desired by travelers. Features a – j are described in Table 2.1 and the text.

ID	Traditional/current practices	Information desired
a-d	Look for high ground to see where the ice is smooth/rough (weather/season-dependent). Try to travel as straight as possible until rough ice is encountered. Follow an existing trail (trails may be used throughout the sea ice season by many people).	Locations of each ice/surface type, particularly for i) high-use areas[2], ii) variable areas[3], and iii) distant/less frequently used areas.
e	Recognise thin ice due to the snow profile (subtle dent in the snow) and/or knowledge of recent temperature/weather conditions.	Locations and timing of thin ice (or open water). Sea ice thickness year-round.
f	Test for ice thickness. Look for open water.	Locations of sea ice/open water. Sea ice thickness/stage of development. Sea ice development over the freeze-up period.
g	Look at ice colour. Avoid areas known to melt early. Check to make sure that people traveling or at camps make it back to town safely (Kugluktuk).	Locations of sea ice/open water, especially as the ice cover breaks and is an impediment to boating. On-ice information needs change to boat and land needs.
h	Reduce/avoid travel on the ice while melt ponds are present. Travel next to cracks as adjacent areas are dryer.	Locations of extensive slush/water on ice
i	Check weather using online forecast[4], VFR station (if available), marine forecast. Talk to people at outpost camps about conditions (though fewer people use camps than in the past).	Ice location, movement, and type, from melt onset to 90% ice-free ocean (spring) and from ice onset to complete freeze-up (fall). Weather conditions. Icebreaker ship presence/routes (spring and fall)
j	Mark fracture location using GPS and/or wood sticks. Share information of where cracks and pressure ridges are traversable.	Locations of ice fractures, especially in areas that have many[5].

2 E.g., between Victoria Island and the mainland
3 E.g., Dolphin & Union Strait, Hadley Bay, M'Clintock Channel
4 E.g., WindyTV forecast (www.windy.com), Norwegian-based weather site (www.yr.no), Environment Canada weather (https://weather.gc.ca), local weather station (linked to https://people.ucalgary.ca/~belse/Brent_Else/WX.html)
5 E.g., leads in Anderson Bay

Table 2.4. Evaluation of SAR-based maps in the context of their ability to provide safety and trafficability information about sea ice conditions a - j, and the potential benefits of the information provided. Features a – j are described in Table 2.1 and the text. Information originates from interview data unless italicized.

ID	Evaluation of SAR	Benefits
a-b	91% of participants want winter SAR-based maps due to accurate roughness observations. Existing travel routes mostly avoided rough areas. Identify smooth ice areas and likely impassable areas. Winter greyscale maps have easily interpretable tones, are preferred experienced SAR users. Classified map categories correspond to local Inuinnaqtun terminology. Classes may show more detail about roughness than greyscale maps due to increased colour contrast and were preferred by people less experienced with SAR. Calm open water may be confused with smooth FYI.	Help plan safe/efficient routes. Roughness location information for less known areas. Accurately estimate and/or reduce[6] trip durations (e.g., important when traveling with small children). Information for search and rescue/ranger patrol operations. Good educational resources.
c	Identify areas of MYI on greyscale maps: bright tone and rounded floe texture. Regions with freshened ice (MYI/river outflow) are "rough" (misclassified).	Identification helps plan safe and efficient routes. May be a destination.
d	Snow detection and its contributions to surface roughness are not shown *and not detectable using C-band SAR.*	Would be useful to understand the snow contribution to surface roughness.
e	Want thin ice areas marked. Fine-scale data may be more helpful. *Thickness is difficult to assess but can be inferred by ice type (coarse-scale).*	Would be educational resources. Help with SAR interpretation. Detection of new areas could help prevent accidents.
f	Greyscale SAR understood by experienced hunters. Useful information about sea ice cover/evolution. Observe wind direction, high current areas (influence on ice), locations where ice accumulates, ice qualities, areas of open water. More difficult to read than winter images, but (often more) helpful as conditions are unknown. Usually more important than spring images. Rapid sea ice changes mean images may be outdated but most people would still check them. May be able to extrapolate subsequent ice conditions using knowledge of weather/environment.	Assess where/when to travel. Access to sea ice evolution information before/as ice becomes trafficable. Spatial information about sea ice/open water/wind.
g	As in f, except conditions more known from travel throughout the season. SAR interpreted for the appropriate transportation mode.	Assess when/where to travel. Spatial information about sea ice/open water/wind during a highly dynamic period.
h	Interest in SAR/other imagery showing melt pond distributions. Products brought not fine scale enough to provide travel information. *Surface fraction covered by melt ponds can be detected (and predicted using winter imagery).* Slush detection not possible directly through SAR-based maps. *Polarimetric analysis untested but may prove useful: HH/VV ratio data is linked to*	Plan routes avoiding on-ice water/slush.

[6] Save ~5 hours between Jenny Lind Island/Cambridge Bay (~20 km) in 2017.
+

	moisture/dielectric permittivity.	
i	Sea ice/open water detection. Shows ice congestion along travel routes, whether ice is present that may move and block travel. Detect when areas become boat accessible[7]. Ship detection possible.	Assess when/where possible routes avoid sea ice. Prepare for larger ocean swells when sea ice is absent. Icebreaker ship traffic: shows whether ice is cleared for boating (spring) or broken and dangerous for snowmobiles (fall).
j	Nearly all are too small to be seen on Sentinel-1 GRD/RADARSAT-2 ScanSAR Wide images. Pressure ridges and leads sometimes visible. 3-band colour composite Sentinel-1 imagery may identify small-scale pressure ridges better than greyscale. *Detection dependent on resolution: finer-scale products/higher-frequency data helpful.*	Useful for safety/navigation. Locations information especially helpful for people who still need to learn approximate ice fracture locations. Fracture detection could help prevent accidents.

[7] E.g., for people who snowmobile to camps and boat back to Kugluktuk, or leave Cambridge Bay and boat to the mainland.

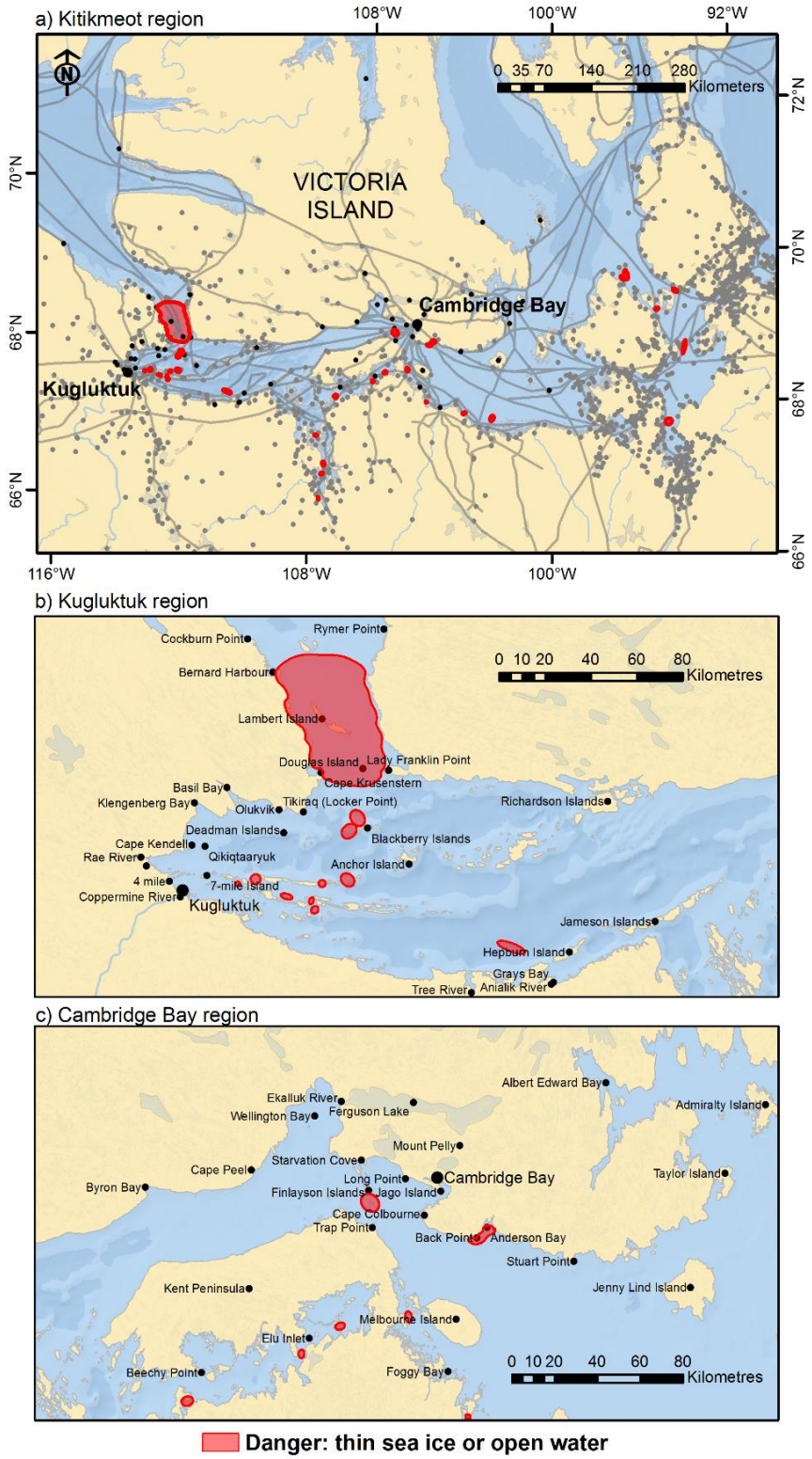

Figure 2.3. Maps showing: a-c) the locations of thin sea ice or open water areas identified by local experts as dangerous seasonally or year-round. Maps show important places

mentioned in interviews (black dots) and dangerous areas across a) the Kitikmeot region, b) the Kugluktuk region, and c) the Cambridge Bay region. This is not a comprehensive list of dangerous areas: some thin sea ice areas are missing near Lewes Island, dangerous areas closer to other Kitikmeot communities would be better known by the residents of those communities, and other areas may appear with a changing climate. a) Main travel routes (grey lines) and important places (grey dots) identified by the Inuit Heritage Trust (http://ihti.ca/eng/iht-proj-plac.html).

2.7.2.3 Extent, scale and resolution

In Kugluktuk, most travel is within Coronation Gulf, but Amundsen Gulf was also identified as an area of interest. The SAR-based maps provided to Cambridge Bay contain the main travel routes, including a route to the mainland via the more seasonally dangerous Finlayson Islands area. Some people travel long distances: from Kugluktuk to Cambridge Bay and beyond the NWT-Nunavut border, or from Cambridge Bay to M'Clintock Channel, Hadley Bay, Bathurst Inlet, King William Island, and Kugluktuk.

The scale and spatial resolution of the SAR-based maps brought to the communities were deemed satisfactory and more helpful than other online products like the CIS weekly charts, particularly for roughness information. People expressed significant interest in information that would only be available on higher-resolution imagery. Agencies providing sea ice information to communities should consider enabling access to higher-resolution imagery, either free or otherwise affordable, as it is within current technological capabilities.

Northerners want access to more frequent SAR images throughout the entire sea ice season. However, sea ice conditions are quite stable once the ice is thick and landfast. Accordingly, it is more important to have frequent shoulder season images, although

timing needs vary by location. For example, in M'Clintock Channel and Victoria Strait region, the sea ice is known to continue to move until mid-January, well after sea ice near Cambridge Bay and Kugluktuk has become landfast. Ideally, SAR-based maps would show current sea ice conditions during freeze-up and break-up, but the 3-4 day revisit frequency of Sentinel-1 means that input images may be several days outdated (ESA, 2018a). Outdated images are not obsolete: they are still understood in the context of recent weather conditions and become part of an image series that shows ice evolution. For example, rapid changes between images may indicate more hazardous conditions.

Both communities would like historical and future imagery to be compiled over time to see how sea ice evolves annually (especially over the freeze-up period), and to identify patterns and discrepancies in yearly sea ice development and roughness.

2.7.2.4 Access

Participants desire SAR-based maps accessible in printed and online formats, as they expect them to be checked like weather reports before excursions. Preferred formats include large print, take-home printouts, books containing sequential images, local television coverage, or online images. Printed maps would be most impactful if kept up-to-date and located centrally (e.g., HTO, Wildlife Office, Library, etc.) and are important for people without internet access. Most participants want maps to take out on the ice, or offline versions on mobile devices. As the internet makes downloading large files problematic, online maps must be available on low bandwidth platforms that are preferably user-friendly and interactive (see section 2.7.4). Many people suggested posting maps on Facebook, as it is a widely-used method of communication; this was done and well received in fall 2018 and winter/spring 2019. Some participants in

Cambridge Bay suggested making the images available on a government website or partnered with existing weather information.

2.7.2.5 Other technology and applications

Overall, there was an overwhelmingly positive response to the SAR-based map technology and a desire to understand and have access to other technologies that can supplement IQ. There is local interest in applying SAR or other technologies to see land and larger lake conditions. Desired lake data include state (ice/water), thickness, and roughness.

Optical imagery was also desired by sea ice travelers, because colour tone can reveal similar conditions as traditional techniques of observing ice colour (e.g., identify thick FYI vs. grey ice). Optical images are also able to show ice-water colour contrasts: Sentinel-2 images brought to the communities as context for the SAR-based maps were well-received because they showed areas that melted early in spring. Several people in Kugluktuk already use coarse optical satellite imagery from online platforms like NASA Worldview to see open water areas and infer sea ice thickness from colour. Furthermore, it may be possible to derive snow surface roughness using multi-angle optical data (Chapter 3).

Sea ice thickness data is desired by sea ice users because it is highly important for safe navigation; interest is compounded due to changes in break-up/freeze-up timing patterns (areas are thin at times of year that in the past would be frozen) as well as the appearance of new thin sea ice areas. Sea ice thickness information would also assist northern residents and scientists by providing contextual information for SAR image interpretation. Ice profilers can measure ice thickness using either electromagnetic

induction (electric conductivity), or ground-penetrating radars (also known as radio echo sounding, which calculates the return time of an electromagnetic pulse reflecting from the sea ice bottom surface (Dammann et al., 2018a; Haas and Druckenmiller, 2010). Several participants in Cambridge Bay noted that ice profilers towed on a sled over the sea ice would be valuable for scientific or industrial projects that require towing equipment heavier than snowmobiles (Druckenmiller et al., 2013). Mass-balance buoys frozen in the sea ice can also be used to provide ice thickness information (Druckenmiller et al., 2013; Richter-Menge et al., 2006). However, Kugluktuk residents are uncertain whether mass-balance buoys would provide helpful information, because thickness varies greatly with the currents; despite this limitation, people in both communities are interested in accessing ice profiler and mass-balance buoy thickness sensors.

2.7.3 Comparison to other trafficability studies

2.7.3.1 Kugluktuk and Cambridge Bay

A study about sea ice and weather in Kugluktuk and Cambridge Bay was conducted by Panikkar et al. (2018), where participants noted similar trafficability concerns and changes. Like this study, they found that a) IQ is not being transferred to younger generations, leading to unsafe travel by inexperienced people, b) technology is helpful and largely desirable but should be used with caution, c) information about sea ice roughness and weather conditions is desired, and d) people generally know the locations and timings of dangerous thin ice. Some people, mostly from Kugluktuk, also discussed the potentially prohibitive expenses associated with travel, particularly in rough ice areas. Panikkar et al. (2018) also recorded observations of environmental changes, including later freeze-up and (possibly) earlier break-up; probable changes in storms, snowfall, and

prevailing winds, and consequently snowdrift formation; new patterns in pressure ridge and lead locations; and increased underwater sediment deposits. These separately obtained conclusions indicate that there are strong and consistent observations of change and information desires in Kugluktuk and Cambridge Bay.

2.7.3.2 Sea ice roughness

Numerous studies mention sea ice roughness as a condition impacting sea ice travel and/or as an information need (Chapter 3; Aporta, 2004; Bell et al., 2014; Dammann et al., 2018b; Druckenmiller et al., 2013; Laidler et al., 2011; Panikkar et al., 2018). Both Dammann et al. (2018b), and Druckenmiller et al. (2013) found that roughness at scales of ~0.1 – 10 m is important for trafficability. Dammann et al. suggest that ice roughness will increase in the Arctic because thin ice is moving at increasing speeds; experiencing more strain, fracturing, and storms; and forming later than normal, hence during the storm season. Trends towards rougher sea ice are also observed by respondents in both our study communities. Consequently, data about sea ice trafficability may prove increasingly valuable. Dammann et al. (2018b) has had success creating a trafficability index using unmanned aircraft system data in conjunction with X- and L-band SAR with advanced interferometry and polarimetry techniques. While rigorous and high quality for the intended study area, the data are costly to obtain and require complex processing.

2.7.3.3 Floe edges

Unlike many other communities, knowledge of floe edge positions is not very important to Kugluktuk and Cambridge Bay residents. Floe edges are high priority

information needs in areas where there is an ice edge that can fracture unexpectedly (Dammann, 2017; Dammann et al., 2018a, 2019; Deemer et al., 2018; Kim et al., 2015; Laidler et al., 2011). There is currently no floe edge near Kugluktuk or Cambridge Bay, though a few participants proposed that floe edges may emerge due to climate change. Several participants recognised that their landfast ice is different and more predictable than in the eastern Canadian Arctic; the sea ice will not break off and begin moving in winter. Some people in Kugluktuk noted that currently there is no reason (e.g., whale presence) to exert the energy to travel the distance to the floe edge. One participant discussed a floe edge feature north of Kugluktuk, from Clifton Point across Dolphin and Union Strait to Ulukhaktok (see Figure 2.1), an area that is a destination for polar bear hunts.

2.7.3.4 Sea ice trail access

Consistent with this study, Ford et al. (2019) found that access to sea ice trails in Inuit Nunangat is decreasing in studied communities based on changing ice concentration, later freeze-up, earlier break-up, wind, visibility, ice thickness, precipitation and temperature, and traveler experience. They found that ice trail access decreased by ~2 days of from 1985-2016 due to environmental changes, which is lower than the approximations of one month decreased access observed by our participants. Like Ford et al. (2019), we observed that the inability to tolerate travel risks significantly impacts modern trail access: an experienced traveler with high risk tolerance has considerably more access to ice trails than a traveler with low-risk tolerance. Education, training, and supplementary technological tools used for navigation and education could therefore drastically change access to the sea ice environment.

However, safety and trafficability are not the only determinants for sea ice route selection. Sea ice trails follow smooth ice, detour around rough and thin ice areas, and are modified when it is recognised that existing trails can be improved, or ice conditions change. Using known trails, which are considered places in and of themselves, has the added benefit of improving safety as it is easier to get help (Aporta, 2004). While trail selection is impacted by safety and experience, it is also influenced by access to destinations, availability of preferred ice types (e.g., desired floe edge characteristics), convenience (e.g., amount of work to make a trail), and tradition (e.g., routes, destinations) (Druckenmiller et al., 2013). Breaking good trails is a source of pride: they are typically set by experienced travellers and followed by the increasing numbers of less experienced “track followers” (Aporta, 2004).

2.7.3.5 Arctic studies using SAR with community stakeholders

Other studies in the Canadian Arctic and Alaska note similar sea ice safety and trafficability conditions to those detailed in Table 2.1. For Kugluktuk and Cambridge Bay, the condition of sea ice roughness is quantified using Sentinel-1 (SAR), Multi-angle Imaging SpectroRadiometer (multi-angle optical), and airborne LiDAR datasets (see Chapter 3). The CIS also provides sea ice charts with data near communities. However, of our participants, only one from each community regularly uses CIS sea ice charts, although they orally disseminate this information with a limited number of others.

For Alaska, Dammann et al. (2018a, 2018b, 2019) have created quantitative assessments of ice trafficability where bearing capacity, surface conditions, and ice motion are investigated. They describe ice quality using nine ice variables: timing/duration, stability, fracture potential, thickness, microstructure/state variables, pre-

existing defects, extent, roughness, and snow and surface water conditions. Of these, only the stability-linked variables are not described by our participants. SAR-derived products showing surface characteristics are shared with the communities over the course of their research project.

Druckenmiller et al. (2013), Laidler et al. (2011), and Bell et al. (2014) provided digital and/or hardcopy SAR images to the communities of Utqiaġvik (formerly Barrow; Alaska); Cape Dorset, Igloolik, and Pangnirtung (Eastern Nunavut); and Nain and North West River (Labrador) respectively. All three studies use restricted SAR datasets and treat them like photos rather than complex datasets. Alaskan residents use the images to locate the sea ice edge and to discriminate between rough and smooth ice. Druckenmiller et al. (2013) found that marking trail locations on SAR images allowed Utqiaġvik hunters to more easily recognise locations.

Eastern Nunavut hunters want information about snow thickness, ice weakness (fracture potential), current-induced thin ice, ice density, and ice thickness (Laidler et al., 2011). The RADARSAT ScanSAR Wide imagery studied improves trip safety and planning by identifying unstable or poor ice, ice roughness, ice type, pressure ridges, as well as ice that impacts boats. They identified a need for higher spatial and temporal SAR resolutions, noting participant desires to resolve cracks, leads, polynyas, ice thickness, and small-scale ice growth using daily images. Expert hunters suggested SAR training access and easier-to-interpret, classified colour products that could be annotated by northerners.

In Labrador, the use of RADARSAT-2 images was combined with in-situ thickness sampling due to the high priority of ice thickness information. The SmartICE

program's initial community consultations revealed that hunters also want information on the locations of surface ice/snow roughness, open water, water-on-ice/melt pond ice lenses, landfast/shear/pack ice, and thin ice areas (termed rattles). They use a combination of RADARSAT-2 ScanSAR Narrow, Standard, and Fine mode products manually classified by locals to resolve small-scale features. While specially-tasked, high resolution images and continuous local input make for high quality products, the outputs are dependent on continuous resources.

2.7.4 Online integration

We created greyscale and classified SAR-based maps through Google Earth Engine (Gorelick et al., 2017): they became available through the SIKU platform (https://beta.siku.org[8]; Figure 2.4) beginning in December 2018. The Sentinel-1 images, part of Google's "COPERNICUS/S1_GRD" image collection, are sent through a near-real time processing chain designed to provide user-friendly sea ice information. The SIKU platform is interactive: users may pan to areas of interest, look backwards through historical imagery and mark dangerous areas or areas of interest. Online maps are less limited in extent and can show a chosen area in detail. As areas become more or less dangerous in the future, information may be uploaded, monitored, and modified by community members.

[8] The address will become https://siku.org once the website's beta testing phase is complete.

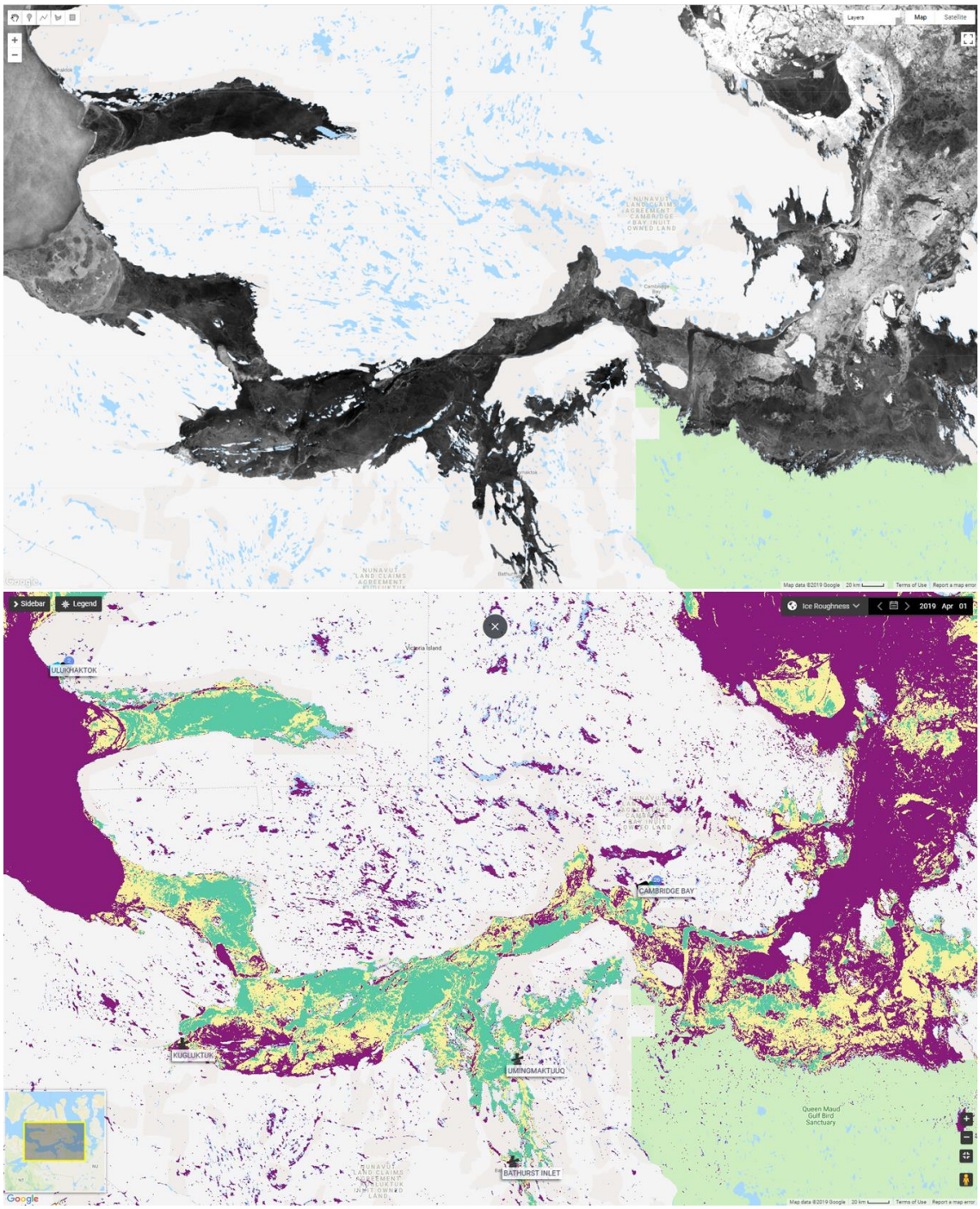

Figure 2.4. Top: greyscale Sentinel-1 HH-band SAR-based map of 1-30 April 2019 images on the Google Earth Engine platform. Bottom: classified roughness map viewed on the SIKU website (https://beta.siku.org) using the selected date of 1 April 2019.

2.8 Conclusions

Changes in both communities and their surrounding environments are impacting sea ice use and uncertainty regarding trafficable conditions. SAR-based maps are a welcome information supplement that complements IQ by providing high spatiotemporal resolution images of sea ice features and seasonal conditions that aid in informing and improving sea ice safety, trafficability, and education.

The sea ice conditions that impact trafficability and safety in Kugluktuk and Cambridge Bay include smooth, moderately rough, and rough sea ice, MYI, snow on ice, thin ice, early ice, late ice, slush/water on ice, ice encountered by boats, and ice fractures. Of these, sea ice surface roughness is considered the main ice condition where benefits to trafficability from SAR-based mapping are regarded as substantial. Both greyscale and classified Sentinel-1-based maps of sea ice surface roughness show good agreement with local understanding and observations, except a) in areas of freshened ice influence (i.e., MYI and riverine output areas), or b) areas of heavy snow. Roughness maps are desired throughout the sea ice season, particularly in fall and winter. Winter Sentinel-1 images show sea ice roughness clearly, while spring and fall conditions are more difficult to interpret on images, and more difficult to assess *in situ*. SAR-based maps would ideally contain ancillary danger warnings depicting typically thin ice areas.

Both soft- and hard-copy greyscale and classified roughness SAR-based maps would be beneficial for the communities, as would training in SAR interpretation. SAR-based maps provide benefits for sea ice education: they allow easy access to sea ice information and can act as discussion foci. For wider sharing of SAR-based maps, regional differences in sea ice conditions must be considered in the context of community

information priorities. Overall, remote sensing is an information source worth exploring further with northern community residents in the context of safe travel and education.

2.9 References

ACIA. (2005). *Arctic climate impact assessment* (p. 1042). New York, New York: Cambridge University Press. Retrieved from www.cambridge.org/9780521865098

Aporta, C. (2004). Routes, trails and tracks: Trail breaking among the Inuit of Igloolik. *Études/Inuit/Studies*, *28*(2), 9–38. https://doi.org/10.7202/013194ar

Aporta, C. (2009). The trail as home: Inuit and their pan-Arctic network of routes. *Human Ecology*, *37*(2), 131–146. https://doi.org/10.1007/s10745-009-9213-x

Arctic Monitoring and Assessment Programme. (2011). *Snow, water, ice and permafrost in the Arctic (SWIPA): Climate change and the cryosphere*. Oslo, Norway. Retrieved from www.amap.no

Bekryaev, R. V., Polyakov, I. V., & Alexeev, V. A. (2010). Role of polar amplification in long-term surface air temperature variations and modern Arctic warming. *Journal of Climate*, *23*(14), 3888–3906. https://doi.org/10.1175/2010JCLI3297.1

Bell, T., Briggs, R., Bachmayer, R., & Li, S. (2014). Augmenting Inuit knowledge for safe sea-ice travel: The SmartICE information system. In *Oceans - St. John's, 2014* (pp. 1–9). https://doi.org/10.1109/OCEANS.2014.7003290

Bertoia, C., Falkingham, J., & Fetterer, F. (1998). Polar SAR data for operational sea ice mapping. In *Analysis of SAR data of the polar oceans* (pp. 201–234). Springer Berlin Heidelberg. https://doi.org/10.1007/978-3-642-60282-5_10

Bhatt, U. S., Walker, D. A., Raynolds, M. K., Comiso, J. C., Epstein, H. E., Jia, G., … Webber, P. J. (2010). Circumpolar Arctic tundra vegetation change is linked to

sea ice decline. *Earth Interactions*, *14*(8), 1–20. https://doi.org/10.1175/2010EI315.1

Brinton, M. (2018). Risk and uncertainty regarding Inuit transportation in the face of climate change. *Boise State University Theses and Dissertations*. https://doi.org/10.18122/td/1372/boisestate

Bush, E., & Lemmen, D. S. (Eds.). (2019). *Canada's changing climate report.* Ottawa, Ontario: Government of Canada. Retrieved from http://publications.gc.ca/collections/collection_2019/eccc/En4-368-2019-eng.pdf

Calihoo, C., & Romaine, T. (2010). Climate change adaptation action plan for Cambridge Bay. Retrieved from https://www.cip-icu.ca/Files/Resources/CAMBRIDGEBAY_CCAP_E

Canadian Ice Service. (2011). *Sea ice climatic atlas: Northern Canadian waters 1981-2010*. Ottawa, Ontario. Retrieved from http://www.ec.gc.ca/glaces-ice/default.asp?lang=En&n=4B35305B-1&printfullpage=true

Chan, Y. K., & Koo, V. C. (2008). An introduction to synthetic aperture radar (SAR). *Progress in Electromagnetics Research B*, *2*, 27–60.

Clark, D. G., Ford, J. D., Berrang-Ford, L., Pearce, T., Kowal, S., & Gough, W. A. (2016a). The role of environmental factors in search and rescue incidents in Nunavut, Canada. *Public Health*, *137*, 44–49. https://doi.org/10.1016/j.puhe.2016.06.003

Clark, D. G., Ford, J. D., Pearce, T., & Berrang-Ford, L. (2016b). Vulnerability to unintentional injuries associated with land-use activities and search and rescue in

Nunavut, Canada. *Social Science & Medicine*, *169*, 18–26. https://doi.org/10.1016/j.socscimed.2016.09.026

Comiso, J. C., & Hall, D. K. (2014). Climate trends in the Arctic as observed from space. *Wiley Interdisciplinary Reviews: Climate Change*, *5*(3), 389–409. https://doi.org/10.1002/wcc.277

Dammann, D. O. (2017). *Arctic sea ice trafficability - New strategies for a changing icescape* (Ph.D.). University of Alaska Fairbanks, United States -- Alaska. Retrieved from https://search.proquest.com/docview/1916037079/abstract/447EFD1B917248E9PQ/1

Dammann, D. O., Eicken, H., Mahoney, A. R., Meyer, F. J., & Betcher, S. (2018a). Assessing sea ice trafficability in a changing Arctic. *Arctic*, *71*(1), 59–75. https://doi.org/10.14430/arctic4701

Dammann, D. O., Eicken, H., Mahoney, A. R., Saiet, E., Meyer, F. J., & George, J. C. "Craig." (2018b). Traversing sea ice: Linking surface roughness and ice trafficability through SAR polarimetry and interferometry. *IEEE Journal of Selected Topics in Applied Earth Observations and Remote Sensing*, *PP*(99), 1–18. https://doi.org/10.1109/JSTARS.2017.2764961

Dammann, D. O., Eriksson, L. E. B., Mahoney, A. R., Eicken, H., & Meyer, F. J. (2019). Mapping pan-Arctic landfast sea ice stability using Sentinel-1 interferometry. *The Cryosphere*, *13*(2), 557–577. https://doi.org/10.5194/tc-13-557-2019

Dawson, J., Hoke, W., Lamers, M., Liggett, D., Ljubicic, G., Stewart, E., & Thoman, R. (2017). *Navigating weather, water, ice and climate information for safe polar*

mobilities. Polar Prediction Project's Societal and Economic Research and Applications Working Group (PPP-SERA) of the World Meteorological Organization (WMO) Geneva, World Meterological Organization. Retrieved from https://www.polarprediction.net/fileadmin/user_upload/www.polarprediction.net/Home/Organization/Task_Teams/PPP-SERA/WWRP_PPP_No_5_2017_11_OCT.pdf

Deemer, G. J., Bhatt, U. S., Eicken, H., Posey, P. G., Hutchings, J. K., Nelson, J., … Creek, K. (2018). Broadening the sea-ice forecaster toolbox with community observations: A case study from the northern Bering Sea. *Arctic Science*, *4*, 47–70. https://doi.org/10.1139/AS-2016-0054

Dierking, W. (2013). Sea ice monitoring by synthetic aperture radar. *Oceanography*, *26*(2). https://doi.org/10.5670/oceanog.2013.33

Dowsley, M., Gearheard, S., Johnson, N., & Inksetter, J. (2010). Should we turn the tent? Inuit women and climate change. *Études/Inuit/Studies*, *34*(1), 151–165.

Druckenmiller, M. L., Eicken, H., George, J. C. "Craig," & Brower, L. (2013). Trails to the whale: Reflections of change and choice on an Iñupiat icescape at Barrow, Alaska. *Polar Geography*, *36*(1–2), 5–29. https://doi.org/10.1080/1088937X.2012.724459

Druckenmiller, M. L., Eicken, H., Johnson, M. A., Pringle, D. J., & Williams, C. C. (2009). Toward an integrated coastal sea-ice observatory: System components and a case study at Barrow, Alaska. *Cold Regions Science and Technology*, *56*(2–3), 61–72. https://doi.org/10.1016/j.coldregions.2008.12.003

Eicken, H., Jones, J., Rohith, M., Kambhamettu, C., Meyer, F., Mahoney, A., & Druckenmiller, M. (2011). Environmental security in Arctic ice-covered seas: From strategy to tactics of hazard identification and emergency response. *Marine Technology Society Journal*. Retrieved from http://seaice.alaska.edu/gi/publications/eicken/11EJRK.pdf

Eicken, H., & Mahoney, A. R. (2015). Sea ice: Hazards, risks, and implications for disasters. In J. T. Ellis & D. J. Sherman (Eds.), *Coastal and Marine Hazards, Risks, and Disasters* (pp. 381–401). Boston: Elsevier. Retrieved from http://www.sciencedirect.com/science/article/pii/B9780123964830000133

Ersahin, K., Brown, L., Kanwar, A., Henley, M., Ross, E., & Fissel, D. (2014). Characterization of hazardous ice using spaceborne SAR and ice profiling sonar: preliminary results. Offshore Technology Conference. https://doi.org/10.4043/24600-MS

ESA. (2018a). Observation scenario archive - Sentinel-1 - Sentinel Online. Retrieved April 21, 2018, from https://sentinel.esa.int/web/sentinel/missions/sentinel-1/observation-scenario

ESA. (2018b). Sentinel-1 SAR User guide introduction. Retrieved October 4, 2018, from https://sentinel.esa.int/web/sentinel/user-guides/sentinel-1-sar

Fisheries and Oceans Canada. (2012). Ice climatology and environmental conditions. In *Ice navigation in Canadian waters* (Revised, pp. 32–78). Ottawa, Ontario: Icebreaking Program, Maritime Services, Canadian Coast Guard, Fisheries and Oceans Canada. Retrieved from http://www.ccg-gcc.gc.ca/Icebreaking/Ice-Navigation-Canadian-Waters/Ice-Climatology-and-Environmental-Conditions

Ford, J. D. (2005). Living with climate change in the Arctic | Worldwatch Institute. *Worldwatch Institute*, *18*(5), 18–21.

Ford, J. D., Clark, D., Pearce, T., Berrang-Ford, L., Copland, L., Dawson, J., … Harper, S. L. (2019). Changing access to ice, land and water in Arctic communities. *Nature Climate Change*, 1. https://doi.org/10.1038/s41558-019-0435-7

Ford, J. D., Couture, N., Bell, T., & Clark, D. G. (2018). Climate change and Canada's north coast: Research trends, progress, and future directions. *Environmental Reviews*, *26*(1), 82–92. https://doi.org/10.1139/er-2017-0027

Ford, J. D., Pearce, T., Gilligan, J., Smit, B., & Oakes, J. (2008). Climate change and hazards associated with ice use in Northern Canada. *Arctic, Antarctic, and Alpine Research*, *40*(4), 647–659. https://doi.org/10.1657/1523-0430(07-040)[FORD]2.0.CO;2

Ford, J. D., & Smit, B. (2004). A framework for assessing the vulnerability of communities in the Canadian Arctic to risks associated with climate change. *Arctic*, *57*(4), 389–400. https://doi.org/10.14430/arctic516

Ford, J. D., Smit, B., & Wandel, J. (2006a). Vulnerability to climate change in the Arctic: A case study from Arctic Bay, Canada. *Global Environmental Change*, *16*(2), 145–160. https://doi.org/10.1016/j.gloenvcha.2005.11.007

Ford, J. D., Smit, B., Wandel, J., & MacDonald, J. (2006b). Vulnerability to climate change in Igloolik, Nunavut: What we can learn from the past and present. *Polar Record*, *42*(2), 127. https://doi.org/10.1017/S0032247406005122

Gauthier, Y., Tremblay, M., Bernier, M., & Furgal, C. (2010). Adaptation of a radar-based river ice mapping technology to the Nunavik context. *Canadian Journal of Remote Sensing*, *36*(S1), S168–S185. https://doi.org/10.5589/m10-018

Gorelick, N., Hancher, M., Dixon, M., Ilyushchenko, S., Thau, D., & Moore, R. (2017). Google Earth Engine: Planetary-scale geospatial analysis for everyone. *Remote Sensing of Environment*, *202*, 18–27. https://doi.org/10.1016/j.rse.2017.06.031

Grimwood, B. S. R., Doubleday, N. C., Ljubicic, G. J., Donaldson, S. G., & Blangy, S. (2012). Engaged acclimatization: Towards responsible community-based participatory research in Nunavut. *The Canadian Geographer / Le Géographe Canadien*, *56*(2), 211–230. https://doi.org/10.1111/j.1541-0064.2012.00416.x

Haas, C., & Druckenmiller, M. L. (2010). Ice thickness and roughness measurements. In H. Eicken, R. Gradinger, K. Shirasawa, D. K. Perovich, & M. Leppäranta (Eds.), *Field techniques for sea ice research* (pp. 49–116). Retrieved from https://epic.awi.de/id/eprint/22664/1/Haa2009c.pdf

Heyes, S. A. (2011). Cracks in the knowledge: Sea ice terms in Kangiqsualujjuaq, Nunavik. *The Canadian Geographer / Le Géographe Canadien*, *55*(1), 69–90. https://doi.org/10.1111/j.1541-0064.2010.00346.x

Howell, S. E. L., Duguay, C. R., & Markus, T. (2009). Sea ice conditions and melt season duration variability within the Canadian Arctic Archipelago: 1979–2008. *Geophysical Research Letters*, *36*(10). https://doi.org/10.1029/2009GL037681

Johnson, K., & Arnold, E. (2010). Climate change adaptation action plan for Kugluktuk. Retrieved from https://www.cip-icu.ca/Files/Resources/KUGLUKTUK_CCAP_E

Kim, M., Im, J., Han, H., Kim, J., Lee, S., Shin, M., & Kim, H.-C. (2015). Landfast sea ice monitoring using multisensor fusion in the Antarctic. *GIScience & Remote Sensing*, *52*(2), 239–256. https://doi.org/10.1080/15481603.2015.1026050

Krupnik, I., & Jolly, D. (2002). *The Earth is faster now: Indigenous observations of Arctic environment change*. Arctic Research Consortium of the United States.

Laidler, G. J. (2006). Inuit and scientific perspectives on the relationship between sea ice and climate change: The ideal complement? *Climatic Change*, *78*(2–4), 407–444. https://doi.org/10.1007/s10584-006-9064-z

Laidler, G. J. (2007). *Ice, through Inuit eyes: Characterizing the importance of sea ice processes, use, and change around three Nunavut communities.* (Ph.D.). University of Toronto, Toronto, Ontario.

Laidler, G. J., Dialla, A., & Joamie, E. (2008a). Human geographies of sea ice: Freeze/thaw processes around Pangnirtung, Nunavut, Canada. *Polar Record*, *44*(4), 335–361. https://doi.org/10.1017/S003224740800750X

Laidler, G. J., & Elee, P. (2008). Human geographies of sea ice: Freeze/thaw processes around Cape Dorset, Nunavut, Canada. *Polar Record*, *44*(1), 51–76. https://doi.org/10.1017/S0032247407007061

Laidler, G. J., Ford, J. D., Gough, W. A., Ikummaq, T., Gagnon, A. S., Kowal, S., … Irngaut, C. (2008b). Travelling and hunting in a changing Arctic: Assessing Inuit vulnerability to sea ice change in Igloolik, Nunavut. *Climatic Change*, *94*(3–4), 363–397. https://doi.org/10.1007/s10584-008-9512-z

Laidler, G. J., Hirose, T., Kapfer, M., Ikummaq, T., Joamie, E., & Elee, P. (2011). Evaluating the Floe Edge Service: How well can SAR imagery address Inuit

community concerns around sea ice change and travel safety? *Canadian Geographer / Le Géographe Canadien*, *55*(1), 91–107. https://doi.org/10.1111/j.1541-0064.2010.00347.x

Laidler, G. J., & Ikummaq, T. (2008). Human geographies of sea ice: Freeze/thaw processes around Igloolik, Nunavut, Canada. *Polar Record*, *44*(2), 127–153. https://doi.org/10.1017/S0032247407007152

Lépy, E. (2008). Information and communication technologies, a tool for risk prevention and accident management on sea ice. *Netcom. Réseaux, Communication et Territoires*, (22-3/4), 255–264. https://doi.org/10.4000/netcom.1678

Letterly, A., Key, J., & Liu, Y. (2018). Arctic climate: Changes in sea ice extent outweigh changes in snow cover. *The Cryosphere*, *12*, 3373–3382. https://doi.org/10.5194/tc-12-3373-2018

Lindsay, R., Haas, C., Hendricks, S., Hunkeler, P., Kurtz, N., Paden, J., … Zhang, J. (2012). Seasonal forecasts of Arctic sea ice initialized with observations of ice thickness. *Geophysical Research Letters*, *39*(21), L21502. https://doi.org/10.1029/2012GL053576

Lindsay, R., & Schweiger, A. (2015). Arctic sea ice thickness loss determined using subsurface, aircraft, and satellite observations. *The Cryosphere*, *9*(1), 269–283. https://doi.org/10.5194/tc-9-269-2015

Markus, T., Stroeve, J. C., & Miller, J. (2009). Recent changes in Arctic sea ice melt onset, freezeup, and melt season length. *Journal of Geophysical Research: Oceans*, *114*(C12), C12024. https://doi.org/10.1029/2009JC005436

Meier, W. N., Hovelsrud, G. K., van Oort, B. E. H., Key, J. R., Kovacs, K. M., Michel, C., … Reist, J. D. (2014). Arctic sea ice in transformation: A review of recent observed changes and impacts on biology and human activity. *Reviews of Geophysics*, *52*(3), 185–217. https://doi.org/10.1002/2013RG000431

Nickels, S., Furgal, C., Buell, M., & Moquin, H. (2005). *Unikkaaqatigiit - Putting the human face on climate change: Perspectives from Inuit in Canada*. Ottawa, Ontario: Inuit Tapiriit Kanatami, Nasivvik Centre for Inuit Health and Changing Environments at Université Laval and the Ajunnginiq Centre at the National Aboriginal Health Organization. Retrieved from http://www.inuitknowledge.ca/sites/ikc/files/attachments/20060726-Unikkaaqatigiit-book-complete-web.pdf

NTI. (2001). *Elder's conference on climate change: Final report* (p. 36). Cambridge Bay, Nunavut: Nunavut Tunngavik Incorporated (NTI).

Nunavut Emergency Management. (2017). *Nunavut emergency management annual report 2015-2016* (No. 252- 4(3)) (p. schar). Government of Nunavut. Retrieved from http://www.assembly.nu.ca/nunavut-emergency-management-annual-report-2015-2016

Overland, J. E. (2009). Meteorology of the Beaufort Sea. *Journal of Geophysical Research: Oceans*, *114*(C1), C00A07. https://doi.org/10.1029/2008JC004861

Panikkar, B., Lemmond, B., Else, B., & Murray, M. (2018). Ice over troubled waters: Navigating the Northwest Passage using Inuit knowledge and scientific information. *Climate Research*, *75*(1). Retrieved from https://www.openchannels.org/literature/22121

Perovich, D. K., Richter-Menge, J. A., Jones, K. F., & Light, B. (2008). Sunlight, water, and ice: Extreme Arctic sea ice melt during the summer of 2007. *Geophysical Research Letters*, *35*(11), L11501. https://doi.org/10.1029/2008GL034007

Pizzolato, L., Howell, S. E. L., Derksen, C., Dawson, J., & Copland, L. (2014). Changing sea ice conditions and marine transportation activity in Canadian Arctic waters between 1990 and 2012. *Climatic Change*, *123*(2), 161–173. https://doi.org/10.1007/s10584-013-1038-3

Prowse, T. D., Furgal, C., Wrona, F. J., & Reist, J. D. (2009). Implications of climate change for Northern Canada: Freshwater, marine, and terrestrial ecosystems. *AMBIO: A Journal of the Human Environment*, *38*(5), 282–289. https://doi.org/10.1579/0044-7447-38.5.282

Richter-Menge, J. A., Perovich, D. K., Elder, B. C., Claffey, K., Rigor, I., & Ivey, M. (2006). Ice mass-balance buoys: A tool for measuring and attributing changes in the thickness of the Arctic sea-ice cover. *Annals of Glaciology*, *44*, 205–210.

Rolph, R. J., Mahoney, A. R., Walsh, J. E., & Loring, P. A. (2018). Impacts of a lengthening open water season on Alaskan coastal communities: Deriving locally relevant indices from large-scale datasets and community observations. *The Cryosphere*, *12*, 1779–1790. https://doi.org/10.5194/tc-12-1779-2018

Scharien, R., Hochheim, K., Landy, J., & Barber, D. (2014). First-year sea ice melt pond fraction estimation from dual-polarisation C-band SAR - Part 2: Scaling in situ to RADARSAT-2. *The Cryosphere*, *8*, 2163–2176. https://doi.org/10.5194/tc-8-2163-2014

Serreze, M. C., Walsh, J. E., Iii, F. S. C., Osterkamp, T., Dyurgerov, M., Romanovsky, V., … Barry, R. G. (2000). Observational evidence of recent change in the Northern high-latitude environment. *Climatic Change*, *46*(1–2), 159–207. https://doi.org/10.1023/A:1005504031923

Stammler-Gossmann, A. (2010). 'Translating' vulnerability at the community level: Case study from the Russian north. In G. K. Hovelsrud & B. Smit (Eds.), *Community Adaptation and Vulnerability in Arctic Regions* (pp. 131–162). Springer Netherlands. https://doi.org/10.1007/978-90-481-9174-1_6

Statistics Canada. (2017a). Cambridge Bay, HAM [Census subdivision], Nunavut and Kitikmeot, REG [Census division], Nunavut (table). 2016 Census. Statistics Canada Catalogue no. 98-316-X2016001. Ottawa. Released November 29, 2017. Retrieved April 8, 2017, from http://www12.statcan.gc.ca/census-recensement/2016/dp-pd/prof/details/page.cfm?Lang=E&Geo1=CSD&Code1=6208073&Geo2=CD&Code2=6208&Data=Count&SearchText=Cambridge%20Bay&SearchType=Begins&SearchPR=01&B1=All&GeoLevel=PR&GeoCode=6208073&TABID=11

Statistics Canada. (2017b). Kugluktuk, HAM [Census subdivision], Nunavut and Kitikmeot, REG [Census division], Nunavut (table). Census Profile. 2016 Census. Statistics Canada Catalogue no. 98-316-X2016001. Ottawa. Released November 29, 2017. Retrieved April 8, 2017, from http://www12.statcan.gc.ca/census-recensement/2016/dp-pd/prof/details/page.cfm?Lang=E&Geo1=CSD&Code1=6208059&Geo2=CD&C

ode2=6208&Data=Count&SearchText=kugluktuk&SearchType=Begins&SearchPR=01&B1=All&TABID=1

Steele, M., Ermold, W., & Zhang, J. (2008). Arctic Ocean surface warming trends over the past 100 years. *Geophysical Research Letters*, *35*(2), L02614. https://doi.org/10.1029/2007GL031651

Stephenson, S. R., Smith, L. C., & Agnew, J. A. (2011). Divergent long-term trajectories of human access to the Arctic. *Nature Climate Change*, *1*(3), 156–160. https://doi.org/10.1038/nclimate1120

Stroeve, J. C., Markus, T., Boisvert, L., Miller, J., & Barrett, A. (2014). Changes in Arctic melt season and implications for sea ice loss. *Geophysical Research Letters*, *41*(4), 2013GL058951. https://doi.org/10.1002/2013GL058951

Stuckenberger, A. N. (2010). Les Inuit et le changement climatique / The Inuit and climate change. *Études/Inuit/Studies*, *34*(1), 5–19.

Teleti, P. R., & Luis, A. J. (2013). Sea ice observations in polar regions: Evolution of technologies in remote sensing. *International Journal of Geosciences*, *4*, 1031–1050.

Tondu, J. M. E., Balasubramaniam, A. M., Chavarie, L., Gantner, N., Knopp, J. A., Provencher, J. F., … D, S. (2014). Working with northern communities to build collaborative research partnerships: Perspectives from early career researchers. *Arctic*, *67*(3), 419–429. https://doi.org/10.14430/arctic4416

Wu, B., Wang, J., & Walsh, J. E. (2006). Dipole anomaly in the winter Arctic atmosphere and Its association with sea ice motion. *Journal of Climate*, *19*(2), 210–225. https://doi.org/10.1175/JCLI3619.1

Chapter 3 - The best of both worlds[9]" - Connecting remote sensing and Arctic communities for safe sea ice travel

Part 2 –Surface roughness

Rebecca A. Segal[a*], Randall K. Scharien[a], Silvie Cafarella[a], Andrew Tedstone[b]
[a]Department of Geography, University of Victoria, Victoria BC, Canada
[b]School of Geographical Sciences, University of Bristol, United Kingdom

3.1 Acknowledgements

This research was supported by the Marine Environmental Observation Prediction and Response (MEOPAR) network and Irving Shipbuilding Inc. project number 1.22, Polar Knowledge Canada (POLAR; project number NST-1718-0024), the W. Garfield Weston Foundation through the Association of Canadian Universities for Northern Studies (ACUNS), the Natural Sciences and Engineering Research Council of Canada (NSERC), the Royal Canadian Geographical Society (RCGS), the Arctic Institute of North America (AINA), the University of Victoria, and the UK Natural Environment Research Council Large Grant NE/M021025. We thank the British Antarctic Survey (BAS) and Technical University of Denmark (DTU) for providing airborne LiDAR data. Thanks to James Balchin for Sentinel-1 video creation. Sentinel-1 data are freely provided by the European Space Agency (ESA). MISR data are provided freely by the

9 Resident of Kugluktuk

Langley Atmospheric Science Data Center at the North American Space Agency (NASA). RADARSAT-2 data (© MacDonald, Dettwiler and Associates Ltd, 2012; all rights reserved) are provided by the Canadian Ice Service (CIS). RADARSAT is an official mark of the Canadian Space Agency (CSA).

3.2 Abstract

This study assesses the utility of two satellite datasets for characterizing sea ice roughness at scales relevant to winter trafficability by Kugluktuk and Cambridge Bay community members in the Canadian Arctic. The satellite datasets are 1) the European Space Agency's C-band synthetic aperture radar, Sentinel-1; and 2) the National Aeronautics and Space Administration's optical Multi-angle Imaging SpectroRadiometer (MISR). Backscatter from Sentinel-1 and the Normalised Difference Angular Index (NDAI) from MISR are both compared to roughness data measured by an airborne LiDAR system. Overall relationships for NDAI and roughness as well as backscatter and roughness are significant (R^2 = 0.65 and 0.66; $p < 0.0001$) when balanced samples of first-year ice (FYI) and multiyear ice (MYI) types are used. For FYI, backscatter is significantly related to roughness ($R^2 = 0.58$, $p < 0.0001$) while the relationship between NDAI and roughness is insignificant. For MYI, NDAI is significantly related to roughness ($R^2 = 0.46$, $p < 0.001$) while backscatter is not, the latter due to consistently high backscatter caused by volume scattering. A comparison of the two satellite datasets finds a strong relationship for deformed FYI ($R^2 = 0.88$, $p < 0.0001$), indicating that radar backscatter is related to the reflectance properties of this ice type. Maps visualizing *smooth ice*, *moderately rough ice*, and *rough ice* categories are created by thresholding NDAI and backscatter, demonstrating a format useful for distribution to northern

communities. Due to the weak capacity of backscatter to predict MYI roughness, a MYI area delineation using the Sentinel-1 H-alpha Wishart classification (Kappa = 0.83) is implemented.

3.3 Introduction

Sea ice surfaces are heterogeneous in time and space, with seasonal and multiyear ice types undergoing thermodynamic and dynamic-deformation processes. Macroscale sea ice topography is characterised by a range of features, including: level, undeformed sea ice; structures formed by convergent or divergent stressors like pressure ridges, cracks, leads, ice rubble, rafted ice, and hummocks; snow features like sastrugi, dunes, and variable depth; and melt features like saturated snow (slush) and melt water ponds. These surface features are linked to season; atmospheric and oceanic forcing; and ice qualities like ice age, salt content, and thickness (Weeks & Ackley, 1982). The result is a wide variety of sea ice topographies with different feature densities, scales and regimes.

Sea ice surface characteristics directly impact the animals and people who use the sea ice (Dammann et al., 2018b; Frost et al., 2004) and ships that travel through sea ice (Bertoia et al., 1998). Indirectly, they also impact ocean biological communities through light transmittance patterns (Horner et al., 1992; Katlein et al., 2015); and the global climate though albedo/heat feedbacks (via topographical melt pond constraint) and sea ice decay (via movement by wind drag) (Martin et al., 2016; Petty et al., 2017; Schröder et al., 2014). Furthermore, sea ice surface characteristics are being altered by climate change, with greater expanses of open water leading to increased dynamic activity, and the transition to a younger, seasonal, sea ice regime leading to the replacement of older ice types with seasonal ice (Krupnik & Jolly, 2002; Martin et al., 2016). As a result, sea

ice surface topography (hereafter *roughness*) is an active area of research across many disciplines, involving a wide variety of sensors and methods of measurement.

While in situ sea ice data are sparse and difficult to obtain, satellites provide information at moderate resolutions and broad scales. Currently there are a wide variety of sea ice roughness characterization methodologies applicable to specific applications and sea ice regimes. The choice of input sensors and output roughness metrics vary depending on data availability, quality, cost, and ease of use (Beckers et al., 2015; Dammann et al., 2018b; Fors et al., 2016; Hong & Shin, 2010; Johansson et al., 2017; Landy et al., 2015; Li, 2018; Martin et al., 2016; Newman et al., 2014; Nolin et al., 2002; Nolin & Mar, 2019; Petty et al., 2016, 2017). Despite the variety of goals and datasets, baseline roughness studies commonly combine or assess broader-scale datasets with finer-scale point-based (e.g., terrestrial LiDAR), linear (e.g., transect), or 3D (e.g., airborne LiDAR) datasets.

While some studies use satellite and/or LiDAR datasets to characterise roughness, few focus on roughness in relation to trafficability by local northern sea ice users (Dammann et al., 2018b; Gauthier et al., 2010). Most Arctic communities are situated adjacent to the marine environment, where sea ice plays an important ecosystem service by connecting communities to hunting grounds, seasonal cabins, recreation activities, and other communities (Chapter 2; Eicken et al., 2009). Roughness impacts travelers, and they desire information about surface conditions in order to plan livelihood activities (Chapter 2; Aporta, 2004; Bell et al., 2014; Dammann et al., 2018b; Druckenmiller et al., 2013; Ford et al., 2008; Laidler et al., 2011). Roughness is important at spatio-temporal scales applicable to travel by snowmobile: sub-metre to metre-scale datasets (>0.1 m to

~10 m) covering large areas at frequent intervals throughout the sea ice season. Consequently, data that are open access or low cost are essential.

Assessments of potential sea ice hazards and impediments to trafficability are readily available to operational and industrial sea ice users in the form of ice charts. These charts, which typically combine C-band synthetic aperture radar (SAR) image data with ancillary sources such as optical, aerial reconnaissance, and in situ observations, are produced with standardised terminologies in Canada, the USA, the Baltic Nations, Japan, and Russia (Bertoia et al., 1998). Sea ice hazards encountered by communities during travel differ from those encountered by ships, as sea ice is used as a platform for activities instead of acting as a hazard for water-based navigation. Consequently, information available to industry users may not be accessible or useful for communities due to technological limitations, jargon, and production at coarse spatio-temporal scales (Bell et al., 2014; Laidler et al., 2011).

In this study, we investigate the utility of two radar and optical satellite-based datasets, the C-band frequency Sentinel-1 SAR and the optical Multi-angle Imaging SpectroRadiometer (MISR), for their utility in estimating winter-period macroscale surface roughness at scales applicable for serving the on-ice trafficability information needs of communities in the Kitikmeot Region of the Western Canadian Arctic (see Chapter 2). Both satellite datasets are assessed by comparing derived image data to high-resolution roughness data measured by an airborne LiDAR system. We identify conditions and locations where relationships between the satellite sensor-computed roughness and LiDAR-measured roughness are strong and where they break down. We

also highlight areas where the two satellite sensors have unequal utility in the quantification of roughness and the subsequent creation of roughness maps.

Sentinel-1 is a constellation of two SAR systems operated by the European Space Agency (ESA) that provides high resolution (40m) imagery every two to four days in the Arctic (ESA, 2018a). The ability of SAR to regularly obtain imagery regardless of cloud cover or darkness, as well as the sensitivity of measured backscatter to surface roughness where dielectric property contrasts occur (air/snow and snow/ice interfaces), makes it desirable for roughness mapping (Dammann et al., 2018a). When surface scattering dominates, rougher surfaces have a greater number of surface components and increased backscatter. Volumetric contributions to backscattering, such as from air bubbles in the case of MYI, occur when the freshened upper ice layer promotes penetration into the volume and are not linked to roughness (Geldsetzer & Yackel, 2009; Hallikainen & Winebrenner, 1992).

MISR is a payload on the Terra platform operated by the National Aeronautics and Space Administration (NASA) that provides optical data from nine cameras with different viewing geometries: one nadir-facing (0˚) and four paired fore- and aft-facing (±26.1˚, ±45.6˚, ±60.0˚, ±70.5˚), all of which capture near-concurrent images (Diner et al., 2002). MISR's descending orbit over the Arctic allows the forward and backward facing cameras to respectively observe forward scattering (typically smooth surfaces) and backward scattering (typically rough surfaces), by taking advantage of the sun's location to the south. Therefore, directional reflectance can be used to infer surface roughness (Nolin, 2004; Nolin & Payne, 2007). MISR has overpasses every one to two days, with a swath width of 380km and a red channel resolution of 275m (National Snow and Ice Data

Center, 2018). It has been used for studies of sea ice and glacier roughness (Nolin et al., 2002; Nolin & Mar, 2019; Nolin & Payne, 2007), ocean texture (oil spill detection) (Chust & Sagarminaga, 2007) and desert dune detection (Wu et al., 2009).

Dataset evaluations are based on the ability to provide robust and accurate roughness information that is useful to northern communities. Therefore we: 1) identify the sea ice characteristics that are local travel-based information needs, 2) incorporate the input of locals in the research methodology and validation process, and 3) design a process that results in both accurate and readily understandable information for incorporation into SAR-based maps. Both 1) and 2) are discussed separately in Chapter 2, while 3) is assessed here for the condition of sea ice surface roughness. In this study, section 3.4 describes the datasets and processing methods; section 3.5 provides multi-scale analysis results and sea ice roughness maps; section 3.6 considers the main strengths and weaknesses of the sensors in the context of products for northern communities; and section 3.7 gives concluding statements.

3.4 Methods

3.4.1 Study area and research design

The study area (Figure 3.1) is of interest to northern residents who travel on sea ice (Chapter 2). The sea ice is landfast and of 100% ice concentration in late winter and spring, which permits surface roughness comparisons from multiple days without the need for tracking movement. The region is characterised by a variety of sea ice types including first year ice (FYI), deformed first year ice (DFYI), and multi-year ice (MYI).

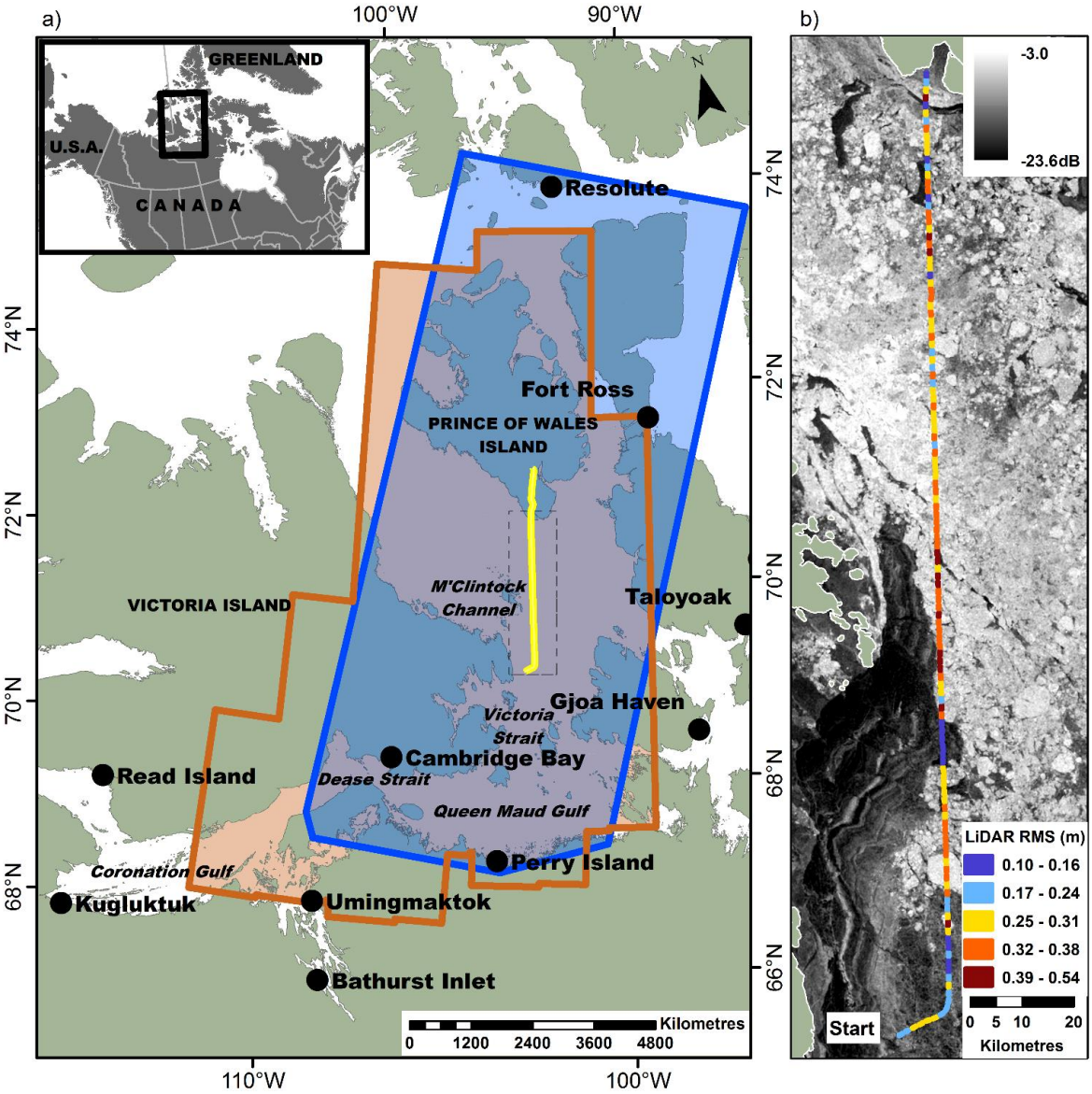

Figure 3.1 a) The study area, showing Sentinel-1 (orange), MISR (blue) and LiDAR (yellow) data coverage. The dashed grey line indicates the coverage of inset b), which shows LiDAR-derived root mean square roughness, overlaid on the 9-14 April 2017 Sentinel-1 mosaic.

FYI can either freeze during calm conditions and be relatively smooth, or freeze while there are varying degrees of wind and wave action and so contain sharp slabs of broken or rafted ice embedded on the sea ice surface. Both surface types are expected for this region. Slabs vary in density and size, which together determine the “degree” of

roughness. Slabs are often small (<1m) but can be more than 6m high (Figure 3.2 a-b). They are typically ~15cm (up to ~60cm) thick, depending on the ice thickness when the surface ice sheet breaks (Figure 3.2c; Chapter 2). DFYI contains the extremes of these rough conditions and is found in areas subject to strong winds and currents when the ice is still consolidating. Pressure ridges also contribute to roughness, with type 1 pressure ridges (locally defined; cracks with ice rubble on the edges; ~1.2m, up to ~4.5m high) and type 2 pressure ridges (ice that has buckled upwards due to pressure; large) causing ice rubble to form above the sea ice surface (Figure 3.2d).

MYI has a hummocky surface that is typically not sharp, but rather smooth and bumpy due to weathering. The junctions between FYI and MYI can be uneven, as MYI may be much thicker than FYI and have a higher freeboard. On top of the sea ice, snow also modifies the surface that is used for travel, by filling in gaps or creating snow-hummocks (Chapter 2). A video clip of the 2016-2017 sea ice season progression in the study region is found in Appendix B section B.1.

All data[10] were captured from 5-20 April 2017, during winter (pre-melt) conditions (mean April 2017 air temperature at Cambridge Bay WMO ID 71925 was -21.8°C). The predominant ice type in Coronation Gulf, Dease Strait, and Queen Maud Gulf was FYI. In Victoria Strait there was DYFI and FYI, and in M'Clintock Channel was a mix of MYI and smaller regions of FYI and DFYI.

[10] Excluding a separate study to assess the effect of incidence angle on SAR backscatter intensity (see Table A.1).

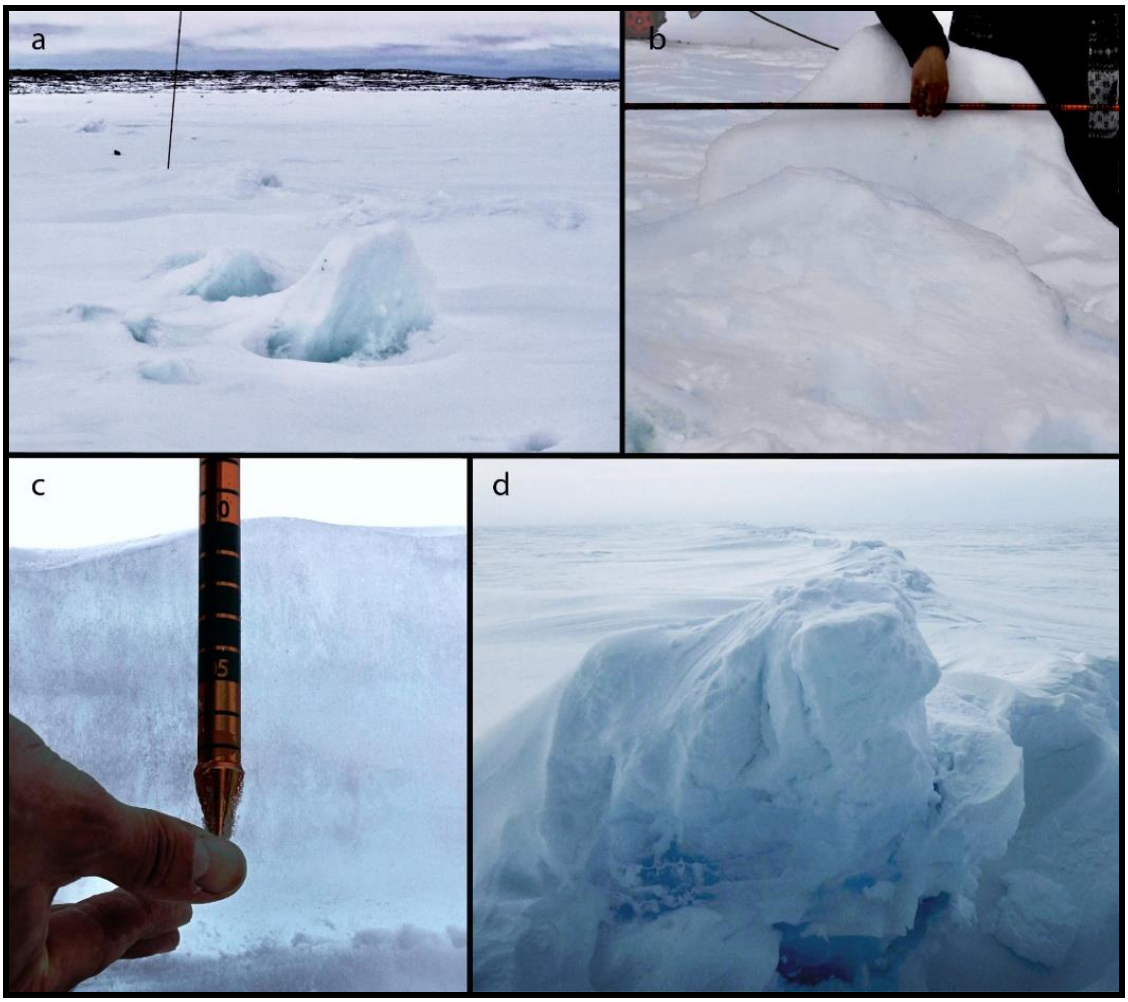

Figure 3.2. Sea ice surface roughness features near Kugluktuk on 28 May 2018 (a-b) and Cambridge Bay on 21 May 2018 (c-d). a) Area of snow-covered moderately rough sea ice with upturned blocks (N 67˚56.936', W 114˚41.526'); b) close-up of a typical ice block seen in the foreground of a), with dimensions: length = 127 cm, width = 24 cm, height = 135 cm, and thickness = 14 cm; c) image showing the thickness of sea ice when it broke (~10 cm, each marked interval is 1 cm); and d) a sea ice fracture (pressure ridge) ~2-3 m in height and ~ 4.5 m wide (N 69˚03.724, W 105˚40.165').

Specifications of the satellite and airborne data covering the areas shown in Figure 3.1 are provided in Table 3.1. The fine-scale resolution (1.0 × 1.0 m) airborne

LiDAR data were collected using a Twin Otter-mounted RIEGL LMS Q-240i-80 on 11 April 2017 as part of ESA's CryoSat Validation Experiment (CryoVEx). The aircraft flew a data collection transect over Victoria Strait and M'Clintock Channel, to Prince of Wales Island (Figure 3.1) at ~300 m above ground level. The 904 nm LiDAR collects data from the air/snow interface over a swath of 400 m by using a maximum scan angle of 80˚ and recording the last returned pulse. The vertical accuracy is on the order of ~10 cm or better due to kinematic GPS uncertainty.

Table 3.1. Information about the sensors and products used to assess sea ice backscatter and surface roughness. Abbreviations are as follows: S = Sentinel; Des = descending; Asc = ascending; EW = extended wide-swath; GRD = ground range detected; FQn = fine quad pol; Bxx=band number; Fxx = Format version number; ALS = airborne laser scanner; SLC = single-look complex; NA = not applicable. SLC images are used in section 3.4.4 exclusively.

Platform	Payload	Date (dd-mmm-yy)	Direction/ Mode	Orbit (Path/Track)	ID(s)	Format
S1A	SAR-C	09-Apr-17	Des/EW	16068 (71)	DFD1, F42F	GRD
S1B	SAR-C	10-Apr-17	Asc/EW	5099 (173)	0A4B, B132	GRD
S1A	SAR-C	11-Apr-17	Des/EW	16097 (100)	3245, E3EA	GRD
					5D71, 3AA2	SLC
S1B	SAR-C	12-Apr-17	Asc/EW	5128 (27)	2A30, B846	GRD
S1B	SAR-C	13-Apr-17	Asc/EW	5143 (42)	240D	GRD
S1A	SAR-C	14-Apr-17	Des/EW	16141 (144)	340A	GRD
Terra	MISR	12-Apr-17	Des/NA	92114 (43)	B30 - B35	F03
Twin Otter	RIEGL LMS Q-240i-80	11-Apr-17	NA/NA	NA	NA	ALS
RADARSAT-2	SAR	05-Apr-17	Des/FQn	48591 (NA)	PDS_05711970, PDS_05711980, PDS_05711990, PDS_05712000	SLC

3.4.2 Data processing

Processed satellite and airborne data described in this section were re-projected to a standard projection (WKID: 32614) to facilitate fine- and broad-scale inter-comparisons. The Global Self-consistent, Hierarchical, High-resolution Shoreline Database (at full resolution and buffered offshore by 300m) is used to mask land in all datasets (Wessel & Smith, 1996).

3.4.2.1 SAR backscatter

Sentinel-1 data were restricted to mid-range incidence angles of 30-39˚ and to the gamma nought calibration, to minimise the effect of incidence angle on backscatter intensity (see Appendix B section B.2). The horizontal transmit-receive (HH) channel was selected due to previously examined sensitivity to sea ice roughness, and since backscatter from sea ice in this channel is typically greater than the high Noise-Equivalent Sigma Zero (NESZ) of Sentinel-1, nominally -22 dB (ESA, 2018b). The Sentinel-1 horizontal transmit and vertical receive (HV) channel was not analyzed due to low backscatter relative to the NESZ and noisy artefacts visible among the sub-swaths in the EW mode. A high NESZ can increase low values (Similä et al., 2010), reducing the effective contrast between smooth and rough ice, if the smooth ice backscatter falls below the NESZ (Dierking & Dall, 2007).

Sentinel-1 images were processed using ESA's Sentinel Application Platform (SNAP) Version 6.0 using the following steps: i) thermal noise removal; ii) HH-band calibration (gamma-nought); iii) speckle filtering (Lee 7×7), iv) sub-setting (incidence angle range 30-39°) and v) map projection. After processing, images were mosaicked, with values averaged in cases of overlapping scenes.

3.4.2.2 MISR NDAI

We processed MISR MI1B2T data from the Cf and Ca cameras (±60.0˚) to surface reflectance using the Simple Model for Atmospheric Correction (SMAC) (Rahman & Dedieu, 1994), and then projected and mosaiced the individual data blocks using the MIB2GEOP ancillary product. Areas with suspected cloud cover were manually masked out (Nolin & Mar, 2019) and then surface reflectance was used to create the normalised difference angular index (NDAI),

$$NDAI = \frac{\rho_{-60} - \rho_{+60}}{\rho_{-60} + \rho_{+60}} \qquad (1)$$

where ρ_{-60} and ρ_{+60} are the Ca and Cf hemispherical-directional reflectances obtained from the sensor's red channel (672 nm), respectively. NDAI is used to approximate roughness and has been proven useful over various cryosphere surfaces such as glacier ice and sea ice, where smooth surfaces have a negative NDAI and rough surfaces have a positive NDAI (Nolin, 2004; Nolin & Payne, 2007).

3.4.2.3 LiDAR-derived roughness

Python's SkyFilt.py program was used to remove processed GPS points with heights falling within 50 m of the aircraft, as in Skourup et al. (2018). Gridded LiDAR points provide a measurement of absolute surface height. The root mean square deviation of surface height is used to estimate surface roughness,

$$Roughness = \sqrt{\frac{1}{n} \sum_{i=1}^{n} (z_i - \bar{z})^2} \qquad (2)$$

where z_i represents height of the gridded LiDAR surface at n grid points within an ROI and $\bar{z}$ are the mean grid heights within the same ROI. ROI dimensions are described in section 3.4.3.

3.4.3 Multi-scale comparisons

A multi-scale approach is used to evaluate a) the congruence of SAR HH backscatter and MISR NDAI datasets; and b) their quantitative relationships with LiDAR-derived roughness. For a), we create a grid of 1.2 by 1.2 km cells separated by 3.8 km intervals in the overlapping MISR and Sentinel-1 data (n=2407) and extract mean HH backscatter and NDAI. We also manually select cells from this grid that represent homogeneous FYI (n=160), DFYI (n=151), and MYI (n=160), using the Sentinel-1 scene and the 10 April 2017 weekly Canadian Ice Service (CIS) ice chart as reference. For b) we create grid cells of 1.2 km length by 0.4 km width, separated by 0.6 km intervals along the LiDAR flight path (n=129) and extract mean HH backscatter, NDAI, and roughness. Since regression analyses are used in these comparisons, output HH backscatter values are converted to decibel (dB) format to meet the normal distribution assumption.

3.4.4 Decomposition and classification using Sentinel-1 and RADARSAT-2

Volume scattering, particularly from MYI, is known to impact the relationship between roughness and backscatter at C-band frequency (Hallikainen & Winebrenner, 1992). To assess whether dual polarimetric Sentinel-1 can be used to accurately delineate MYI areas, we compute the H-Alpha dual-pol decomposition and apply the Wishart Classification to Sentinel-1 images (Rodrigues et al., 2003; Cloude, 2007; Gill & Yackel, 2012). The following processing chain is used on two 11 April 2017 Sentinel-1 images in SLC format (Table 3.1): i) TOPSAR-Split (to select EW swaths 2-4), ii) radiometric calibration, iii) TOPSAR deburst, iv) polarimetric matrices (C2 coherency matrix), v) polarimetric speckle filter (refined Lee 7x7), vi) polarimetric classification (H-Alpha dual

pol Wishart classification), vii) sub-setting (incidence angle range 30-39°), viii) map projection, and ix) mosaicking. Output classes from the Wishart classifier are collapsed, based on visual inspection, to highlight the separation of MYI from FYI, with class FYI < 3.5 and class MYI ≥ 3.5.

As dual-polarization decompositions are less commonly used and less understood for sea ice applications than decompositions of fully polarimetric datasets, we also process four RADARSAT-2 FQn scenes using the H-A-Alpha decomposition to assess Sentinel-1 decomposition performance (Table 3.1). The available RADARSAT-2 images have incidence angles ranging from 39.6-42.2°. Processing for these decompositions is done by i) radiometric calibration, ii) polarimetric matrices (C3 coherency matrix), iii) polarimetric speckle filter (refined Lee 7x7), iv) polarimetric classification (H-A-Alpha Quad Pol Wishart classification), and v) map projection. The classification product classes are collapsed using the same threshold as the classified Sentinel-1 imagery.

Accuracies of both the dual-pol and quad-pol Wishart classifications are assessed through comparison to 100 random points, which were classified though expert visual inspection of Sentinel-1 HH backscatter (dB) images.

3.5 Results

3.5.1 Broad-scale comparison

The results from our broadscale comparison indicate that HH backscatter and NDAI are generally in agreement except in areas of MYI. We found low values in smooth FYI areas, with HH backscatter and NDAI medians equal to -18.53 dB and -0.04 respectively (Figure 3.3), as well as high values in DFYI areas, with medians equal to -

13.49 dB and 0.01 respectively. In Figure 3.3, the high reach of the interquartile range for HH backscatter is likely due to MYI, where there is a clear difference between the HH backscatter and NDAI. For DFYI, there is a strong significant relationship between HH backscatter and NDAI (R^2 = 0.88; p <0.0001; Figure 3.4), indicating that radar backscatter is related to the reflectance properties of this ice type as captured by the NDAI. Significant relationships between HH backscatter and NDAI are not found for FYI and MYI (Figure B.2).

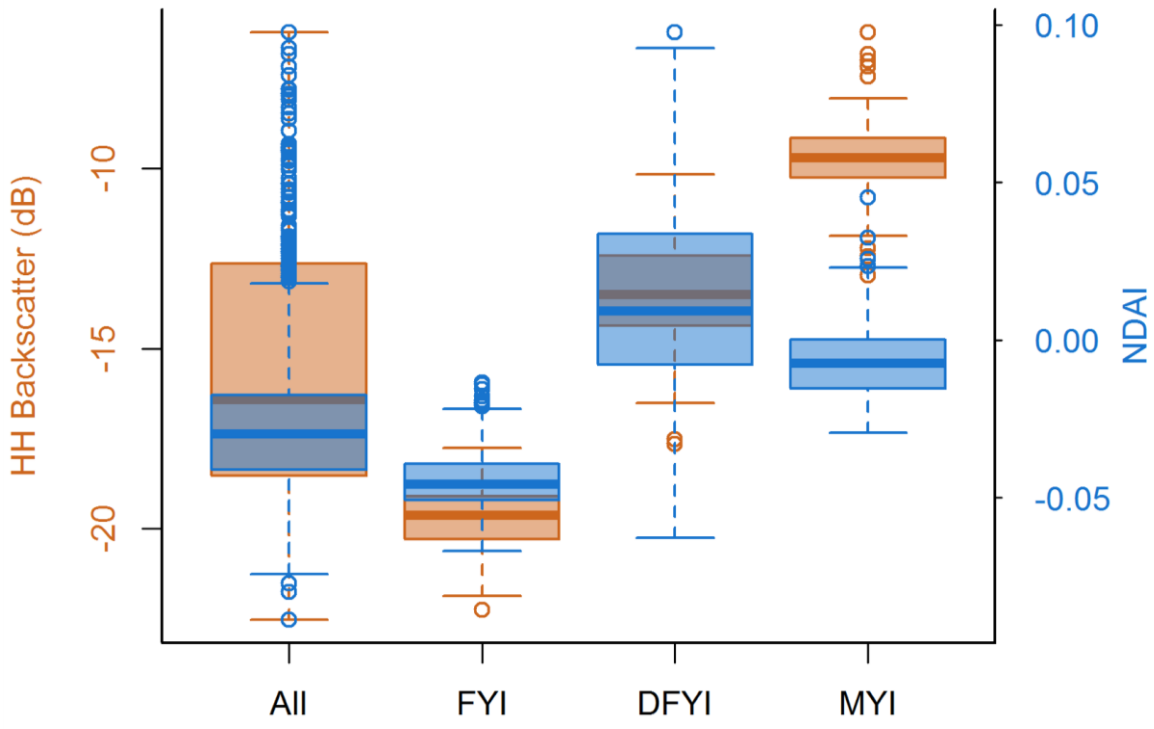

Figure 3.3. Box and whisker plot showing HH backscatter and NDAI by sea ice type.

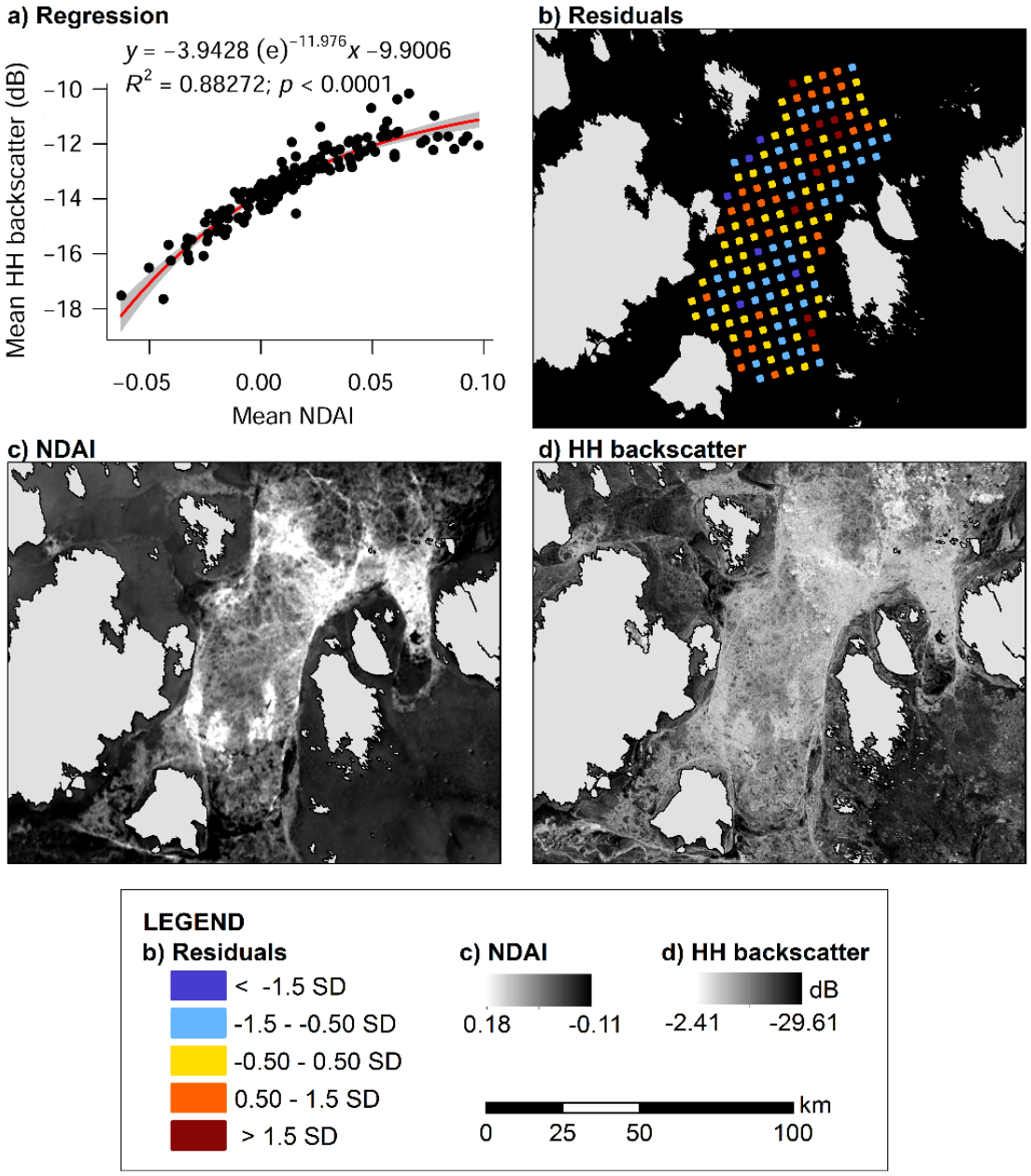

Figure 3.4. For DFYI in Victoria Strait: a) relationship between mean HH backscatter and NDAI; b) standard regression residuals from a) plotted spatially; c) NDAI; and d) HH backscatter.

3.5.2 Fine-scale comparison

HH backscatter and NDAI from FYI have lower values than MYI and mixed ice areas (Figure 3.5). For FYI, NDAI is not significantly related to roughness (Figure 3.6a; R^2 = 0.13, p = 0.07), while for HH backscatter this relationship is significant (Figure 3.6b; R^2 = 0.58, p <0.0001). Conversely, in areas of MYI, NDAI is significantly related to roughness whereas HH backscatter is not (Figure 3.6c-d; R^2 = 0.46, p <0.001 versus R^2 = 0.01, p = 0.54, respectively). Using homogeneous ice types and balanced numbers of FYI and MYI samples, both NDAI and HH backscatter are shown to have similar significant relationships with roughness (Figure 3.6e-f; R^2=0.65 and R^2=0.66 respectively; p <0.0001). An unbalanced approach, using all available samples, showed similar but slightly weaker relationships compared to the balanced approach (NDAI: R^2=0.50, p <0.0001; HH backscatter: R^2=0.55, p <0.0001). When regressed directly using the balanced dataset, HH backscatter can be predicted using NDAI (R^2=0.63, p <0.0001).

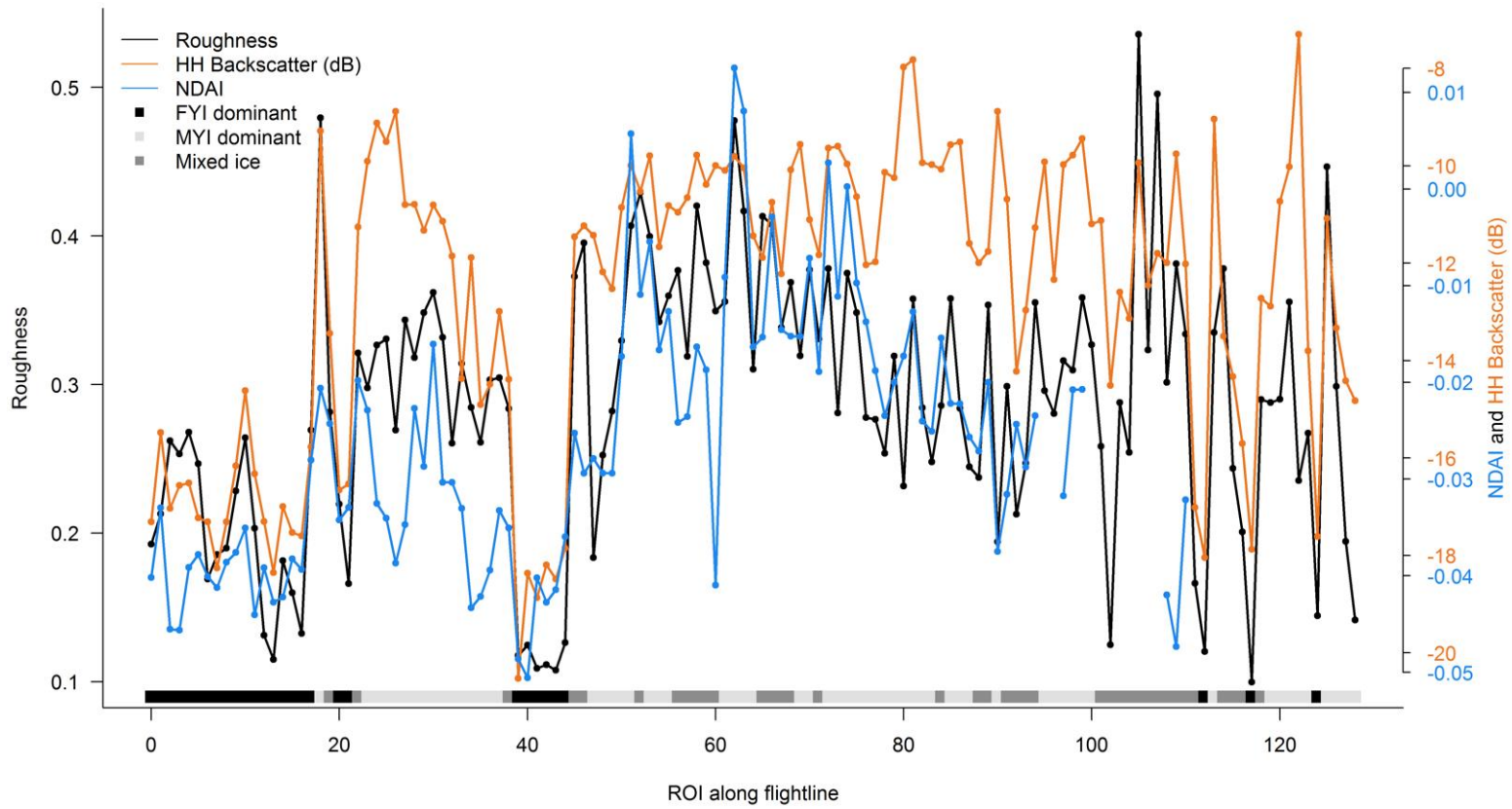

Figure 3.5. Measured sea ice surface roughness (black) compared to Sentinel-1 HH backscatter (orange) and MISR NDAI (blue) along a LiDAR flightline from Victoria Strait to M'Clintock Channel.

The dotted horizontal lines in Figure 3.6 show the NDAI and HH backscatter thresholds used to create pseudo-roughness maps displaying *smooth ice*, *moderately rough ice*, and *rough ice* types (Figure 3.7). Thresholds were determined by visually inspecting the measured roughness along the LiDAR track. Quantitatively, however, each class encompasses a range of measured roughness, with cases of similar roughness measurements falling into different roughness categories (Figure 3.6). Thus, the *moderately rough ice* category provides space between the *smooth ice* and *rough ice* categories. A MYI classification is overlaid on the HH backscatter roughness map (Figure 3.7; see Section 3.5.3). Note that where the Sentinel-1 maps (Figure 3.7b,d) show areas of MYI, NDAI still shows the roughness categories.

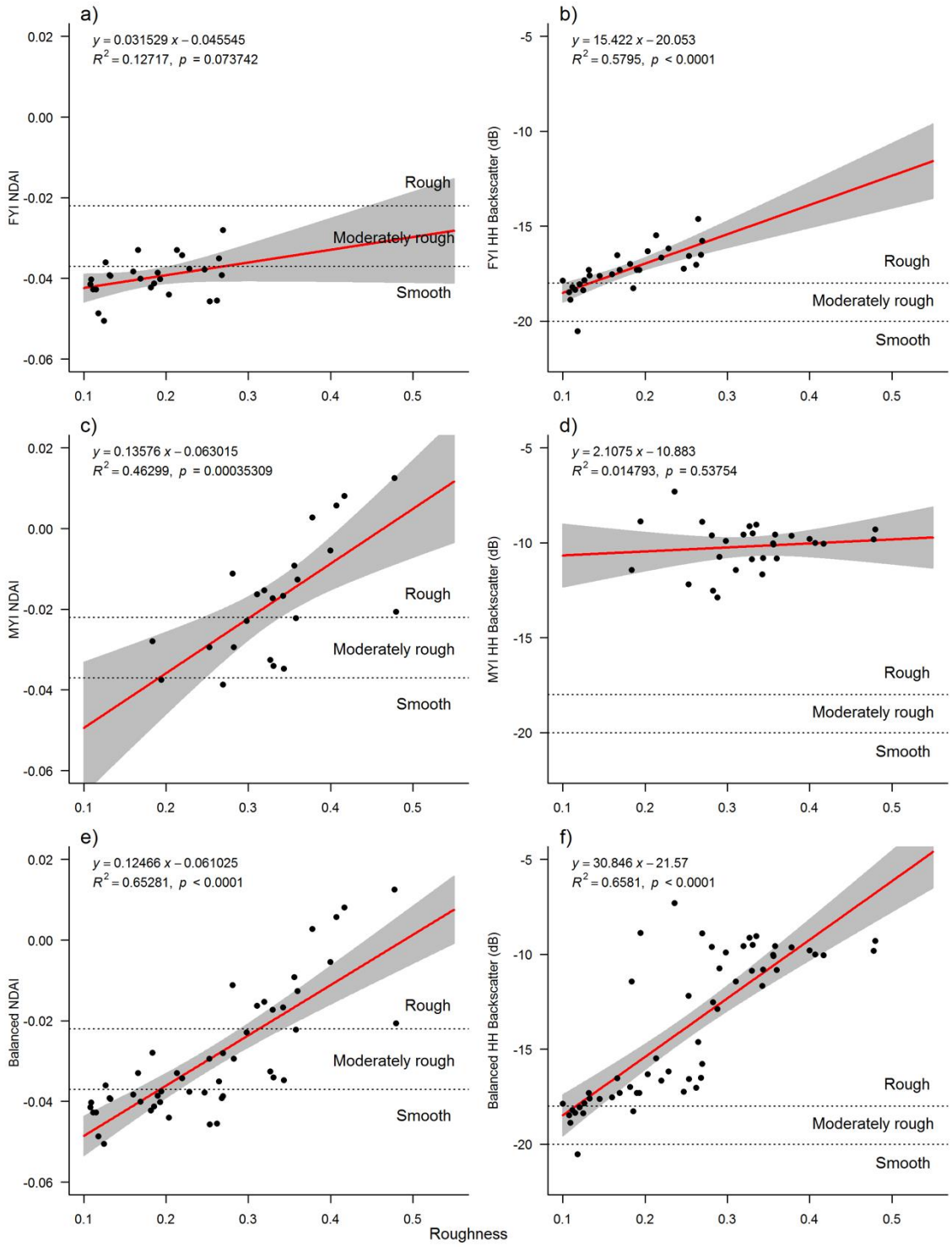

Figure 3.6. Relationship of surface roughness to satellite-derived roughness by ice type: a) NDAI for FYI, b) HH backscatter for FYI, c) NDAI for MYI, d) HH backscatter for MYI, e)

NDAI for a balanced set of ROIs by ice type (N = 29 for FYI and N = 28 for MYI), and f) HH backscatter for a balanced set of ROIs by ice type (*N* = 26 for FYI and *N* = 23 for MYI). Plots show linear regressions with 95% confidence intervals and threshold values (dotted horizontal lines) used for the creation of maps showing *smooth ice, moderately rough ice*, and *rough sea ice.*

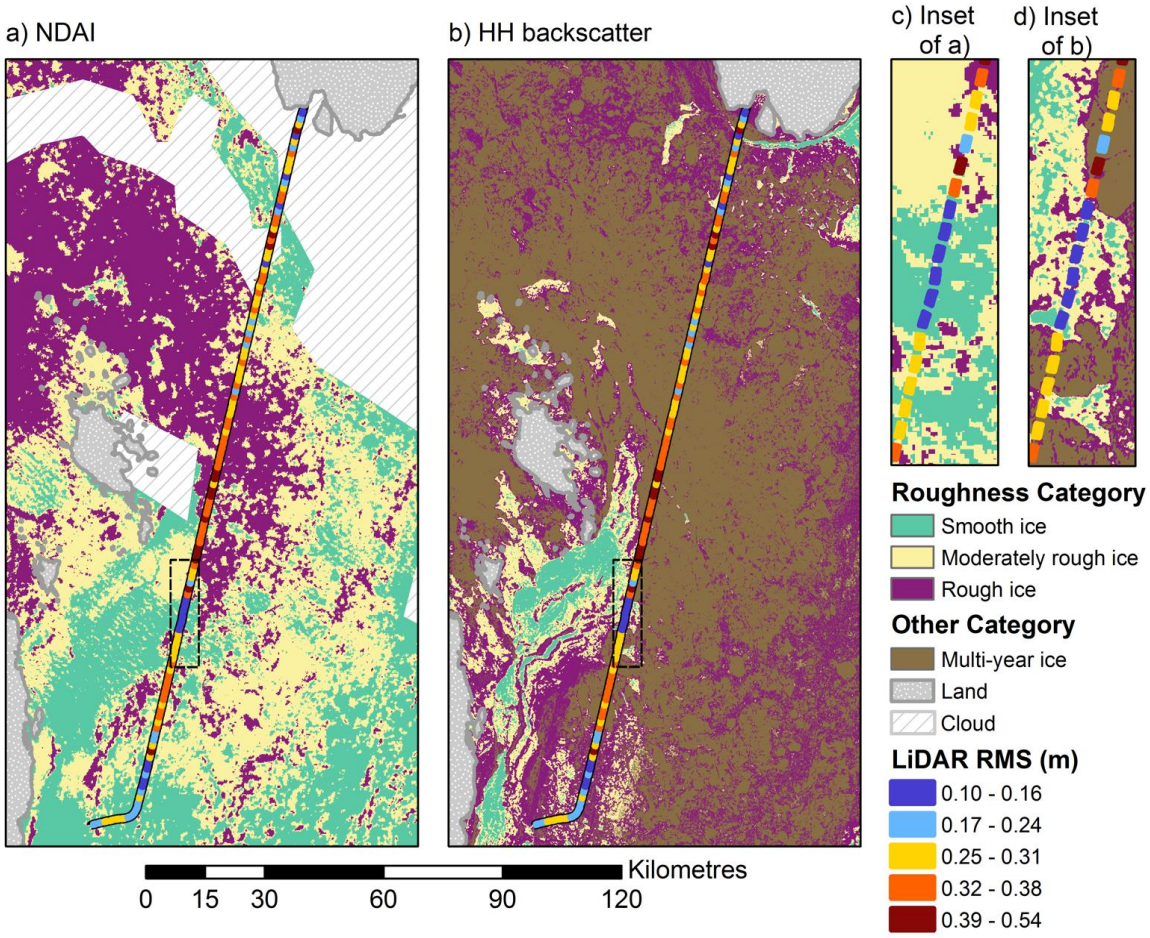

Figure 3.7. Thresholded roughness maps from a) NDAI and b) HH backscatter. Overlaid ROIs show measured roughness along a LiDAR flight path. Insets of c) NDAI and d) HH backscatter, are indicated by a dotted black line.

3.5.3 Roughness indices

Modelled sea ice roughness, rather than thresholded roughness, is also of interest in many contexts because it applies observed relationships to satellite imagery and outputs relevant and relatable data (Dammann et al., 2018b; Gegiuc et al., 2018). The models are based on NDAI- and HH-backscatter relationships to roughness that have R^2 values in the range of 0.65 (Figure 3.6e-f) but should be treated with caution due to their application outside the fine-scale validation range. However, smooth and rough ice areas are generally consistent between sensors, as shown in Figure 3.8. For example, smooth ice ringed by rougher ridges is observed in Queen Maud Gulf, and deformed ice is observed in Victoria Strait. The NDAI-derived roughness is generally higher than HH backscatter-derived roughness in areas of FYI (e.g., Dease Strait and portions of M’Clintock Channel) and DFYI (e.g., Victoria Strait). In areas of MYI, including portions of M’Clintock Channel, the HH backscatter-derived roughness is greater.

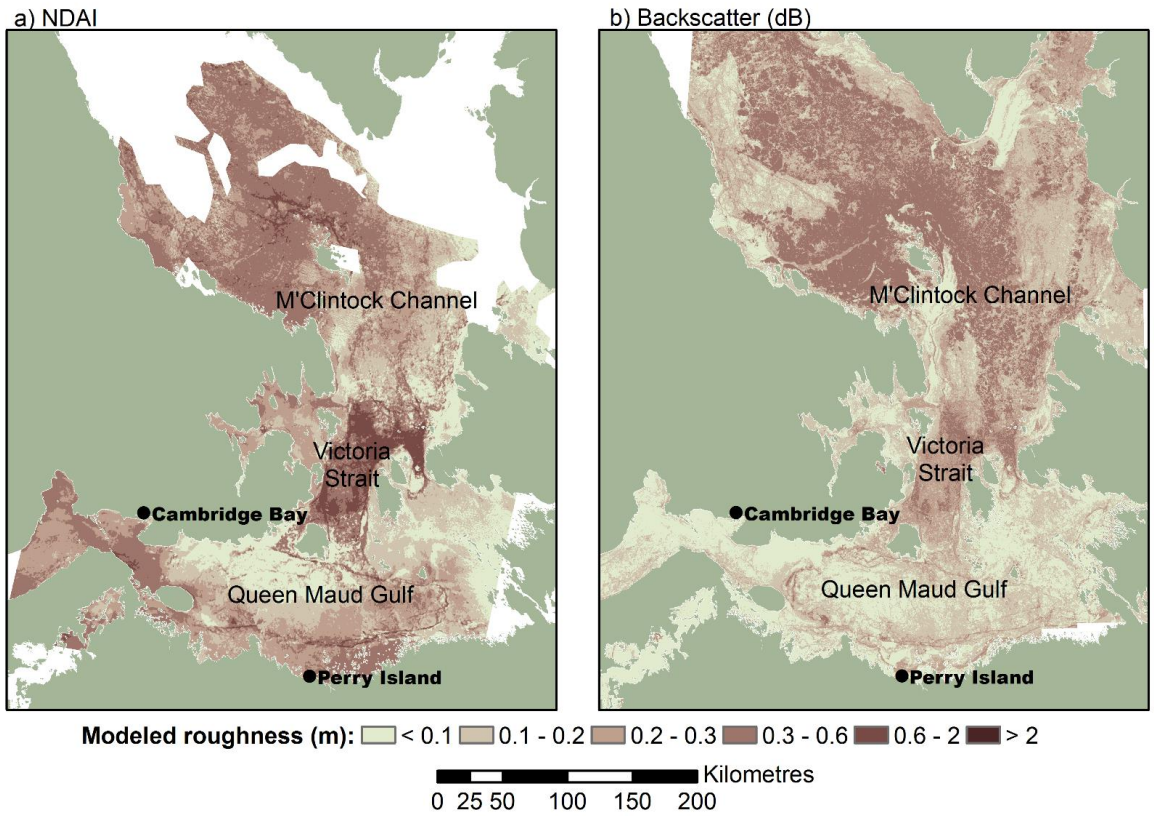

Figure 3.8. Modeled roughness based on regression fits from measured roughness and a) NDAI and b) HH backscatter from Figure 3.6.

3.5.4 Ice type classification

The MYI delineations using Sentinel-1 and RADARSAT-2 classifications are similar, with both producing overall accuracy values of Kappa = 0.83 (Figure 3.9, Table 3.2). There is also generally good agreement with the coarser-scale CIS regional weekly ice chart for the same time period (Figure 3.9c). MYI, seen in Figure 3.9d as bright and (typically) rounded ice floes, qualitatively correspond to the classifications. However, there are differences between the classifications (Figure 3.9e-g). The Sentinel-1 classification identified more MYI than the RADARSAT-2 classification, as seen by the blue colour in Figure 3.9e.

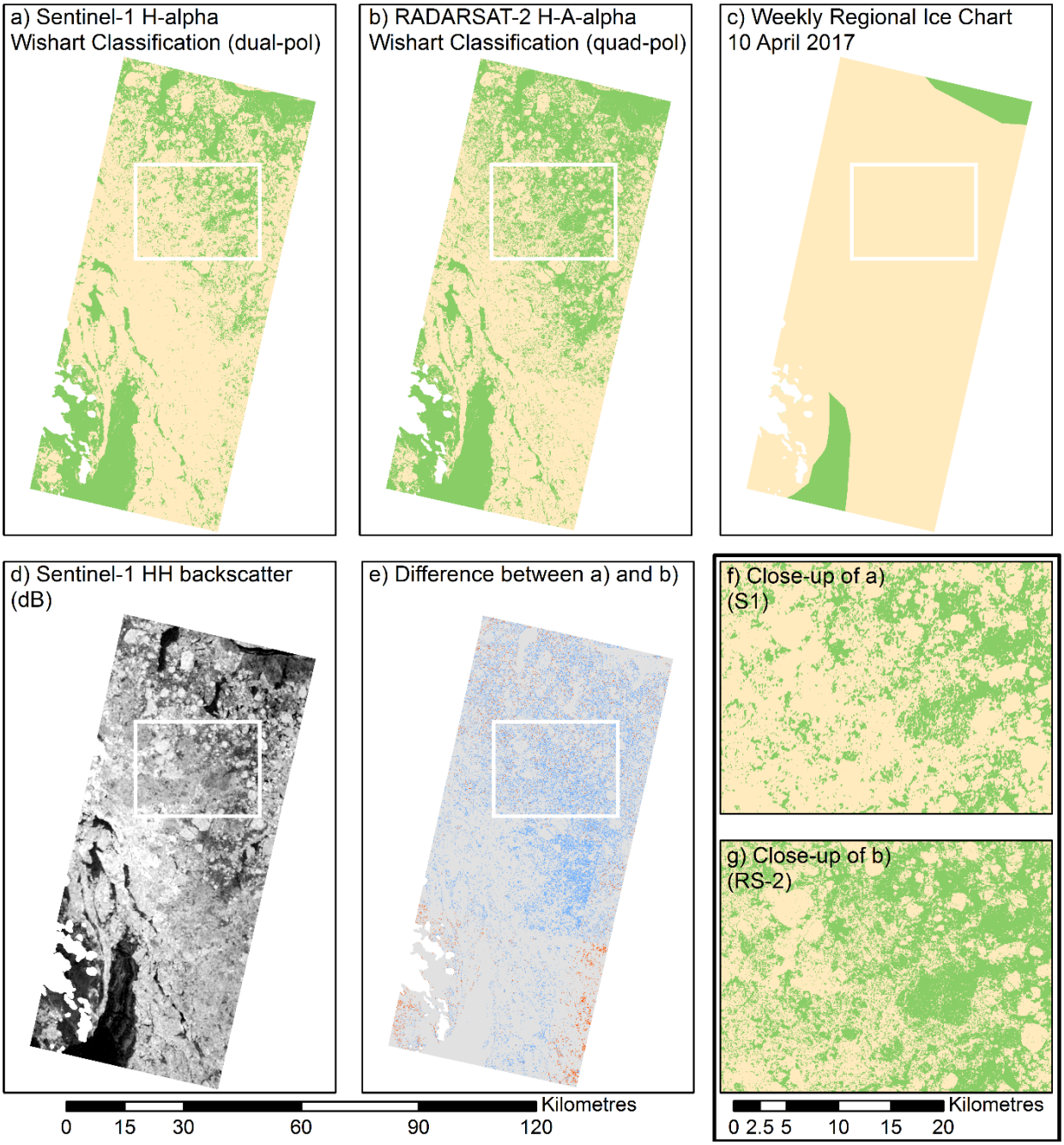

Figure 3.9. Evaluation of a) the Sentinel-1-based H-alpha dual pol Wishart classification and its ability to detect areas of MYI (yellow) and FYI (green). Images are from April 2017 in Victoria Strait. Comparisons are made to: b) the RADARSAT-2-based H-A-alpha quad pol Wishart classification, c) the corresponding weekly regional sea ice chart produced by the Canadian Ice Service; and d) Sentinel-1 HH backscatter (in dB). In e) the difference

between the a) and b) is shown, with grey representing areas where the two classifications agree, and blue (red) representing areas where Sentinel-1 found MYI (FYI) but RADARSAT-2 found FYI (MYI). Images f) and g) are insets of a) and b) respectively, denoted by the white boxes in the outset images.

Table 3.2. Confusion matrices for MYI detection using a H-alpha Wishart classification on Sentinel-1 imagery (dual-pol) and H-A-alpha Wishart classification on RADARSAT-2 imagery (quad-pol). Producer's accuracy measures the probability of omission error whereas user's accuracy measures commission error. Kappa is a measure of actual vs. chance agreement in the classification, as calculated in Congalton (1991).

Classification	Class	MYI	FYI	User's Accuracy	Kappa
Dual-pol	MYI	59	8	0.881	
	FYI	0	32	1	
	Producer's accuracy	1	0.8	0.919	
	Kappa				0.827
Quad-pol	MYI	55	4	0.932	
	FYI	4	36	0.9	
	Producer's accuracy	0.932	0.9	0.919	
	Kappa				0.832

3.6 Discussion

3.6.1 MISR NDAI

NDAI is comparable across snow-covered ice regimes as MISR has also been used to study Greenland ice sheets, Antarctic sea ice, and an Antarctic ice shelf (Li, 2018; Nolin et al., 2001). Unfortunately, data about expected NDAI values in cryospheric environments are not readily available. Nolin et al. (2002) and Nolin & Payne (2007) found that NDAI and LiDAR roughness from glacier ice are strongly related, with R^2 values of 0.27 – 0.74 and correlations approaching $r = 0.9$ (except in areas of smooth ice;

r = 0.1), respectively. Better functionality of MISR NDAI for rougher surfaces is also seen in our study, with significant relationships found for MYI between NDAI and roughness, and for DFYI between NDAI and HH backscatter. Insignificant relationships in FYI may be due in part to low roughness levels that are difficult to detect using reflectance variations.

More research is needed to understand the sub-pixel geophysical properties like feature spatial scale, orientation, and solar illumination that impact angular MISR datasets, and the effects of different multi-angle techniques on roughness calculations. For sea ice environments this means that accounting for snow properties (e.g., grain size and density) as well as feature distributions and orientations (e.g., of snow dunes and sastrugi) will likely lead to stronger and more consistent relationships with sea ice roughness. Better understanding of sub-pixel geophysical properties may also help reconcile the findings of two studies that observed different relationships with roughness using MISR-based (but not NDAI-based) techniques, described below.

Using a nearest neighbor approach within an optimal prediction radius, Nolin & Mar (2019) found that their MISR-based roughness calculations are more strongly related to measured roughness over smooth sea ice (0-20 cm; R^2 = 0.52) than rough sea ice (0-100 cm; R^2 = 0.39) in the Beaufort Sea. The same study also found that MISR-based roughness has about half the variance of LiDAR-based roughness, especially in areas of roughness exceeding 20 cm. This discrepancy may be due to Nolin & Mar's LiDAR-MISR comparison methods, inclusion of the nadir camera angle, the application to a different and potentially mobile ice regime, or sub-pixel influences that are not yet fully understood.

Contradictions in MISR observations of roughness were also found in a study of Chinese dunes (Wu et al., 2009). Their site with the least macroscale roughness and Aeolian sandy soils had more backward scattering than the rougher sites with small coarse-grain sand dunes and Aeolian sandy soils. Wu et al. concluded that rough surfaces usually, but not always, produce more backward scattering than smooth surfaces. Exceptions may be due to sub-pixel sand ripples (which rise and fall vertically) and the orientation of dune facets that modify the angular pattern of reflectance.

3.6.2 Sentinel-1 HH backscatter

As expected, HH backscatter from smooth FYI has low values and a small range, meaning that high backscatter from DFYI may be separated with minimal overlap between the two categories. Results from this study, and previous studies covering various Arctic regions, show that HH backscatter from FYI generally increases with increasing deformation (Table A.2). HH backscatter values for FYI and DFYI within and near the Canadian Arctic Archipelago (CAA) are remarkably similar to this study, and extrapolation of our mapping methods to this region may be possible with minimal modification. However, contextual knowledge is critical because SAR backscatter is influenced by a number of parameters in addition to surface roughness, including the local radar beam incidence angle (at scales greater than the wavelength), inhomogeneities in the ice (e.g., air bubbles, cracks, crystal structure), orientation of ice features, dielectric properties including brine in snow and brine at the snow-sea ice interface, the signal to noise ratio, as well as frequency, polarization, and spatial resolution (Dierking & Dall, 2007). Other regions or ice types may require specialised datasets for mapping surface properties; for example, to map Koksoak River ice near the community of Kuujjuaq,

Gauther et al. (2010) required fine-scale radar, hydrographic vectors, and digital elevation models.

Low MYI salinity allows C-band SAR to penetrate the upper sea ice volume, where scattering occurs from air bubbles and other particles within the sea ice volume; this results in consistently high backscatter regardless of surface roughness (Geldsetzer & Yackel, 2009; Hallikainen & Winebrenner, 1992; Kim et al., 1984; Perovich et al., 1998). The salinity of MYI is typically much lower than FYI, in the range of 0.1-3 ppt for MYI compared to 5-8 ppt for 1-2 m thick FYI (Weeks, 1981) due to desalination processes that occur at warmer (summer) temperatures. Freshened sea ice due to riverine inputs also behaves similarly, as identified in Chapter 2.

Marking the spatial extent of MYI and riverine output areas could be an alternative to using optical-derived roughness indices, because travelers have a wealth of contextual information about MYI navigation. Using the Sentinel-1 H-alpha Wishart Classification we found evidence that MYI areas are identifiable during the winter (pre-melt) period. Similarly, Englebrecht et al. (2017) compared a Sentinel-1 H-alpha decomposition to a RADARSAT-2 H-A-alpha decomposition for the purpose of mapping burned zones, and found that changes could be detected using either sensor. The use of Sentinel-1 polarimetry to identify ice type is opportune because the freshened ice can be separated from FYI areas using the same images as the roughness classification, resulting in temporally and spatially-cohesive information. However, while we found similar classification accuracy for Sentinel-1 and RADARSAT-2 (Kappa = 0.83 for both sensors), Englebrecht et al. (2017) found that Sentinel-1 had lower overall accuracy and Kappa values than RADARSAT-2 by ~3% and 0.15 respectively, possibly due to dual-

pol scattering mechanism separation difficulties. Further research is necessary to confirm that our findings are scalable and applicable to riverine output areas, as high noise effects and artefacts in the HV channel may be problematic.

3.6.3 Impact of snow

Snowmobile trafficability is impacted by a combination of snow and ice surface roughness. As an optical sensor, MISR views reflectance at the snow surface, provided there is no atmospheric interference. Unfortunately, Sentinel-1 C-band SAR penetrates through cold and dry snow to the sea ice. Consequently, areas with ice rubble covered by snow may remain rough according to C-band SAR (Manninen, 1997), but are actually perceived as smooth, trafficable surfaces by travelers. Conversely, wind-roughened snow decreases trafficability. This roughening may or may not increase SAR roughness (Manninen, 1997): microwave sensors can be impacted by snow properties (e.g., density, grain size, salinity, temperature, ice crusts) (Johansson et al., 2017; Perovich et al., 1998). Snow and the upper ice layers are systematically related, but only coarse estimates of ice roughness can be made from surface measurements (Manninen, 1997), and mismatches between the snow and sea ice surface will decrease the accuracy of SAR-based roughness maps.

There is currently no efficient and cost-effective method for using satellites to measure on-ice snow depth at the fine scales (<~300 m) desired to improve sea ice roughness maps for community use. However, snow depth has been estimated at larger scales using passive microwave data (Rostosky et al., 2018), Ku- and Ka-band altimeters (Lawrence et al., 2018), or at small temporal scales using airborne or in-situ studies (e.g., using Operation IceBridge data) (Kurtz & Farrell, 2011; Lawrence et al., 2018; Newman

et al., 2014). However, the knowledge of a) prevailing winds, which redistribute snow; b) location, as the central Arctic has very thin snow depths (Newman et al., 2014); c) ice type, as smooth FYI generally has shallower snow depths than DFYI and MYI (Kurtz & Farrell, 2011; Newman et al., 2014), and d) date, as snow accumulates over the season; all allow experienced sea ice users to infer probable snow coverage. In situ measurements show a mean snow depth on smooth FYI of ~8 cm at Cambridge Bay between October and May, deceasing by ~0.8 cm/year (1960-2014), with linear growth over the season, peaking in May (Howell et al., 2016).

3.6.4 Other data and recommendations

This study focuses on evaluating available datasets for the purpose of providing information to communities. Other satellites or satellite modes that are available for a cost would offer other benefits. For example, northern sea ice users would benefit from high-resolution data. While the spatial resolution of open-access Sentinel-1 images in this region (40 m) is significantly higher than the MISR images (275 m), both provide data at scales useful for investigating roughness. However, with higher resolution datasets, information from small-scale roughness features like pressure ridges and other features (e.g., ice cracks) could be resolved. These finer-scale features also impact trafficability and safety, as features like pressure ridges may not be crossable along their entire length.

Other data types like multi-angle and stereo-pair imagery, or other radar frequencies like L- and X-bands, also offer the potential to provide information on sea ice roughness (Table A.3). However, there are currently no other radar frequencies with freely available data or as extensive a research history for sea ice mapping applications as C-band. See Appendix B section B.5 for a discussion of current and near-future satellite

datasets that may be useful (high quality and/or affordable) for providing sea ice surface trafficability information to northern communities.

3.7 Conclusions

The MISR and Sentinel-1 roughness proxies, NDAI and HH polarization backscatter respectively, show similar spatial patterns of roughness and are significantly related to measured roughness, with R^2 = 0.65 and 0.66 for balanced samples of FYI and MYI types (p < 0.0001). Maps displaying *smooth ice, moderately rough ice,* and *rough ice* types based on thresholded NDAI and HH backscatter reveal that it is possible to create clear and simple products for use by northerners from open-access datasets. Overlaying a *multi-year ice* layer on the HH backscatter map provides extra utility and accuracy.

Roughness map advantages and limitations are associated with sensor type and geophysical context. MISR NDAI can show freshened ice roughness and has the potential to be adapted for freshwater ice environments like Arctic lakes or Antarctica. Sentinel-1 HH backscatter has a finer spatial scale, wider temporal availability, is not impacted by clouds, and is more accurate for FYI roughness. MISR NDAI is not a good roughness proxy for relatively smooth FYI, and is limited by atmospheric conditions (e.g., clouds, darkness). Sentinel-1 HH backscatter is not a good roughness proxy in freshened ice (e.g., MYI, riverine output), or where the snow roughness differs from ice roughness.

Future qualitative and quantitative data collection would be useful for further refining the roughness thresholds considered trafficable in northern communities. The collection and analysis of high-resolution validation data close to the focus communities, as well as an evaluation of higher resolution (i.e., <40m) and complimentary datasets

(e.g., RCM, X-and L-band SAR, multispectral) would provide additional data for understanding of community-scale sea ice roughness. Further analysis could also address other identified information needs like ice fractures and slush/water on ice (Chapter 2; Scharien et al., 2017).

3.8 References

Aporta, C. (2004). Routes, trails and tracks: Trail breaking among the Inuit of Igloolik. *Études/Inuit/Studies*, *28*(2), 9–38. https://doi.org/10.7202/013194ar

Beckers, J. F., Renner, A. H. H., Spreen, G., Gerland, S., & Haas, C. (2015). Sea-ice surface roughness estimates from airborne laser scanner and laser altimeter observations in Fram Strait and north of Svalbard. *Annals of Glaciology*, *56*(69), 235–244. https://doi.org/10.3189/2015AoG69A717

Bell, T., Briggs, R., Bachmayer, R., & Li, S. (2014). Augmenting Inuit knowledge for safe sea-ice travel: The SmartICE information system. In *Oceans - St. John's, 2014* (pp. 1–9). https://doi.org/10.1109/OCEANS.2014.7003290

Bertoia, C., Falkingham, J., & Fetterer, F. (1998). Polar SAR data for operational sea ice mapping. In *Analysis of SAR data of the polar oceans* (pp. 201–234). Springer Berlin Heidelberg. https://doi.org/10.1007/978-3-642-60282-5_10

Chust, G., & Sagarminaga, Y. (2007). The multi-angle view of MISR detects oil slicks under sun glitter conditions. *Remote Sensing of Environment*, *107*(1–2), 232–239. https://doi.org/10.1016/j.rse.2006.09.024

Cloude, S. (2007). The dual polarisation entropy/alpha decomposition: A PALSAR case study. *Proceedings of the 3rd International Workshop on Science and Applications of SAR Polarimetry and Polarimetric Interferometry*, 1–6.

Congalton, R. G. (1991). A review of assessing the accuracy of classifications of remotely sensed data. *Remote Sensing of Environment*, *37*(1), 35–46. https://doi.org/10.1016/0034-4257(91)90048-B

Dammann, D. O., Eicken, H., Mahoney, A. R., Meyer, F. J., Freymueller, J. T., & Kaufman, A. M. (2018a). Evaluating landfast sea ice stress and fracture in support of operations on sea ice using SAR interferometry. *Cold Regions Science and Technology*, *149*, 51–64. https://doi.org/10.1016/j.coldregions.2018.02.001

Dammann, D. O., Eicken, H., Mahoney, A. R., Saiet, E., Meyer, F. J., & George, J. C. "Craig." (2018b). Traversing sea ice: Linking surface roughness and ice trafficability through SAR polarimetry and interferometry. *IEEE Journal of Selected Topics in Applied Earth Observations and Remote Sensing*, *PP*(99), 1–18. https://doi.org/10.1109/JSTARS.2017.2764961

Dierking, W., & Dall, J. (2007). Sea-ice deformation state from synthetic aperture radar imagery—Part I: Comparison of C- and L-band and different polarization. *IEEE Transactions on Geoscience and Remote Sensing*, *45*(11), 3610–3622. https://doi.org/10.1109/TGRS.2007.903711

Diner, D. J., Beckert, J. C., Bothwell, G. W., & Rodriguez, J. I. (2002). Performance of the MISR instrument during its first 20 months in Earth orbit. *IEEE Transactions on Geoscience and Remote Sensing*, *40*(7), 1449–1466. https://doi.org/10.1109/TGRS.2002.801584

Druckenmiller, M. L., Eicken, H., George, J. C. "Craig," & Brower, L. (2013). Trails to the whale: Reflections of change and choice on an Iñupiat icescape at Barrow, Alaska. *Polar Geography*, *36*(1–2), 5–29. https://doi.org/10.1080/1088937X.2012.724459

Eicken, H., Lovecraft, A. L., & Druckenmiller, M. L. (2009). Sea-ice system services: A framework to help identify and meet information needs relevant for observing networks. *Arctic*, *62*(2), 119–136. https://doi.org/10.14430/arctic126

Engelbrecht, J., Theron, A., Vhengani, L., & Kemp, J. (2017). A simple normalized difference approach to burnt area mapping using multi-polarisation C-band SAR. *Remote Sensing*, *9*(8), 764. https://doi.org/10.3390/rs9080764

ESA. (2018a). Observation scenario archive - Sentinel-1 - Sentinel Online. Retrieved April 21, 2018, from https://sentinel.esa.int/web/sentinel/missions/sentinel-1/observation-scenario

ESA. (2018b). Sentinel-1 SAR User guide introduction. Retrieved October 4, 2018, from https://sentinel.esa.int/web/sentinel/user-guides/sentinel-1-sar

Ford, J. D., Pearce, T., Gilligan, J., Smit, B., & Oakes, J. (2008). Climate change and hazards associated with ice use in Northern Canada. *Arctic, Antarctic, and Alpine Research*, *40*(4), 647–659. https://doi.org/10.1657/1523-0430(07-040)[FORD]2.0.CO;2

Fors, A. S., Brekke, C., Gerland, S., Doulgeris, A. P., & Beckers, J. F. (2016). Late summer Arctic sea ice surface roughness signatures in C-Band SAR data. *IEEE Journal of Selected Topics in Applied Earth Observations and Remote Sensing*, *9*(3), 1199–1215. https://doi.org/10.1109/JSTARS.2015.2504384

Frost, K. J., Lowry, L. F., Pendleton, G., & Nute, H. R. (2004). Factors affecting the observed densities of ringed seals, Phoca hispida, in the Alaskan Beaufort Sea, 1996-99. *Arctic*, *57*(2), 115–128.

Gauthier, Y., Tremblay, M., Bernier, M., & Furgal, C. (2010). Adaptation of a radar-based river ice mapping technology to the Nunavik context. *Canadian Journal of Remote Sensing*, *36*(S1), S168–S185. https://doi.org/10.5589/m10-018

Gegiuc, A., Similä, M., Karvonen, J., Lensu, M., Mäkynen, M., & Vainio, J. (2018). Estimation of degree of sea ice ridging based on dual-polarized C-band SAR data. *The Cryosphere*, *12*(1), 343–364. https://doi.org/10.5194/tc-12-343-2018

Geldsetzer, T., & Yackel, J. J. (2009). Sea ice type and open water discrimination using dual co-polarized C-band SAR. *Canadian Journal of Remote Sensing*, *35*(1), 73–84. https://doi.org/10.5589/m08-075

Hallikainen, M., & Winebrenner, D. P. (1992). The physical basis for sea ice remote sensing. In *Microwave remote sensing of sea ice* (pp. 29–46). American Geophysical Union. https://doi.org/10.1029/GM068p0029

Hong, S., & Shin, I. (2010). Global trends of sea ice: Small-scale roughness and refractive index. *Journal of Climate*, *23*(17), 4669–4676. https://doi.org/10.1175/2010JCLI3697.1

Horner, R., Ackley, StephenF., Dieckmann, GerhardS., Gulliksen, B., Hoshiai, T., Legendre, L., … Sullivan, CorneliusW. (1992). Ecology of sea ice biota: 1. Habitat, terminology, and methodology. *Polar Biology*, *12*(3–4). https://doi.org/10.1007/BF00243113

Howell, S. E. L., Laliberté, F., Kwok, R., Derksen, C., & King, J. (2016). Landfast ice thickness in the Canadian Arctic Archipelago from observations and models. *The Cryosphere*, *10*(4), 1463–1475. https://doi.org/10.5194/tc-10-1463-2016

Johansson, A. M., King, J. A., Doulgeris, A. P., Gerland, S., Singha, S., Spreen, G., & Busche, T. (2017). Combined observations of Arctic sea ice with near-coincident colocated X-band, C-band, and L-band SAR satellite remote sensing and helicopter-borne measurements. *Journal of Geophysical Research: Oceans*, *122*(1), 669–691. https://doi.org/10.1002/2016JC012273

Katlein, C., Arndt, S., Nicolaus, M., Perovich, D. K., Jakuba, M. V., Suman, S., … German, C. R. (2015). Influence of ice thickness and surface properties on light transmission through Arctic sea ice: Light transmission in Arctic sea ice. *Journal of Geophysical Research: Oceans*, *120*(9), 5932–5944. https://doi.org/10.1002/2015JC010914

Kim, Y.-S., Moore, R. K., & Onstott, R. G. (1984). *Theoretical and experimental study of radar backscatter from sea ice* (Technical Report No. RSL-TR 331-37) (p. 168). Lawrence, Kansas: Remote Sensing Laboratory, University of Kansas.

Krupnik, I., & Jolly, D. (2002). *The Earth is faster now: Indigenous observations of Arctic environment change*. Arctic Research Consortium of the United States.

Kurtz, N. T., & Farrell, S. L. (2011). Large-scale surveys of snow depth on Arctic sea ice from Operation IceBridge. *Geophysical Research Letters*, *38*(20), n/a-n/a. https://doi.org/10.1029/2011GL049216

Laidler, G. J., Hirose, T., Kapfer, M., Ikummaq, T., Joamie, E., & Elee, P. (2011). Evaluating the Floe Edge Service: How well can SAR imagery address Inuit community concerns around sea ice change and travel safety? *Canadian Geographer / Le Géographe Canadien*, *55*(1), 91–107. https://doi.org/10.1111/j.1541-0064.2010.00347.x

Landy, J. C., Isleifson, D., Komarov, A. S., & Barber, D. G. (2015). Parameterization of centimeter-scale sea ice surface roughness using terrestrial LiDAR. *IEEE Transactions on Geoscience and Remote Sensing*, *53*(3), 1271–1286. https://doi.org/10.1109/TGRS.2014.2336833

Lawrence, I. R., Tsamados, M. C., Stroeve, J. C., Armitage, T. W. K., & Ridout, A. L. (2018). Estimating snow depth over Arctic sea ice from calibrated dual-frequency radar freeboards. *The Cryosphere*, *12*(11), 3551–3564. https://doi.org/10.5194/tc-12-3551-2018

Li, Y. (2018). *Sea ice and ice sheet surface roughness characterization and its effects on bi-directional reflectance* (Thesis). Texas A & M University, College Station, Texas. Retrieved from https://oaktrust.library.tamu.edu/handle/1969.1/173578

Manninen, A. T. (1997). Surface roughness of Baltic sea ice. *Journal of Geophysical Research: Oceans*, *102*(C1), 1119–1139. https://doi.org/10.1029/96JC02991

Martin, T., Tsamados, M., Schroeder, D., & Feltham, D. L. (2016). The impact of variable sea ice roughness on changes in Arctic Ocean surface stress: A model study: Arctic ocean surface stress. *Journal of Geophysical Research: Oceans*, *121*(3), 1931–1952. https://doi.org/10.1002/2015JC011186

National Snow and Ice Data Center. (2018). Terra vs. Aqua. Retrieved October 23, 2018, from https://nsidc.org/data/modis/terra_aqua_differences

Newman, T., Farrell, S. L., Richter-Menge, J. A., Conner, L. N., Kurtz, N. T., Elder, B. C., & McAdoo, D. (2014). Assessment of radar- derived snow depth over Arctic sea ice. *Journal of Geophysical Research: Oceans*, *119*(12), 8578–8602. https://doi.org/10.1002/2014JC010284

Nolin, A. W. (2004). Towards retrieval of forest cover density over snow from the Multi-angle Imaging SpectroRadiometer (MISR). *Hydrological Processes*, *18*(18), 3623–3636. https://doi.org/10.1002/hyp.5803

Nolin, A. W., Fetterer, F. M., & Scambos, T. A. (2002). Surface roughness characterizations of sea ice and ice sheets: Case studies with MISR data. *IEEE Transactions on Geoscience and Remote Sensing*, *40*(7), 1605–1615. https://doi.org/10.1109/TGRS.2002.801581

Nolin, A. W., & Mar, E. (2019). Arctic sea ice surface roughness estimated from multi-angular reflectance satellite imagery. *Remote Sensing*, *11*(1), 50. https://doi.org/10.3390/rs11010050

Nolin, A. W., & Payne, M. C. (2007). Classification of glacier zones in western Greenland using albedo and surface roughness from the Multi-angle Imaging SpectroRadiometer (MISR). *Remote Sensing of Environment*, *107*(1–2), 264–275. https://doi.org/10.1016/j.rse.2006.11.004

Nolin, A. W., Stroeve, J. C., Scambos, T. A., & Fetterer, F. (2001). Cryospheric applications of MISR data. In *IGARSS 2001. Scanning the present and resolving the future. Proceedings. IEEE 2001 International Geoscience and Remote Sensing Symposium (Cat. No.01CH37217)* (Vol. 3, pp. 1219–1221 vol.3). https://doi.org/10.1109/IGARSS.2001.976798

Perovich, D. K., Longacre, J., Barber, D. G., Maffione, R. A., Cota, G. F., Mobley, C. D., … Roesler, C. S. (1998). Field observations of the electromagnetic properties of first-year sea ice. *IEEE Transactions on Geoscience and Remote Sensing*, *36*(5), 1705–1715. https://doi.org/10.1109/36.718639

Petty, A. A., Tsamados, M. C., & Kurtz, N. T. (2017). Atmospheric form drag coefficients over Arctic sea ice using remotely sensed ice topography data, spring 2009-2015. *Journal of Geophysical Research: Earth Surface*, *122*, 1472–1490.

Petty, A. A., Tsamados, M. C., Kurtz, N. T., Farrell, S. L., Newman, T., Harbeck, J. P., … Richter-Menge, J. A. (2016). Characterizing Arctic sea ice topography using high-resolution IceBridge data. *The Cryosphere*, 19.

Rahman, H., & Dedieu, G. (1994). SMAC: A simplified method for the atmospheric correction of satellite measurements in the solar spectrum. *International Journal of Remote Sensing*, *15*(1), 123–143. https://doi.org/10.1080/01431169408954055

Rodrigues, A., Corr, D., Partington, K., Pottier, E., & Ferro-Famil, L. (2003). Unsupervised Wishart Classifications of Sea-Ice using Entropy, Alpha and Anisotropy decompositions. *Proceedings of POLinSAR 2003*, 1-6. Frascati, Italy.

Rostosky, P., Spreen, G., Farrell, S. L., Frost, T., Heygster, G., & Melsheimer, C. (2018). Snow depth retrieval on Arctic sea ice from passive microwave radiometers - Improvements and extensions to multiyear ice using lower frequencies. *Journal of Geophysical Research: Oceans*, *123*(10), 7120–7138. https://doi.org/10.1029/2018JC014028

Scharien, R. K., Segal, R., Nasonova, S., Nandan, V., Howell, S. E. L., & Haas, C. (2017). Winter Sentinel-1 backscatter as a predictor of spring Arctic sea ice melt pond fraction. *Geophysical Research Letters*, *44*(24), 12,262-12,270. https://doi.org/10.1002/2017GL075547

Schröder, D., Feltham, D. L., Flocco, D., & Tsamados, M. (2014). September Arctic sea-ice minimum predicted by spring melt-pond fraction. *Nature Climate Change*, *4*(5), 353–357. https://doi.org/10.1038/nclimate2203

Similä, M., Mäkynen, M., & Heiler, I. (2010). Comparison between C band synthetic aperture radar and 3-D laser scanner statistics for the Baltic Sea ice. *Journal of Geophysical Research: Oceans*, *115*(C10). https://doi.org/10.1029/2009JC005970

Skourup, H., Simonsen, S. B., Sørensen, S. L., Helm, V., Hvidegaard, S. M., Bella, D. A., & Forsberg, R. (2018). *ESA CryoVEx/EU ICE-ARC 2016: Airborne field campaign with ASIRAS radar and laser scanner over Austfonna, Fram Strait and the Wandel Sea* (Technical Report No. ESA Contract No. 4000110600/14/NL/FF/lf (CCN3)) (p. 70). Lyngby, Denmark: DTU Space, National Space Institute, Dansih Technical University. Retrieved from https://earth.esa.int/documents/10174/134665/CryoVEx-Spring-2016-final-report

Weeks, W. F. (1981). Sea ice: The potential of remote sensing. *Oceanus*, *24*, 39–48.

Weeks, W. F., & Ackley, S. F. (1982). *The Growth, Structure, and Properties of Sea Ice* (CRREL Monograph 82-1) (p. 136). Hanover, NH: National Technical Information Service.

Wessel, P., & Smith, W. H. F. (1996). A global, self-consistent, hierarchical, high-resolution shoreline database. *Journal of Geophysical Research: Solid Earth*, *101*(B4), 8741–8743. https://doi.org/10.1029/96JB00104

Wu, Y., Gong, P., Liu, Q., & Chappell, A. (2009). Retrieving photometric properties of desert surfaces in China using the Hapke model and MISR data. *Remote Sensing of Environment*, *113*(1), 213–223. https://doi.org/10.1016/j.rse.2008.09.006

Chapter 4 - Conclusions

Remote sensing products showing sea ice features at scales that impact sea ice trafficability have been requested by sea ice users both within and outside the Western Canadian Arctic (Bell et al., 2014; Dammann et al., 2018; Laidler et al., 2011; Panikkar et al., 2018). Generation of data products that assist on-ice trafficability is dependent on sustained collaboration where information needs and relevant metrics are described and assessed by local sea ice users, and improvements in technology and data interoperability that increasingly allow for the production of customised products and product sharing techniques (Knol et al., 2018). A key step in product development is ensuring that quality products are created, with accuracies that are understood. For the condition of sea ice surface roughness, investigating two very different sensors (SAR and multi-angle optical) allowed us to gain insight into the conditions where each is able to observe sea ice roughness accurately. This information can now be used to guide the creation of sea ice informational products.

4.1 Summary

This research focuses on sea ice trafficability relevant to the communities of Kugluktuk and Cambridge Bay in Nunavut, located in the Western Canadian Arctic. The objectives of this thesis are 1) to identify impediments to community sea ice trafficability and safety that may be ameliorated using remote sensing information, and 2) to assess the effectiveness of two open-access satellite sensors for their ability to provide information about sea ice roughness at a scale useful to northern communities. These objectives are

addressed in Chapters 2 and 3 by using interviews, interactive map discussions, and thematic analysis, as well as quantitative assessments of remotely sensed datasets.

Chapter 2 finds that social and technological changes in communities accompanied by changes in the sea ice environment have caused increased uncertainty regarding trafficable conditions. Access to SAR-based maps for the purpose of complementing IQ is strongly desired by nearly all study participants (91%). A wide range of conditions that impact sea ice trafficability and safety are identified, and include smooth, moderately rough, and rough ice types, MYI, snow on ice, thin ice, early ice, late ice, slush/water on ice, ice encountered by boats, and ice fractures. SAR-based maps are judged by locals as effective at aiding and informing sea ice safety, trafficability, and education. Benefits from access to SAR are regarded as most substantial for the condition of sea ice surface roughness, for these two communities.

Chapter 3 demonstrates that MISR NDAI and Sentinel-1 HH backscatter, two satellite-based roughness proxies, can both be useful in the creation of maps with roughness information for communities. Both datasets are open-access and have satellite overpasses at least once every four days, although Sentinel-1 EW images have higher spatial resolution than the MISR red band (40 m vs 275 m) and are more likely to be available as they are not impacted by clouds or darkness. Based on an accuracy assessment done using fine-scale airborne LiDAR roughness, it is found that roughness maps for communities are most accurate if they use HH backscatter in areas of FYI (R^2 = 0.58, $p < 0.0001$), and NDAI in areas of MYI ($R^2 = 0.46$, $p = 0.0004$). In areas of MYI, NDAI is more useful for roughness maps because HH backscatter observes very high roughness due to volume scattering in the freshened, low-salinity ice. However, the

accuracies of the roughness proxies are very similar for a balanced selection of FYI and MYI types, with significant relationships and R^2 values of 0.65 (NDAI) and 0.66 (HH backscatter). This chapter confirms that HH backscatter becomes a poor roughness proxy in areas of low salinity ice (e.g., MYI or areas of riverine input) and in areas where the snow surface roughness is decoupled from the ice surface roughness. It also demonstrates that the dual-polarization H-alpha Wishart classification may be effective at identifying MYI using Sentinel-1 HH-HV polarised images (Kappa = 0.827).

4.2 Community engagement with remote sensing products

Many Kugluktuk and Cambridge Bay residents desire to understand and have access to technologies that can supplement IQ. Consequently, there was an overwhelmingly positive response to the SAR-based maps brought to the northern communities. Residents communicated that the SAR-based greyscale and classified maps have been successfully used for navigation purposes by local hunters, search and rescue, rangers, and wildlife guides. Throughout the duration of this thesis project, SAR-based maps of specific dates and/or regions were requested numerous times by northern residents via phone call, email, and social media. Northern organization employees suggested that SAR-based map information should be included in educational campaigns or projects where it is relevant to demonstrate sea ice use or to identify sea ice conditions (e.g., provide access for schools, shipping impact studies, etc.). Residents from other communities have found these SAR-based maps through personal contacts, social media, SIKU, CBC News, and other researchers. Consequently, outreach from residents who live in other communities (e.g., in Northern Quebec, the Northwest Territories, and Nunavut) show that there is broader interest in SAR-based sea ice maps for communities.

4.3 Future research and recommendations

This thesis represents a first look at the sea ice information needs of two Western Canadian Arctic communities. It is also the first to explore the utility of open-access satellite datasets for characterising sea ice roughness at scales relevant to communities. Thus, a large part of its value comes from identifying areas for further research. Future research will hopefully improve the access and value of remotely sensed imagery in Arctic communities, where it is currently underutilised. Further research is recommended in the following areas:

- Assessments of sea ice information priorities in other Arctic communities would be beneficial. Communities described in scientific literature had different priorities due to their social and environmental contexts: for example, Cape Dorset, Igloolik, and Pangnirtung residents expressed concern about identifying the floe edge location (Laidler et al., 2011).
- It would be valuable to continue improvements to the availability, content, and accessibility of remote sensing-based products. Improvements could derive from: 1) further consulting with locals about refinement of the SAR-based maps, MISR-based maps, and online SIKU platform; 2) developing a continuous two-way communication stream between locals and remote sensing experts for use in ice feature validation; 3) addressing other identified information needs (MYI, snow on ice, thin ice, early ice, late ice, slush/water on ice, ice encountered by boats, and ice fractures); 4) implementing a procedure for providing hard-copy maps in the communities, 5) providing training for SAR and other remote sensing product

use, which is desired by locals from both communities, and 6) offering maps to groups that may use sea ice data for educational purposes.

- Further tests for the detection of MYI using the Sentinel-1 dual-polarisation H-alpha Wishart classification are necessary to see how well the classification performs in other sea ice environments. If favourable, the creation of a fourth sea ice roughness class, “MYI,” would be a worthwhile addition to SAR-based roughness maps.
- It would be useful to assess new satellites (e.g., RCM) and/or fine-scale datasets (e.g., ground-truth, airborne LiDAR) for their abilities to characterise sea ice roughness. Other datasets and modes (e.g., high resolution) may also provide complementary information for detecting sea ice features.

4.4 References

Bell, T., Briggs, R., Bachmayer, R., & Li, S. (2014). Augmenting Inuit knowledge for safe sea-ice travel: The SmartICE information system. In *Oceans - St. John's, 2014* (pp. 1–9). https://doi.org/10.1109/OCEANS.2014.7003290

Dammann, D. O., Eicken, H., Mahoney, A. R., Saiet, E., Meyer, F. J., & George, J. C. "Craig." (2018). Traversing sea ice: Linking surface roughness and ice trafficability through SAR polarimetry and interferometry. *IEEE Journal of Selected Topics in Applied Earth Observations and Remote Sensing*, *PP*(99), 1–18. https://doi.org/10.1109/JSTARS.2017.2764961

Knol, M., Arbo, P., Duske, P., Gerland, S., Lamers, M., Pavlova, O., … Tronstad, S. (2018). Making the Arctic predictable: The changing information infrastructure of Arctic weather and sea ice services. *Polar Geography*, *41*(4), 279–293. https://doi.org/10.1080/1088937X.2018.1522382

Laidler, G. J., Hirose, T., Kapfer, M., Ikummaq, T., Joamie, E., & Elee, P. (2011). Evaluating the Floe Edge Service: How well can SAR imagery address Inuit community concerns around sea ice change and travel safety? *Canadian Geographer / Le Géographe Canadien*, *55*(1), 91–107. https://doi.org/10.1111/j.1541-0064.2010.00347.x

Panikkar, B., Lemmond, B., Else, B., & Murray, M. (2018). Ice over troubled waters: Navigating the Northwest Passage using Inuit knowledge and scientific information. *Climate Research*, *75*(1). Retrieved from https://www.openchannels.org/literature/22121

Appendix A

Table A.1. Semi-structured interview question guideline for May-June 2017 field season.

Themes	Follow-up questions
Experience	▪ Do you, or did you, travel on the sea ice? Why do people travel on sea ice? ▪ Is there anything else you want me to know about sea ice and/or travel?
Hazard identification and technology	▪ How do you choose travel routes? ▪ How much do your routes change from year to year? ▪ Using a map/image, can you point out: o Routes that are good for travel/have high traffic? o Areas where travel does not happen. Why? ▪ What are the features that make an area good for travel? Poor for travel? Unsafe? ▪ Can you point to (or draw) areas on this map where this feature is found? ▪ What are the main hazards for travel? Impediments to travel? o How do they vary by season? ▪ What features (or ice conditions) would be useful to know about when making travel plans? ▪ Do you already use remote sensing images to aid your travel? If so, what information do you use from them? ▪ Are there areas where remote sensing information would be very useful (i.e., areas I should focus on)? o How do you think remote sensing images/analysis can help with this? ▪ What impact does technology have on travel?
Spatiotemporal sea ice use and change	▪ Where do people travel to/from Kugluktuk/Cambridge Bay? o Does this depend on the season? ▪ When does a normal season for sea ice travel start/end? ▪ Have you noticed any changes in sea ice that impact travel? o Where? o When? Over the past 3, 5, or 20 years? o Is it changing more lately? o Are the changes related to seasons? o Who do they impact? ▪ What features would be useful to know about when tracking change (or lack of change) over long time periods? o Do you think remote sensing can help us look at changes in sea ice conditions? What would be helpful to track? ▪ Is there anything in addition to, or instead of, remote sensing data that would be helpful (e.g., web cam, met station data, etc.).
Site-specific questions	▪ What is interesting here? ▪ What part of this image/map/photo is important? ▪ Explain what you see? ▪ What is significant about this area, feature, or process? ▪ How does this kind of feature impact you? The community? Travel or safety? ▪ Is this a normal sea ice feature?

A.1 SAR processing

Of the two available Sentinel-1 image bands, HH-polarization (horizontal transmit and receive) was used since it is sensitive to ice type and surface roughness, and data from smooth sea ice in this region are above the sensor noise floor (Scharien et al., 2017). A standard processing chain was applied to Sentinel-1 HH images (Table A.2) using ESA's Sentinel Application Platform (SNAP) Version 6.0: i) thermal noise removal; ii) calibration (Gamma-nought); iii) speckle filtering (Lee 7×7), iv) conversion to decibels (dB), and v) map projection. SAR intensity was displayed using a histogram stretch range limited to the marine data.

Table A.2. Information about the Sentinel-1 products processed and used in maps brought to the communities. Where indicated (*), classified maps were also created. Abbreviations are as follows: S = Sentinel; Des = descending; Asc = ascending; and EW = extended wide-swath. All images are in ground range detected (GRD) format.

Platform (Direction/Mode)	Date (dd-mmm-yy)	Orbit (Track)	ID	Location
S1A (Des/EW)	12-Mar-18	020983 (86)	56B6	Kugluktuk
S1A (Des/EW)	5-Mar-18	020881 (159)	970B	Kugluktuk
S1A (Des/EW)	20-Feb-18	020691 (144)	BD41	Cambridge Bay
S1A (Des/EW)	11-Jan-18	020108 (86)	3D38	Kugluktuk
S1A (Des/EW)	4-Jan-18	020006 (159)	E84A	Kugluktuk
S1B (Asc/EW)	4-Jan-18	009022 (71)	859F	Cambridge Bay
S1A (Des/EW)	3-Jan-18	019991 (144)	1C50	Cambridge Bay
S1A (Des/EW)	4-Nov-17	019116 (144)	DAF2	Cambridge Bay
S1B (Asc/EW)	7-Nov-17	008176 (100)	1813	Cambridge Bay
S1B (Asc/EW)	1-Jul-17	006295 (144)	FC51	Cambridge Bay
S1B (Asc/EW)	22-Jun-17	006164 (13)	92F3	Kugluktuk
S1A (Des/EW)	30-Mar-17	015922 (100)	90B7	Victoria Strait
S1A (Des/EW)	28-Mar-17	015893 (71)	3595	Cambridge Bay
S1B (Asc/EW)	18-Mar-17	004764 (13)	57E5	Kugluktuk
S1B (Des/EW)	17-Mar-17	004749 (173)	0AE8	Cambridge Bay
S1A (Des/EW)	23-Feb-17	015412 (115)	A7D2	Kugluktuk
S1B (Des/EW)	25-Nov-16	003116 (115)	3225	Kugluktuk
S1A (Des/EW)	21-Apr-16	010920 (173)	317F	Cambridge Bay
S1A (Des/EW)	9-Apr-16	010745 (173)	132B	Cambridge Bay
S1A (Des/EW)	12-Mar-16	010337 (115)	DD0B	Kugluktuk

A.2 References

Scharien, R. K., Segal, R., Nasonova, S., Nandan, V., Howell, S. E. L., & Haas, C. (2017). Winter Sentinel-1 backscatter as a predictor of spring Arctic sea ice melt pond fraction. *Geophysical Research Letters*, *44*(24), 12,262-12,270. https://doi.org/10.1002/2017GL075547

Appendix B

B.1 Study region sea ice regime

Video S1 <*Vic_Strait_Sent_1_2016_2017.avi*> shows a time sequence of Sentinel-1 GRD EW images (HH polarization in dB) over the Victoria Strait region from July 2016 to October 2017. The sea ice began freezing North of Victoria Island, in M'Clintock Channel, where some MYI floes were present (mid-October 2016). Ice formed near land and spread throughout the southern portion of the study region, while open water in M'Clintock Channel and leads in Victoria Strait persisted. Areas of smooth ice formed and persisted in wind- and current-sheltered areas (e.g., part of M'Clintock Channel and Queen Maud Gulf). Victoria Strait showed north-south axis movement of sea ice and underwent ice deformation processes that continued late into winter, resulting in very rough sea ice. In spring, the sea ice began breaking at the northern and southern edges of Victoria Strait, and the ice in the strait began forming large leads. Open water then formed near land, before appearing in the south and moving northwards.

B.2 HH backscatter processing

We processed 17 Sentinel-1 HH-band extra wide swath (EW) scenes captured between 12 March and 15 April 2017 during cold conditions, when the backscatter contribution from sea ice is stable and differences in backscatter between images are due to changes in incidence angle. Image processing consisted of i) thermal noise removal; ii) calibration (both Sigma-nought and Gamma-nought); iii) speckle filtering (Lee 5×5), and iv) map projection. Backscatter statistics and incidence angle were calculated for two FYI

ROIs (19.6 km^2 and 17.6 km^2) and three MYI ROIs (7.5 km^2, 9.8 km^2, and 19.7 km^2). Results from this analysis are shown in Figures B.1 and B.2. We chose to use a gamma-nought calibration for the roughness comparisons in order to reduce sensitivity to incidence angle (Figure B.2) (Dierking & Busche, 2006; Dierking & Dall, 2007). Alternatively, some other studies opt to adjust SAR images to remove the effects of incidence angle on backscatter, either by applying scaling or corrections using backscatter from dark and light reference areas (Gegiuc et al., 2018; Makynen et al., 2002; Martinez-Agirre et al., 2017; Melling, 1998).

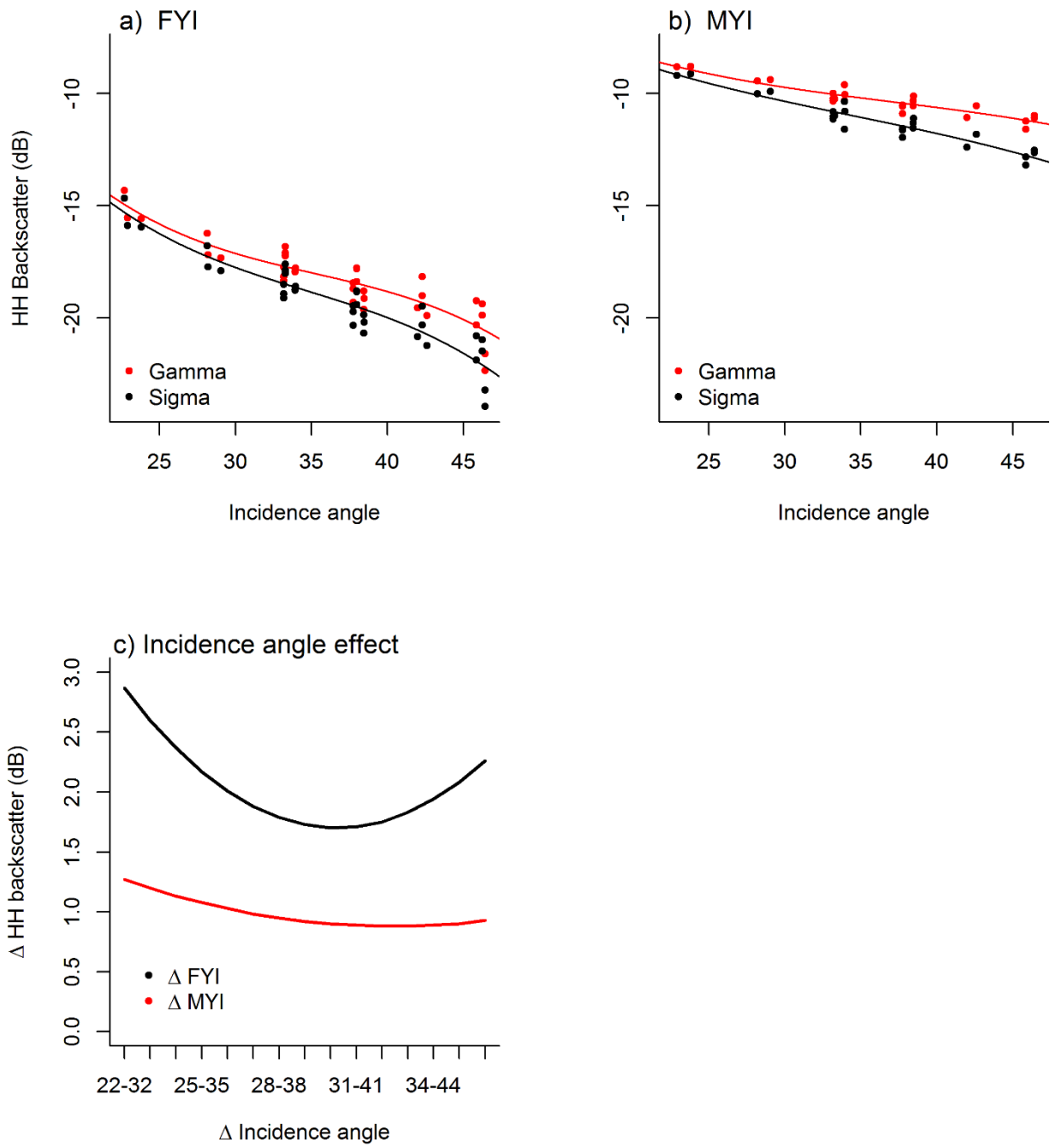

Figure B.1. Sentinel-1 HH-band backscatter from a) FYI and b) MYI targets, given as cubic functions of incidence angle for gamma-nought and sigma-nought calibrations. The effect of incidence angle is less for gamma-nought calibration and is similar between FYI and MYI types. In c) the effect of ten-degree incidence angle intervals is shown as HH gamma nought backscatter ranges, for FYI and MYI types.

Table B.1. Information about the sensors and products used to investigate the effect of incidence angle on Sentinel-1 backscatter over FYI and MYI in M'Clintock Channel, winter 2017. Abbreviations are as follows: S = Sentinel; Des = descending; Asc = ascending; EW = extended wide-swath; GRD = ground range detected.

Platform	Payload	Date (dd-mmm-yy)	Dir/Mode	Orbit (Track)	ID	Format
S1A	SAR-C	16-Mar-17	Des/EW	15718 (71)	CC2C	GRD
S1A	SAR-C	16-Mar-17	Des/EW	15718 (71)	661C	GRD
S1A	SAR-C	20-Mar-17	Des/EW	15776 (129)	E279	GRD
S1A	SAR-C	09-Apr-17	Des/EW	15776 (129)	DFD1	GRD
S1A	SAR-C	11-Apr-17	Des/EW	16097 (100)	E3EA	GRD
S1B	SAR-C	12-Mar-17	Des/EW	4676 (100)	7B4F	GRD
S1B	SAR-C	14-Mar-17	Des/EW	4705 (129)	4ACF	GRD
S1B	SAR-C	17-Mar-17	Des/EW	4749 (173)	0AE8	GRD
S1B	SAR-C	22-Mar-17	Asc/EW	4822 (71)	F378	GRD
S1B	SAR-C	26-Mar-17	Asc/EW	4880 (129)	74C6	GRD
S1B	SAR-C	27-Mar-17	Asc/EW	4895 (144)	B970	GRD
S1B	SAR-C	29-Mar-17	Asc/EW	4924 (173)	55F6	GRD
S1B	SAR-C	31-Mar-17	Asc/EW	4953 (27)	0B83	GRD
S1B	SAR-C	01-Apr-17	Asc/EW	4968 (42)	6869	GRD
S1B	SAR-C	10-Apr-17	Asc/EW	5099 (173)	B132	GRD
S1B	SAR-C	12-Apr-17	Asc/EW	5128 (27)	2A30	GRD
S1B	SAR-C	15-Apr-17	Asc/EW	5172 (71)	DA2D	GRD

B.3 NDAI and HH backscatter relationships by ice type

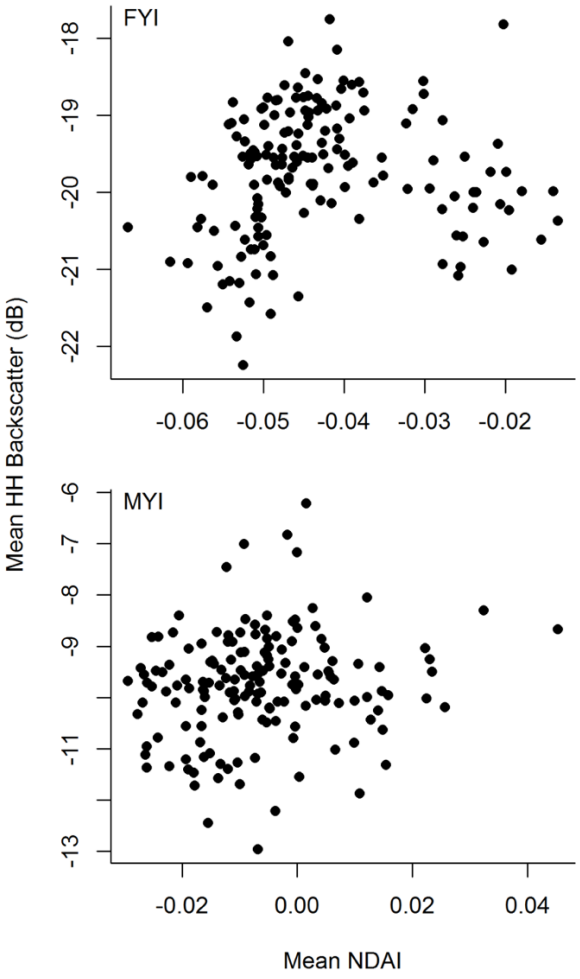

Figure B.2. Relationship between mean Sentinel-1 HH backscatter and mean MISR NDAI for FYI (top) and MYI (bottom) types.

B.4 HH backscatter by region

Table B.2. FYI C-band HH backscatter observed across Arctic roughness regimes.

Region	FYI		Rough FYI		Incidence angle[11]	Source
	Backscatter (dB)	*Value description*	*Backscatter (dB)*	*Value description*		
Kitikmeot	-18.53 -19.7 -22.2 to -19.7	FYI median FYI mean FYI range	-13.49 -13.3 -17.6 to -10.2	DFYI median DFYI mean DFYI range	30-40°	This study
Cornwallis Island, Nunavut	-19.3	FYI mean	-16.1	Rough FYI mean	26.0-45.2°	Geldsetzer and Yackel (2009)
Franklin Bay, Northwest Territories	-20.45 -21-74	FYI mean	-11.73 -12.23 -9.66 -10.12	Rough FYI[12] mean DFYI[13] mean	31-33° 35-37° 31-33° 35-37°	Gill and Yackel (2012)
Beaufort Sea/ Amundsen Gulf	-23 to -19	FYI range	-14 to -13	DFYI range	30-40°	Gupta et al. (2014)
Beaufort Sea/ Amundsen Gulf	-22 to -18	FYI range	-14 to -13	DFYI range	30-40°	Gupta, Scharien and Barber (2013)
Eastern Beaufort Sea	~-22 to -19.8	FYI range	~-12.5	FYI ridge range	20.1-25.9°	Melling (1998)
Southwestern Hudson Bay	-13 -15	FYI mean	-10 -7.5 -11.5 -9	Rough FYI mean DFYI mean Rough FYI mean DFYI mean	29° 29° 39° 39°	Hossain et al. (2014)
Svalbard Fram Strait Barents Sea	-15 to -7.5 -14.5 to -9 -16.5 to -10	FYI range	-11 to -4.5 -6.5 to -4 -11.5 to -6.5	Broken ice range FYI ridge range Brash/rubble range	30-45°	Dierking (2010)
Baltic Sea	~ -19 (data points all < -16.5)	Model predictions of >80% level ice	~ -12 (data points all > -17)	Model predictions of <20% level ice	23.2-25.3°; 40.3-42.5°	Similä Mäkynen and Heiler (2010)
Baltic Sea	-20 -25 -16 -14	Dry snow; FYI Wet snow; FYI	-17 -21 -13 -17	Dry snow, rough FYI Dry snow, slightly DFYI[14]	23° 45° 23° 45°	Mäkynen and Hallikainen (2004)

[11] Limited to 30-40° if possible
[12] Broken or uneven FYI with protruding blocks and/or edges
[13] Rubble ice, ridges, and/or boulders >1m in sle
[14] Contains ice ridges and uneven surfaces; level ice components in this zone are usually >100m

			-10 -13 -12 -11 -11 -11	Dry snow, highly DFYI[15] Wet snow, slightly DFYI Wet snow, highly DFYI	23° 45° 23° 45° 23° 45°	
Baltic Sea	-15	FYI mean	-9	DFYI mean	45°	Dierking and Dall (2007)
Baltic Sea	-13.5 to -11 -16.25 to -14.25	FYI range	-8.25 to -7 -12.5 to -9.5	Rough fast FYI mean	20° 33°	Eriksson et al. (2010)
Baltic Sea	-21.5 to -10 -21.5 to -10 -21 to -5	FYI range from proportion of observations >0.05 (Jan.) (Feb.) (Mar.)	-19.5 to -19; -18.5 to -11.5 -16 to -10.5 -17 to -11	Ridged ice range from proportion of observations >0.05 (Jan.) (Feb.) (Mar.)	20-49° (corrected)	Gegiuc et al. (2018)

B.5 Other data and recommendations (continued)

Radar systems are sensitive to the sea ice surface at scales of the radar wavelength: the C-band wavelength is ~5.7 cm, L-band ~23.6 cm, and X-band ~3.1 cm (Richards, 2009). Several studies using the longer L-band wavelength have found that deformation features have a higher contrast to smooth ice than higher frequencies and are less sensitive to small-scale roughness, ice type, and spring conditions (Arkett et al., 2008; Dierking & Busche, 2006; Eriksson et al., 2010). L-band HH polarization at larger incidence angles (35-42°) was found to be particularly useful for characterizing surface deformation, and detected a higher fractional area of DFYI than C-band SAR in the Baltic Sea (Dierking & Busche, 2006; Dierking & Dall, 2007), likely because C-band backscatter is very sensitive to small-scale (several wavelength)

[15] Level ice components usually <100m, with lower proportional area than DFYI

deformations, which can obscure larger-scale features (Dierking et al., 1997), and makes the contrast between level and deformed ice at L-band higher for small height undulations (e.g., rafted ice) (Dierking & Dall, 2007). L-band SAR has also proven useful during freeze-up, as the frequency is less sensitive to new ice frost-flower roughness and thus backscatter and texture are more related to ice thickness (and larger-scale roughness) (Arkett et al., 2008).

Shorter wavelength X-band SAR is more sensitive to snow and air bubbles in the upper ice layer than lower frequencies, responding with higher volume scattering and consequently shallower penetration into the sea ice (Eriksson et al., 2010; Richards, 2009). This frequency separates level FYI and level MYI from new and young ice more easily than lower frequencies and has greater contrast between sea ice and calm water, making it sensitive to spring melt (Eriksson et al., 2010). The main differences between X- and C-band frequencies are at micro-scale surface interactions (mm-cm; to which L-band is less sensitive), rather than differences related to macro-scale roughness (Eriksson et al., 2010; Richards, 2009). Eriksson et al. (2010) found that co-pol backscatter from X-band appeared similar to C-band, and cross-pol X-band data similar to L-band, with deformation features easier to recognise at L-band than at X-band. While X- and C-band datasets (but not L-band) provide similar information (Eriksson et al., 2010; Mäkynen & Hallikainen, 2004), several studies report that multifrequency data is helpful for identifying roughness (Arkett et al., 2008; Eriksson et al., 2010; Milillo et al., 2015). For example, ice blocks >30 cm on relatively level ice could be identified by their high backscatter across X-, C- and L-band, while smooth level ice exhibited reduced backscatter at lower frequencies (Eriksson et al.,

2010). Consequently, access to multiple frequencies would provide more information for community sea ice maps. Unfortunately, the cost (L-and X-band), low temporal resolution (L-band) and small swath size (X-band) of the current X- and L-band satellites makes their current utility for frequent and large-scale data collection limited. Region-based subscription offered by companies like ICEYE, Planet and DigitalGlobe, may prove to be more cost-effective options for monitoring sea ice near particular communities.

Multiple SAR polarization parameters can also have utility for discriminating rough sea ice from level ice, or for identifying degrees of deformation. Studies have found that multiple C-band channel combinations (Drinkwater et al., 1992; Gill & Yackel, 2012), cross-pol ratios (Dierking & Dall, 2007; Gegiuc et al., 2018), co-pol ratios (Dierking & Dall, 2007; Johansson et al., 2017), and other measures of depolarization, intensity, decomposition, etc., can contain information about roughness (Brekke et al., 2015; Casey et al., 2014; Fors et al., 2016; Hossain et al., 2014; Moen et al., 2013), though it remains necessary to interpret the data in the context of seasonal and ice/snow properties (Fors et al., 2015). While multiple polarization parameters can increase the effectiveness of roughness mapping, there is evidence that the HH channel works well for detecting rough sea ice and is generally as strong as any other single metric (Fors et al., 2015; Gegiuc et al., 2018; Gill & Yackel, 2012; Xu et al., 2017).

Other data types, including multi-angle and stereo-pair optical data, can also provide information on sea ice elevation and roughness. MISR and other optical satellites (e.g., DigitalGlobe’s WorldView-1-4, GeoEye-1) or platforms (e.g., airborne or UAV) can capture multiple off-nadir images from one platform or from coincident

but separate orbits, allowing for the creation of digital elevation and roughness models (Dammann et al., 2018; Li, 2018; Shean et al., 2016). Fine-scale optical datasets can also assess roughness using ice feature shadows (Zakharov et al., 2015). However, most multi-angle and high-resolution optical images are only commercially available (Table B.3). Other methods of obtaining sea ice roughness include CryoSat-2 radar altimetry (Kurtz et al., 2014; Shepherd et al., 2012), although backscatter angle can cause roughness errors. ICESat laser altimetry measures elevation, but ellipsoidal coverage is not continuous and is affected by the roughness found within each ellipse (Kurtz et al., 2008). Scatterometers are sensitive to surface roughness, among other parameters (Gupta, 2015; Nghiem et al., 2007; Remund & Long, 2014).

Table B.3. Current and near-future satellite-based payloads that may be useful (high quality and/or affordable) for providing sea ice surface trafficability information to northern communities.

Data Type	Programme(s) and relevant payloads	Agency	Availability	Example roughness studies
C-band SAR	Sentinel-1 (SAR-C)	ESA, EC	Open access	(Dierking, 2010; Martinez-Agirre et al., 2017)
C-band SAR	RADARSAT-2 (SAR)	CSA	Restricted	(Brekke et al., 2015; Ersahin et al., 2014; Fors et al., 2016; Gauthier et al., 2010; Gegiuc et al., 2018; Hossain et al., 2014; Johansson et al., 2017; Mussells, 2015; Xu et al., 2017; Zakharov et al., 2015)
C-band SAR	RADARSAT Constellation Mission (SAR RCM)	CSA	TBD	(Nasonova et al., 2018)
X-band SAR	TerraSAR-X (SAR-X) and TanDEM-X (SAR-X)	DLR	Restricted	(Dammann et al., 2018; Johansson et al., 2017; Linow, 2015; Yitayew et al., 2018; Zakharov et al., 2015)
X-band SAR	COSMO-SkyMed (SAR-2000)	ASI	Restricted	
X-band SAR	ICEYE-X1	ICEYE	Restricted	
X-band SAR	SEOSAR/Paz (SAR-X)	CDTI	Restricted	
L-band SAR	ALOS-2 (PALSAR-2)	JAXA	Restricted	(Dammann et al., 2018; Johansson et al., 2017)
X- and L-band SAR, Panchromatic, Multispectral, NIR; RGB video	OptiSAR, Deimos-1 -2 (SLIM6, HIRAIS); Theia, Iris	Urthecast	Restricted	
Multispectral	Terra (ASTER, MISR)	NASA	Open access	(Nolin & Mar, 2019; Nolin & Payne, 2007; Nolin et al., 2002; Wu et al., 2009; Chust & Sagarminaga, 2007)
Multispectral	Sentinel-2 (MSI)	ESA, EC	Open access	
Panchromatic and multispectral	DigitalGlobe Constellation (WorldView-1-4: WV60, WV110, WV110, SpaceView-110; and GeoEye-1: GIS)	DigitalGlobe	Restricted	(Brekke et al., 2015; Shean et al., 2016; Zakharov et al., 2015)
Multispectral, RGB, and NIR	RapidEye (REIS); SkySat-1; SkySat-2; SkySat-3; SkySat-5; SkySat-6; SkySat-7; Flock-2e; Flock-2e'; Flock-2p; Flock-3p	Planet	Restricted	
Altimeter	Sentinel-3 (SRAL)	ESA, EC, EUMETSAT	Open access	

B.6 References

Arkett, M., Flett, D., Abreu, R. D., Clemente-Colon, P., Woods, J., & Melchior, B. (2008). Evaluating ALOS-PALSAR for Ice Monitoring - What Can L-band do for the North American Ice Service? In *IGARSS 2008 - 2008 IEEE International Geoscience and Remote Sensing Symposium* (Vol. 5, pp. V-188-V–191). https://doi.org/10.1109/IGARSS.2008.4780059

Brekke, C., Grahn, J., & Doulgeris, A. P. (2015). Quad-polarimetric SAR for roughness and deformation characterization of sea ice at Hopen. In *Proceedings of POLinSAR 2015* (Vol. 729). Frascati, Italy. Retrieved from http://www.npcarcticpotentialreport.org/pdf/tp/5-5_Summary_of_Current_Ice_Characterization_Research-Norway-Russia-Europe.pdf

Casey, J. A., Beckers, J., Busche, T., & Haas, C. (2014). Towards the retrieval of multi-year sea ice thickness and deformation state from polarimetric C- and X-band SAR observations. In *2014 IEEE Geoscience and Remote Sensing Symposium* (pp. 1190–1193). https://doi.org/10.1109/IGARSS.2014.6946644

Chust, G., & Sagarminaga, Y. (2007). The multi-angle view of MISR detects oil slicks under sun glitter conditions. *Remote Sensing of Environment*, *107*(1–2), 232–239. https://doi.org/10.1016/j.rse.2006.09.024

Dammann, D. O., Eicken, H., Mahoney, A. R., Saiet, E., Meyer, F. J., & George, J. C. “Craig.” (2018). Traversing sea ice: Linking surface roughness and ice trafficability through SAR polarimetry and interferometry. *IEEE Journal of*

Selected Topics in Applied Earth Observations and Remote Sensing, *PP*(99), 1–18. https://doi.org/10.1109/JSTARS.2017.2764961

Dierking, W. (2010). Mapping of different sea ice regimes using images from Sentinel-1 and ALOS synthetic aperture radar. *IEEE Transactions on Geoscience and Remote Sensing*, *48*(3), 1045–1058. https://doi.org/10.1109/TGRS.2009.2031806

Dierking, W., & Busche, T. (2006). Sea ice monitoring by L-band SAR: An assessment based on literature and comparisons of JERS-1 and ERS-1 imagery. *IEEE Transactions on Geoscience and Remote Sensing*, *44*(4), 957–970. https://doi.org/10.1109/TGRS.2005.861745

Dierking, W., Carlstrom, A., & Ulander, L. M. H. (1997). The effect of inhomogeneous roughness on radar backscattering from slightly deformed sea ice. *IEEE Transactions on Geoscience and Remote Sensing*, *35*(1), 147–159. https://doi.org/10.1109/36.551943

Dierking, W., & Dall, J. (2007). Sea-ice deformation state from synthetic aperture radar imagery—Part I: Comparison of C- and L-band and different polarization. *IEEE Transactions on Geoscience and Remote Sensing*, *45*(11), 3610–3622. https://doi.org/10.1109/TGRS.2007.903711

Drinkwater, M. R., Kwok, R., Rignot, E., Israelsson, H., Onstott, R. G., & Winebrenner. (1992). Potential applications of polarimetry to the classification of sea ice. In F. D. Carsey (Ed.), *Microwave remote sensing of sea ice* (Vol. 68, pp. 419–430). Washington DC: American Geophysical Union.

Eriksson, L. E. B., Pemberton, P., Lindh, H., & Karlson, B. (2010). Evaluation of new spaceborne SAR sensors for sea-ice monitoring in the Baltic Sea. *Canadian Journal of Remote Sensing*, 19.

Ersahin, K., Brown, L., Kanwar, A., Henley, M., Ross, E., & Fissel, D. (2014). Characterization of hazardous ice using spaceborne SAR and ice profiling sonar: preliminary results. Offshore Technology Conference. https://doi.org/10.4043/24600-MS

Fors, A. S., Brekke, C., Gerland, S., Doulgeris, A. P., & Beckers, J. F. (2016). Late summer Arctic sea ice surface roughness signatures in C-Band SAR data. *IEEE Journal of Selected Topics in Applied Earth Observations and Remote Sensing*, *9*(3), 1199–1215. https://doi.org/10.1109/JSTARS.2015.2504384

Fors, A. S., Brekke, C., Gerland, S., Doulgeris, A. P., & Eltoft, T. (2015). Extraction of late summer sea ice properties from polarimetric SAR features in C-and X-band. In *Proceedings of POLinSAR 2015* (pp. 1–5). Frascati, Italy.

Gauthier, Y., Tremblay, M., Bernier, M., & Furgal, C. (2010). Adaptation of a radar-based river ice mapping technology to the Nunavik context. *Canadian Journal of Remote Sensing*, *36*(S1), S168–S185. https://doi.org/10.5589/m10-018

Gegiuc, A., Similä, M., Karvonen, J., Lensu, M., Mäkynen, M., & Vainio, J. (2018). Estimation of degree of sea ice ridging based on dual-polarized C-band SAR data. *The Cryosphere*, *12*(1), 343–364. https://doi.org/10.5194/tc-12-343-2018

Geldsetzer, T., & Yackel, J. J. (2009). Sea ice type and open water discrimination using dual co-polarized C-band SAR. *Canadian Journal of Remote Sensing*, *35*(1), 73–84. https://doi.org/10.5589/m08-075

Gill, J. P. S., & Yackel, J. J. (2012). Evaluation of C-band SAR polarimetric parameters for discrimination of first-year sea ice types. *Canadian Journal of Remote Sensing*, *38*(3), 306–323. https://doi.org/10.5589/m12-025

Gupta, M. (2015). Various remote sensing approaches to understanding roughness in the marginal ice zone. *Physics and Chemistry of the Earth, Parts A/B/C*, *83–84*, 75–83. https://doi.org/10.1016/j.pce.2015.05.003

Gupta, M., Barber, D. G., Scharien, R. K., & Isleifson, D. (2014). Detection and classification of surface roughness in an Arctic marginal sea ice zone: Surface roughness in MIZ. *Hydrological Processes*, *28*(3), 599–609. https://doi.org/10.1002/hyp.9593

Gupta, M., Scharien, R. K., & Barber, D. G. (2013). C-band polarimetric coherences and ratios for discriminating sea ice roughness. *International Journal of Oceanography*, *2013*(567182), 1–13. http://dx.doi.org/10.1155/2013/567182

Hossain, M., Yackel, J., Dabboor, M., & Fuller, M. C. (2014). Application of a three-component scattering model over snow-covered first-year sea ice using polarimetric C-band SAR data. *International Journal of Remote Sensing*, *35*(5), 1786–1803. https://doi.org/10.1080/01431161.2013.879345

Johansson, A. M., King, J. A., Doulgeris, A. P., Gerland, S., Singha, S., Spreen, G., & Busche, T. (2017). Combined observations of Arctic sea ice with near-coincident colocated X-band, C-band, and L-band SAR satellite remote sensing and helicopter-borne measurements. *Journal of Geophysical Research: Oceans*, *122*(1), 669–691. https://doi.org/10.1002/2016JC012273

Kurtz, N. T., Galin, N., & Studinger, M. (2014). An improved CryoSat-2 sea ice freeboard retrieval algorithm through the use of waveform fitting. *The Cryosphere*, *8*(4), 1217–1237. https://doi.org/10.5194/tc-8-1217-2014

Kurtz, N. T., Markus, T., Cavalieri, D. J., Krabill, W., Sonntag, J. G., & Miller, J. (2008). Comparison of ICESat data with airborne laser altimeter measurements over Arctic sea ice. *IEEE Transactions on Geoscience and Remote Sensing*, *46*(7), 1913–1924. https://doi.org/10.1109/TGRS.2008.916639

Li, Y. (2018). *Sea ice and ice sheet surface roughness characterization and its effects on bi-directional reflectance* (Thesis). Texas A & M University, College Station, Texas. Retrieved from https://oaktrust.library.tamu.edu/handle/1969.1/173578

Linow, S. (2015, January). *What can polarimetric SAR data tell us about snow accumulation on polar ice sheets?* Presentation presented at the ESA POLinSAR 2015 - 1st BIOMASS Science Workshop, ESA-ESRIN, Frascati, Italy. Retrieved from https://www.researchgate.net/publication/272348126_What_can_polarimetric_SAR_data_tell_us_about_snow_accumulation_on_polar_ice_sheets

Mäkynen, M., & Hallikainen, M. (2004). Investigation of C- and X-band backscattering signatures of Baltic Sea ice. *International Journal of Remote Sensing*, *25*(11), 2061–2086. https://doi.org/10.1080/01431160310001647697

Makynen, M. P., Manninen, A. T., Simila, M. H., Karvonen, J. A., & Hallikainen, M. T. (2002). Incidence angle dependence of the statistical properties of C-band HH-polarization backscattering signatures of the Baltic Sea ice. *IEEE Transactions on*

Geoscience and Remote Sensing, *40*(12), 2593–2605. https://doi.org/10.1109/TGRS.2002.806991

Martinez-Agirre, A., Álvarez-Mozos, J., Lievens, H., Verhoest, N. E. C., & Giménez, R. (2017). Influence of surface roughness sample size for C-band SAR backscatter applications on agricultural soils. *IEEE Geoscience and Remote Sensing Letters*, *14*(12), 2300–2304. https://doi.org/10.1109/LGRS.2017.2762434

Melling, H. (1998). Detection of features in first-year pack ice by synthetic aperture radar (SAR). *International Journal of Remote Sensing*, *19*(6), 1223–1249. https://doi.org/10.1080/014311698215702

Milillo, P., Riel, B., Minchew, B., Yun, S.-H., Simons, M., & Lundgren, P. (2015). On the synergistic use of SAR constellations' data exploitation for earth science and natural hazard response. *IEEE Journal of Selected Topics in Applied Earth Observations and Remote Sensing*, *PP*(99), 1–6. https://doi.org/10.1109/JSTARS.2015.2465166

Moen, M.-A. N., Doulgeris, A. P., Anfinsen, S. N., Renner, A. H. H., Hughes, N., Gerland, S., & Eltoft, T. (2013). Comparison of feature based segmentation of full polarimetric SAR satellite sea ice images with manually drawn ice charts. *The Cryosphere*, *7*(6), 1693–1705. https://doi.org/10.5194/tc-7-1693-2013

Mussells, O. (2015). *Observing pressured sea ice in the Hudson Strait using RADARSAT: Implications for shipping* (Thesis). Université d'Ottawa / University of Ottawa. Retrieved from http://www.ruor.uottawa.ca/handle/10393/33358

Nasonova, S., Scharien, R. K., Geldsetzer, T., Howell, S. E. L., & Power, D. (2018). Optimal compact polarimetric parameters and texture features for discriminating

sea ice types during winter and advanced melt. *Canadian Journal of Remote Sensing*, *44*(4), 390–411. https://doi.org/10.1080/07038992.2018.1527683

Nghiem, S. V., Rigor, I. G., Perovich, D. K., Clemente- Colón, P., Weatherly, J. W., & Neumann, G. (2007). Rapid reduction of Arctic perennial sea ice. *Geophysical Research Letters*, *34*(19). https://doi.org/10.1029/2007GL031138

Nolin, A. W., Fetterer, F. M., & Scambos, T. A. (2002). Surface roughness characterizations of sea ice and ice sheets: Case studies with MISR data. *IEEE Transactions on Geoscience and Remote Sensing*, *40*(7), 1605–1615. https://doi.org/10.1109/TGRS.2002.801581

Nolin, A. W., & Mar, E. (2019). Arctic sea ice surface roughness estimated from multi-angular reflectance satellite imagery. *Remote Sensing*, *11*(1), 50. https://doi.org/10.3390/rs11010050

Nolin, A. W., & Payne, M. C. (2007). Classification of glacier zones in western Greenland using albedo and surface roughness from the Multi-angle Imaging SpectroRadiometer (MISR). *Remote Sensing of Environment*, *107*(1–2), 264–275. https://doi.org/10.1016/j.rse.2006.11.004

Remund, Q. P., & Long, D. G. (2014). A decade of QuikSCAT scatterometer sea ice extent data. *IEEE Transactions on Geoscience and Remote Sensing*, *52*(7), 4281–4290. https://doi.org/10.1109/TGRS.2013.2281056

Richards, J. A. (2009). *Remote sensing with imaging radar*. Berlin, Heidelberg: Springer Berlin Heidelberg. Retrieved from http://link.springer.com/10.1007/978-3-642-02020-9

Shean, D. E., Alexandrov, O., Moratto, Z. M., Smith, B. E., Joughin, I. R., Porter, C., & Morin, P. (2016). An automated, open-source pipeline for mass production of digital elevation models (DEMs) from very-high-resolution commercial stereo satellite imagery. *ISPRS Journal of Photogrammetry and Remote Sensing*, *116*, 101–117. https://doi.org/10.1016/j.isprsjprs.2016.03.012

Shepherd, A., Ivins, E. R., A, G., Barletta, V. R., Bentley, M. J., Bettadpur, S., … Zwally, H. J. (2012). A reconciled estimate of ice-sheet mass balance. *Science*, *338*(6111), 1183–1189. https://doi.org/10.1126/science.1228102

Similä, M., Mäkynen, M., & Heiler, I. (2010). Comparison between C band synthetic aperture radar and 3-D laser scanner statistics for the Baltic Sea ice. *Journal of Geophysical Research: Oceans*, *115*(C10). https://doi.org/10.1029/2009JC005970

Wu, Y., Gong, P., Liu, Q., & Chappell, A. (2009). Retrieving photometric properties of desert surfaces in China using the Hapke model and MISR data. *Remote Sensing of Environment*, *113*(1), 213–223. https://doi.org/10.1016/j.rse.2008.09.006

Xu, L., Clausi, D. A., Li, F., & Wong, A. (2017). Weakly supervised classification of remotely sensed imagery using label constraint and edge penalty. *IEEE Transactions on Geoscience and Remote Sensing*, *55*(3), 1424–1436. https://doi.org/10.1109/TGRS.2016.2623942

Yitayew, T. G., Dierking, W., Divine, D. V., Eltoft, T., Ferro-Famil, L., Rösel, A., & Negrel, J. (2018). Validation of sea-ice topographic heights derived from TanDEM-X interferometric SAR data with results from laser profiler and photogrammetry. *IEEE Transactions on Geoscience and Remote Sensing*, *56*(11), 6504–6520. https://doi.org/10.1109/TGRS.2018.2839590

Zakharov, I., Bobby, P., Power, D., Saunders, K., & Warren, S. (2015). Monitoring hazardous sea ice features using satellite imagery (Vol. OTC-25570-MS). Presented at the OTC Arctic Technology Conference, Copenhagen, Denmark: Offshore Technology Conference. http://dx.doi.org/10.4043/25570-MS